University College London

The influence of increased Kallikrein 5 in keratinocytes in inflammatory immuno-response

Xin Huang

A thesis submitted to the University College London for the Degree of Doctor of Philosophy

UCL Great Ormond Street Hospital Institute of Child Health

2023

Declaration

I, Xin Huang, confirm that the work presented in my thesis is my own. Where information has been derived from other sources, I confirm that this has been indicated in the thesis. No portion of the work referred to in the thesis has been submitted in support of an application for another degree or qualification of this or any other university or other institute of learning.

Abstract

Atopic dermatitis (AD) is a multi-factorial inflammatory skin disease caused by genetic and environmental factors. AD has a disrupted skin barrier, resulting in external allergens easily penetrating through the barrier and leading to Th2 immune response. Abnormalities of proteins in the skin can cause dysfunctional skin barrier and enhanced serine proteases Kallikrein 5 (KLK5) is one of them. Studies showed enhanced KLK5 could impair the skin barrier integrity by over-degrading the adhesion protein and upregulate cytokines. I proposed to investigate the relationship between enhanced KLK5 in keratinocytes and immuno-response in the skin.

The transcriptome changes were first examined in keratinocytes overexpressing KLK5. The results showed no differentiated genes directly related to immuno-response. However, genes involved in the TGF-β signaling were down-regulated. Secondly, the culture media from keratinocytes with KLK5 overexpression were checked. Increased IL-2 and IL-6 and decreased TSLP were found. To confirm if these cytokines play a paracrine effect on Th2 immuno-response in the skin, human naïve $CD4^+$ T cells were treated with this conditional medium. Increase of Th2 differentiation was found in treated cells from three out of six donors, suggesting there might be a link between enhanced KLK5 in keratinocytes and Th2 differentiation with individual variations. Finally, based on the evidence that KLK5 was enhanced in AD-lesional skin but not in non-lesional skin, a cell model with inducible KLK5-GFP overexpression was developed using the lentiviral vector containing TRE3GS promoter controlled by doxycycline. The KLK5-GFP over-expression was observed following doxycycline induction, and it could be reversed once Doxycycline treatment was withdrawal.

In conclusion, enhanced KLK5 in keratinocytes down-regulated TGF-β signaling and increased cytokine secretions in keratinocytes, which could influence Th2 differentiation in certain donors. An inducible KLK5 overexpression keratinocyte model was also developed, providing a new tool for investigating KLK5 activity and skin barrier function.

Impact statement

This study focused on the relation between KLK5 overexpression and immune response in AD. The transcriptome study in keratinocytes overexpressing KLK5 revealed differentially expressed pathways related to the down-regulated TGF-β signalling and *FLG2*. Potential interactions between keratinocytes with KLK5 overexpression and immune cells might lead to Th2 immune response.

These results could be beneficial for multiple fields. First, this is the first whole transcriptome screening keratinocytes overexpressing KLK5, which provided information regarding to the pathological role of KLK5 overexpression in the immune response in AD. The differentially expressed pathways found in the study and interactions with immune cells also emphasized the importance of KLK5 in the patho-mechanism of AD. The development of inducible KLK5 expression cell model could be a useful tool for studying therapeutic strategies for AD, which will benefit to the pharmaceutical research.

Second, AD is a chronic inflammatory skin disease, which affects patients' life qualities from various perspectives. This study addressed the importance of KLK5 overexpression in the pathological mechanism of AD and provided more insights regarding to the treatments for AD. AD patients might benefit from therapeutic interventions on control of KLK5 regulation in skin lesions.

Acknowledgements

First of all, my sincere gratitude goes to Professor Wei-Li Di, for supervising my MSc project six years ago and giving me this opportunity to pursue my PhD degree in her group. Thank her so much for all the time and effort she contributes to this project, for her patience and guidance while I was fresh to PhD, for pushing me forward while I felt it was beyond my ability, for building me who I am in science today.

Second, I am so grateful to have Professor Veronica Kinsler as my secondary supervisor, who is always super supportive whenever and whatever I needed and offered her valuable opinions to my work. Thank her for her encouragement and giving effective solutions regarding whatever problems I had.

Next, I would like to thank all the patients and their families for their contributions to this project. Thank all the colleagues whom I worked with, the group members in Professor Wei-Li Di's group, in Professor Veronica Kinsler's group, office neighbours in Professor Tessa Crompton's group, laboratory neighbours Dr Ying Hong and Dr Barbara Jenson. I would like to point out the great support from Dr Vignesh Jayarajan for his valuable suggestions and being a trustworthy friend all the time.

Next, I express my gratefulness to my family and friends for their endless support to me. Thank my friend Wenxin Fan for being there despite 8-hour jet lag. Thank my mother for supporting my choice even if she did not fully agree with it. My special appreciation goes to my late grandfather, who always wanted to see the moment when I finish my PhD. Thank him for raising me up and teaching me when I was a kid and did not know anything about his world.

Finally, I would like to thank myself for deciding to come to UK seven years ago despite of many disagreements. Thank life for enlightening me to learn from the patients and their families I encountered during my internship in the hospital. It has been a life-changing journey and thank myself for not giving up when those moments of failing hit. If I had the same chance again, I would make the same decision.

Table of Contents

List of figures

Chapter 1

Chapter 3

Chapter 4

Chapter 5

List of tables

Chapter 2

Chapter 3

Chapter 4

Abbreviations

KLK5	Kallikrein 5
GFP	Green fluorescence protein
AD	Atopic Dermatitis
SC	Stratum Corneum
SG	Stratum Granulosum
SS	Stratum Spinosum
SB	Stratum Basale
CE	Cornified envelope
NMFs	Natural moisturizing factors
TEWL	Transepidermal water loss
AMPs	Antimicrobial peptides
PRRs	Pattern recognition receptors
TLRs	Toll-like receptors
NLRs	NOD-like receptors
PAMPs	Pathogen-associated molecular patterns
ILs	Interleukins
TSLP	Thymic stromal lymphopoietin
TNF-α	Tumor necrosis factor-alpha
APCs	Antigen-presenting cells
Tregs	Regulatory T cells
NK cells	Nature Killer cells
LCs	Langerhans cells
MHC	Major histocompatibility complex
TCR	T cell receptor
TRMs	Resident memory T cells
GWAS	Genome-wide association studies
DSG	Desmoglein
DSC	Desmocollin
IgE	Immunoglobulin E
LEKTI	Lympho-epithelial Kazal-type-related inhibitor
NS	Netherton Syndrome
KLKs	Kallikrein-related peptidases
SCTE	Stratum corneum tryptic enzyme

ELA2	Elastase 2
PAR2	Proteinase-activated receptor 2
FLG	Filaggrin
FLG2	Filaggrin 2
DMEM	Dulbecco's Modified Eagle Medium
FBS	Fetal bovine serum
PBS	Phosphate buffered saline
Pen/Strap	Penicillin and streptomycin
MOI	Multiplicity of infection
P_{adj}	Adjusted p value
KC-UT	Untransduced keratinocytes
KC-GFP	Keratinocytes containing GFP transgene
KC-KLK5	Keratinocytes containing KLK5-GFP transgene
qPCR	Quantitative polymerase chain reaction
PBMCs	Peripheral blood mononuclear cells
RPMI	Roswell Park Memorial Institute
IRES	Internal ribosome entry site
LV-GFP	Lentivirus containing GFP transgene
LV-KLK5	Lentivirus containing KLK5-GFP transgene
SFFV	Spleen focus-forming virus
RNA-seq	RNA sequencing
DEGs	Differentially expressed genes
RT	Reverse transcription
RIN	RNA integrity nuber
PI	Propidium Iodid
RM-UT	Conditional media from untransduced keratinocyte culture
RM-GFP	Conditional media from keratinocytes containing GFP culture
RM-KLK5	Conditional media from keratinocytes containing KLK5-GFP culture
Tet-GFP	Tet-One-Puro vector containing GFP transgene
Tet-KLK5	Tet-One-Puro vector containing KLK5-GFP transgene
293T cells	HEK 293T cells
LV-Tet-GFP	Inducible lentivirus containing GFP transgene
LV-Tet-KLK5	Inducible lentivirus containing KLK5-GFP transgene

MFI	Mean fluorescence intensity
KC-Tet-UT	Keratinocytes without inducible lentivirus
KC-Tet-GFP	Keratinocytes containing inducible lentivirus with GFP transgene
KC-Tet-KLK5	Keratinocytes containing inducible lentivirus with KLK5-GFP transgene
NFATc2	Nuclear factor of activated T cells c2
SOCS1	Suppressor of cytokine signaling 1
IFNγ	Interferon gamma
IP3	3,4,5-inositol triphosphate

Chapter 1: Introduction

1.1 The skin

The skin is one of the largest organs in the human body. It plays a crucial role by acting as a protective barrier between internal homeostasis and external environment. Its multi-function also contributes to absorption, secretion, immune regulation, sensory perception etc (Hsu and Fuchs 2022). The skin is composed of three major compartments: epidermis, dermis and subcutaneous tissue (**Figure 1.1**). The epidermis is at the outermost layer of the skin, which serves as a remarkable shield to prevent excessive water loss and guard against harmful microorganisms. The dermis is underneath the epidermis, which is a connective tissue layer that contributes to the strength, elasticity, and sensation of the skin. The subcutaneous layer is the deepest layer of the skin, which consists of adipose (fat) cells, blood vessels and nerves. The structure of the skin is complex, consisting of specialized cells that work together to maintain its integrity and functionality, such as keratinocytes in the epidermis, fibroblasts in the dermis and adipose cells in the subcutaneous tissue. Each cell type plays a crucial role. Keratinocytes are essential for maintaining the integrity and functionality of the skin, of which the proliferation and differentiation function allow the self-renewal of the epidermis. They also build a defensive layer to prevent skin inflammation. Fibroblasts form the collagen matrix to support dermis layer and also regulate dermal immune response. Adipocytes primarily compose adipose tissue and provide energy to the skin. The coordination among different cells contribute to the maintenance of the functional skin.

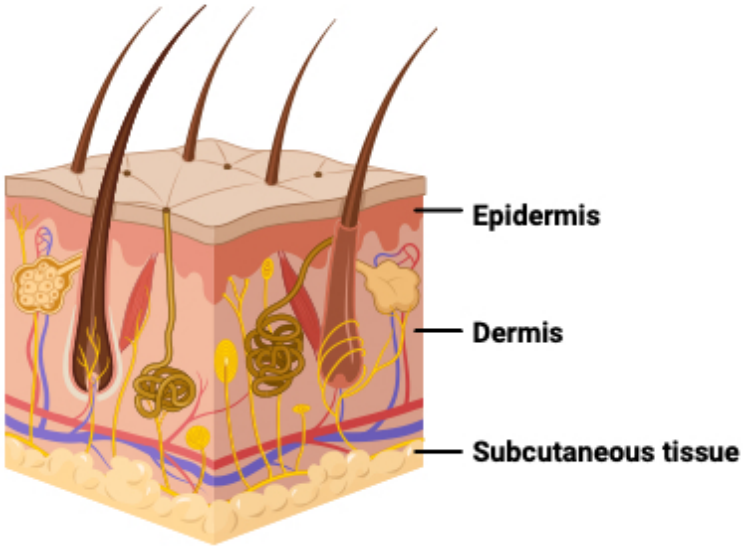

Figure 1.1 Three skin layers

There are three layers in skin: epidermis, dermis and subcutaneous tissue from the outermost to the innermost. This image was made by BioRender.

1.1.1 The epidermis

The epidermis plays a critical role in protecting the body from a wide range of external threats. It acts as a formidable defense system, shielding the delicate tissues and organs beneath it from physical, chemical and microbial damage. The structure of the epidermis is designed to provide strength, rigidity and resilience. It is composed of multiple layers of cells, known as keratinocytes. Keratinocytes are highly specialized cells that produce a tough, fibrous protein known as keratin. Keratin is essential for the epidermis to fulfil its protective role effectively.

The epidermis is organized into four layers, which are Stratum Corneum (SC), Stratum Granulosum (SG), Stratum Spinosum (SS) and Stratum Basale (SB) (**Figure 1.2**) (ECKERT 1989, Walt 1989, Matsui and Amagai 2015). Keratinocyte stem cells are located in SB, which actively proliferate to SS (ECKERT 1989, Walt 1989, Matsui and Amagai 2015). While keratinocytes proliferate from SB to

upper layers, they start to differentiate until they reach to SC (ECKERT 1989, Walt 1989, Matsui and Amagai 2015). The whole process normally takes 28 days (ECKERT 1989, Walt 1989, Matsui and Amagai 2015). This process is defined as desquamation, which eliminates dead skin cells, debris and potentially harmful microorganisms, maintaining the integrity of the epidermal barrier.

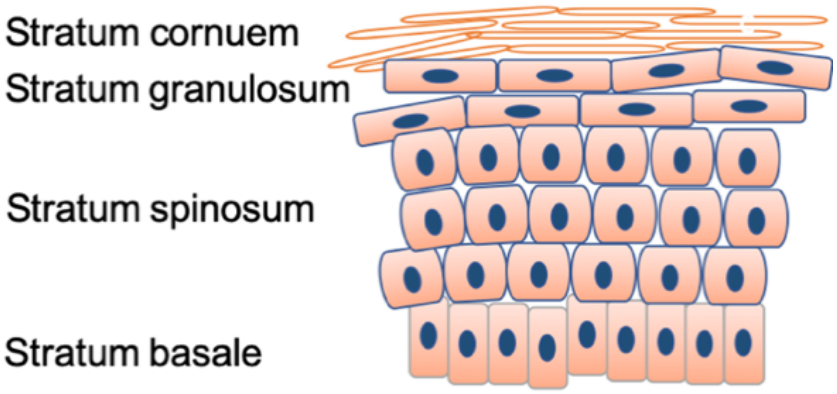

Figure 1.2 Multiple layers in epidermis

The epidermis consists of four layers from inner skin to the outermost skin: stratum basale, stratum spinosum, stratum granulosum and stratum corneum.

Stratum basale (SB), also known as the innermost layer, is a dynamic and vital component responsible for the continuous renewal of the skin. It consists mainly of basal cells, which form a single layer. These highly proliferative cells constantly undergo mitosis as they move upward towards the skin's surface until they are eventually shed from the outermost layer called the stratum corneum (SC) (ECKERT 1989, Walt 1989, Matsui and Amagai 2015). The regenerative capabilities of the basal layer are evident in various biological processes. During wound healing, basal cells rapidly proliferate and migrate to the site of the wound, initiating the formation of new tissue. These cells actively participate in the re-epithelialization process, ensuring the closure of the wound and the restoration of skin integrity. Moreover, the basal layer's ability to renew cells helps maintain

a balance between cell proliferation and differentiation. This delicate equilibrium ensures the continuous renewal of the epidermis while preserving its overall structure and functionality. Achieving this balance involves intricate signalling pathways and interactions between the basal cells and their microenvironment (Losquadro 2017).

The Stratum Spinosum (SS), also known as the spinous layer, is a crucial part of the epidermis. The stratum spinosum consists of differentiated keratinocytes, which are polygonal-shaped cells. These keratinocytes are linked together by desmosomes, giving the layer its unique spiky appearance. The desmosomes establish robust connections that offer structural support and aid in preserving the skin's integrity.

The stratum granulosum is positioned between the stratum spinosum and the stratum corneum, forming the middle layer of the epidermis. It is most prominently observed in areas of the skin that experience frequent friction and pressure, such as the palms of the hands and the soles of the feet. Under microscopic examination, the stratum granulosum shows as a thin layer composed of flattened polygonal cells with dark-staining granules (Yousef, Alhajj et al. 2023). One of the primary roles of the stratum granulosum is to facilitate cellular terminal differentiation, where keratinocytes undergo the conversion into specialized cells, corneocytes. This process involves distinct alterations in cellular structure and the accumulation of granules within the cytoplasm. These granules, formed by filaggrin, play a vital role in preserving skin hydration by binding to water molecules. As keratinocytes transition into corneocytes, the filaggrin granules congregate, contributing to the creation of the skin's natural moisturizing factors.

Besides, the stratum granulosum also participates in the production and release of lipid-rich substances, including ceramides. These lipids can involve in the formation of skin barrier in SC. Moreover, the stratum granulosum also regulates and maintains the acidic pH in the skin, which is vital for the optimal enzymatic activity and the prevention of microbial colonization (Yousef, Alhajj et al. 2023).

As keratinocytes migrate to the outermost of the skin, they form the SC surrounded by cornified envelope merged in lipid lamellae (cornified layer) (Elias 1983). This is also known as the skin barrier, which serves as the defensive frontline. This will be further discussed in the next section.

1.1.2 The skin barrier

The epidermal skin barrier refers to the cornified layer of epidermis. Serving as the first defensive line, skin barrier is a complex structure that is responsible for protecting the body from environmental stressors, regulating water loss and maintaining overall skin health. It is primarily composed of corneocytes, which undergo terminal differentiation in the SC and lose their nucleus and other cellular organelles, becoming densely packed with keratin filaments. This process leads to the formation of a protective layer of corneocytes that shields the underlying skin layers (**Figure 1.3**). A monolayer of insoluble structural protein transformed from plasma membrane and covalently linked including filaggrin, loricrin, involucrin etc. encompass each corneocyte, shaping a ‘cornified envelope’ (CE). Lipids secreted by lamellar granules bind to each CE covalently, forming the *‘brick’* in the system. The extracellular space is filled with excessive lipids orderly, naming lamellae membrane, the *‘mortar’* in the system. Corneodesmosomes function like *‘iron rods’* that link CE intercellularly. These structures provide

mechanical strength and cohesion to the skin barrier. Corneodesmosomes are composed of various proteins, including desmoglein, desmocollin, and corneodesmosin, which facilitate the adhesion between adjacent corneocytes. With the intact *'brick, mortar and iron rods'* system, skin barrier provides protection to human body (Elias 1983, Cork, Robinson et al. 2006, Cork, Danby et al. 2009, Yang, Seok et al. 2020).

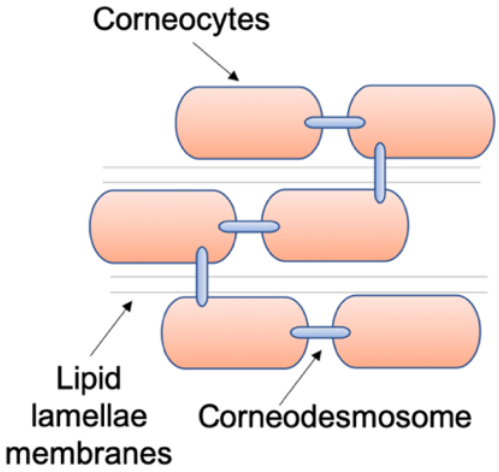

Figure 1.3 The "brick, mortar and iron rod" system in the skin barrier

Corneocytes bond by insoluble protein and a layer of lipids form cornified envelopes, representing "bricks". The remaining lipids form lipid lamellae membranes in the extracellular space, which is the "mortar". Each cornified envelope is connected by corneodesmosomes, the "iron rods" in the system.

Another important component in the skin barrier is Filaggrin, which is encoded by *FLG* gene. It is a monomer subunit that was broken down from Profilaggrin. Filaggrin participates in the final stages of keratinocyte differentiation by bundling with Keratin 1 and Keratin 10 and other intermediate filaments, which facilitates the collapse of keratinocyte to transform to flattened corneocytes (Manabe, Sanchez et al. 1991, Candi, Schmidt et al. 2005, Kim and Lim 2021). In addition, filaggrin could be degraded into natural moisturizing factors (NMFs) by various

proteases, which help maintain the skin pH and protect from ultraviolet radiation (Barresi, Stremnitzer et al. 2011, Joo, Han et al. 2012, Kim and Lim 2021).

The stratum corneum's health and function are essential for maintaining overall skin health and preventing various skin conditions. Recent studies have showed the intricate mechanism in SC also help prevent UV-induced damage (Biniek, Levi et al. 2012). SC also plays a vital role in regulating water loss from the body and preventing excessive dehydration. The lipids present in the stratum corneum act as a waterproof barrier to reduce the transepidermal water loss (TEWL) (Cork, Robinson et al. 2006, Cork, Danby et al. 2009). Besides, the pH balance in the skin is also regulated by SC. Maintaining acidic pH from 4 to 6 is essential for the optimal functioning of enzymes involved in barrier maintenance and antimicrobial defense. Disruptions in the skin's pH balance can lead to altered barrier function and susceptibility to infections and skin disorders (Proksch 2018). As part of the frontline defensive mechanism, SC also participates in the skin immunity by producing antimicrobial peptides (AMPs), such as defensins and cathelicidins, which have direct antimicrobial activity against a wide range of pathogens (Pasupuleti, Schmidtchen et al. 2012). The immunomodulation in SC is conducted by multiple ways. SC serves as a first physical defensive line to prevent external allergens causing immune response in skin. Besides, the keratinocytes in this layer could secrete inflammation-related molecules, such as IL-8, IL-10 and TSLP, which could interact with immune cells like dendritic cells and T cells (Zhu, Underwood et al. 2017, Nguyen and Soulika 2019). For instance, epidermal TNF-α and TSLP altered CD40, which activates LC to present antigens to $CD8^+$ T cell (Polak, Ung et al. 2017). Disruptions in the skin barrier can lead to dysregulated immune responses, contributing to the development of chronic

inflammatory skin conditions, such as atopic dermatitis (Langan, Irvine et al. 2020).

1.1.3 The epidermal immunity

Epidermal immunity remains an important function in the skin. As the frontline of defensive system, epidermis contribute enormously to the immune response, particularly the epidermal immune cells. Keratinocytes, as 90% of all epidermal cells, are not only contribute to the establishment of a structurally robust and functionally proficient epidermal structure, but also regulating skin immunity via pro-inflammatory/inflammatory molecules or pathways. Keratinocytes contribute to the antimicrobial defence of the skin by expressing various antimicrobial peptides (AMPs). Antimicrobial peptides (AMPs), such as defensins and cathelicidins, display a wide-ranging capacity to combat bacteria, fungi and viruses, serving as an innate immune defense mechanism (Piipponen, Li et al. 2020). Keratinocytes are also capable of recognizing and responding to microbial pathogens through the expression of pattern recognition receptors (PRRs). These receptors include Toll-like receptors (TLRs) and NOD-like receptors (NLRs), which detect conserved microbial components referring to pathogen-associated molecular patterns (PAMPs) (Piipponen, Li et al. 2020, Das, Mounika et al. 2022). Upon sensing PAMPs, keratinocytes activate intracellular signalling pathways, resulting in the production of pro-inflammatory cytokines and chemokines. This immune response initiates the recruitment and activation of immune cells, such as neutrophils and macrophages, to clear the pathogens (Najor, Fitz et al. 2017, Piipponen, Li et al. 2020, Das, Mounika et al. 2022).

Keratinocytes can also produce various signalling molecules and cytokines that function in the immunomodulation (Grone 2002, Piipponen, Li et al. 2020, Das, Mounika et al. 2022). Interleukins (ILs) are a major group of cytokines produced by keratinocytes. For example, IL-1α and IL-1β are pro-inflammatory cytokines that mediate immune responses by inducing the production of other cytokines, activating immune cells, and promoting tissue remodeling (Murphy, Robert et al. 2000). Keratinocytes could secret IL-6 and IL-8, which play roles in inflammation and immune cell recruitment (Jonathan N.W.N. Barker 1991, Dienz and Rincon 2009, Parrado, Canellada et al. 2012, Zhu, Underwood et al. 2017), while IL-10 exhibits anti-inflammatory properties and helps maintain immune homeostasis (Rene de Waal Malefyt 1991). Thymic stromal lymphopoietin (TSLP) is also released by the keratinocytes and involved in several signalling pathways including irritation and itching in the diseases (Tatsuno, Fujiyama et al. 2015). Tumor necrosis factor-alpha (TNF-α) is another key cytokine produced by keratinocytes, involved in inflammation, cell survival and immune cell activation (Bradley 2008). TNF-α plays a crucial role in psoriasis and other chronic inflammatory skin conditions (Kristensen, Chu et al. 1993, Ettehadi, Greaves et al. 1994). Other molecules, such as chemokines CCL2, CCL3, CCL5, CXCL1 and CXCL8, also function in the immune response that promote the recruitment and activation of immune cells, including neutrophils, monocytes/macrophages and T cells. These chemokines play critical roles in immune surveillance, inflammation, and wound healing process (Grone 2002, Kany, Vollrath et al. 2019, Piipponen, Li et al. 2020).

Keratinocytes actively communicate and collaborate with various immune cells within the skin microenvironment. These interactions play a crucial role in shaping

the immune response and maintaining immune tolerance. Keratinocytes themselves could serve as antigen-presenting cells (APCs) and can present microbial antigens to T cells, initiating adaptive immune responses (Piipponen, Li et al. 2020, Das, Mounika et al. 2022). It was found the T cells stimulated with activated keratinocytes could express a distinct cytokine profile with the production of IL-2 and IL-4 but not IFN-γ (Goodman, Nestle et al. 1994). Keratinocytes can also interact with Dendritic cells (DCs), of which the crosstalk in between balances the immune activation and tolerance. The activation and differentiation of other cells, like regulatory T cells (Tregs), can be induced by keratinocytes to promote an immunosuppressive microenvironment that prevents excessive immune responses and maintains skin homeostasis (Soumelis, Reche et al. 2002, Piipponen, Li et al. 2020, Das, Mounika et al. 2022).

Other factors could also influence skin inflammation, including skin immune cells. The major immune cells involved in this biological process are Langerhans cells, T cells, Nature Killer (NK) cells and Mast cells. As the major dendritic cells in epidermis, Langerhans cells (LCs) are distinctive antigen-presenting cells found within the epidermis and form a crucial part of the skin's immune system. They are characterized by their distinctive morphology, which includes long dendritic processes that extend between neighbouring keratinocytes. LCs express several unique surface markers, such as CD1a and Langerin (CD207), which distinguish them from other dendritic cell subsets (Liu, Zhu et al. 2021). They possess an impressive capacity to capture antigens in the skin environment and initiate immune responses (Polak, Newell et al. 2012). When encountering antigens, LCs employ receptor-mediated endocytosis to internalize them and process them into peptide fragments. These peptides are then presented on their cell surface in

association with major histocompatibility complex (MHC) molecules (Collin and Milne 2016). When LCs migrate from the epidermis to the draining lymph nodes, they encounter naïve T cells. The antigen-MHC complex on the surface of LCs interacts with specific T cell receptors, leading to T cell activation and the initiation of adaptive immune responses. Moreover, LCs have been shown to play a role in the regulation of immune tolerance and the development of allergic reactions (Polak, Newell et al. 2012). Studies have demonstrated that LCs can induce tolerance to harmless antigens by promoting the generation of regulatory T cells, which dampen immune responses and prevent excessive inflammation (Polak, Ung et al. 2017). These provide insights into the plasticity and functional diversity of LCs, highlighting their involvement in both protective and pathological immune responses (Clayton, Vallejo et al. 2017).

The skin-resident T cells play a crucial role in the immune surveillance and defense against pathogens, tumors, and inflammatory skin diseases. Dendritic epidermal T cells are a unique subset of T cells that reside exclusively in the epidermis. They express a semi-invariant γδ T cell receptor (TCR) and pattern recognition receptors that enable them to recognize pathogen-associated molecular patterns present on invading microorganisms. They also migrate to the injured area upon the secretion of cytokines/chemokines and promptly initiate immune responses and modulate the inflammation in the skin (Clark 2010). Epidermal T helper cells ($CD4^+$ T cells) and cytotoxic T cells ($CD8^+$ T cells) are found in the epidermis as well as the underlying dermis. $CD4^+$ T cells exert their influence through the secretion of cytokines, which serve as key regulators of immune cell activation and differentiation. $CD4^+$ T cells are specialized to recognize antigens presented by antigen-presenting cells, such as Langerhans

cells in epidermis. Once activated, $CD4^+$ T cells provide the necessary help to other immune cells by releasing cytokines that shape the immune response. Unlike $CD4^+$ T cells, $CD8^+$ T cells primarily function in direct cell killing, which are also known as cytotoxic T cells. $CD8^+$ T cells identify antigens presented in the context of MHC class I molecules. This recognition initiates the discharge of cytotoxic agents, including perforin and granzymes, leading to the cell death in the target cells (Kortekaas Krohn, Aerts et al. 2022). Other skin-resident T cells like regulatory T cells and resident memory T cells (TRMs) also function in epidermal immunity by exhibiting immunosuppressive properties and maintaining long-term immune memory (Schenkel, Fraser et al. 2014, Ali, Zirak et al. 2017).

Apart from LC and T cells, Natural Killer cells, which are traditionally associated with innate immunity, are also found in the epidermis. NK cells possess cytotoxic activity and are involved in the rapid elimination of infected or transformed cells. Recent research has highlighted the ability of epidermal NK cells to mediate immunosurveillance in the skin, providing protection against viral infections and tumors. Moreover, they interact with other immune cells, such as LCs and T cells, to orchestrate immune responses and maintain skin homeostasis (Sun, Kim et al. 2021). Another immune cells in skin, Mast cells, are presented both in dermis and epidermis. They play a critical role in allergic reactions and inflammation by releasing various mediators upon activation, including histamine and cytokines, which further influence both innate and adaptive immune responses (Hershko 2017).

The disrupted skin immunity may lead to various skin disorders, including Atopic Dermatitis (AD) and psoriasis etc. Understanding the role of skin barrier in skin

immunity is essential for improving the management and treatment of disease conditions, ultimately enhancing skin health and quality of life for affected individuals.

1.2 Atopic Dermatitis

Due to the critical role in maintaining skin health and integrity, when the skin barrier is compromised or dysfunctional, it can lead to various skin disorders. One of them is Atopic Dermatitis. Atopic Dermatitis (AD, eczema) is a chronic inflammatory skin disease with eczematous lesions, xerosis (dryness) and pruritus (itch). AD affects people of all ages, but it is more prevalent in infants and children which affects up to 20% of children in the UK (Deckers, McLean et al. 2012, Laughter, Maymone et al. 2021). There is variation of prevalence between different age groups and countries. The prevalence has increased dramatically in recent decades (Deckers, McLean et al. 2012). Apart from typical clinical phenotypes described above, patients with AD also often have moderately elevated IgE levels. The manifestations of AD usually develop during childhood and 1%-3% of them persist into adulthood (Wallach and Taieb 2014). Daily skin care is applied to children with AD, including emollients and reducing exposure to exogenous allergens where appropriate. Topical corticosteroids or anti-inflammatory immunomodulators are also prescribed to patients (Cork, Danby et al. 2009). AD can have a significant impact on the quality of life for individuals and their families.

1.2.1 Clinical phenotypes

AD is a complex skin disorder characterized by a diverse clinical phenotype. Its presentation can vary widely in terms of age of onset, distribution, morphology,

associated symptoms and disease course. It typically begins in infancy or childhood. The hallmark of AD is intense itching, which leads to scratching, further exacerbating the condition. The primary lesions of AD are characterized by erythema (redness), xerosis and pruritus. These lesions can be localized or widespread, affecting various areas of the body, including the face, neck, flexural areas (inner elbows and knees), hands, and feet (Langan, Irvine et al. 2020). Based on the onset of the disease, AD can be classified into acute and chronic phases. The acute phase of AD refers to the period of intense inflammation and symptom exacerbation experienced by individuals with this condition. It is characterized by a sudden onset or worsening of AD symptoms, leading to significant discomfort and distress for the affected individuals. During the acute phase of AD, patients often experience a sudden flare-up of symptoms, which may include erythema and edema, vesicles and papules, intense itching and excoriations. The affected skin becomes red, inflamed, and swollen due to increased blood flow and fluid accumulation in the tissues. The skin temperature may increase at this stage. As a result of the inflammatory response, small fluid-filled blisters (vesicles) and raised bumps (papules) may develop on the skin. Pruritus is one of the hallmark symptoms of AD and is particularly severe during the acute phase. Itching can be relentless and unbearable, leading to constant scratching, which further exacerbates the inflammation. Continuous scratching of the itchy skin can cause excoriations, resulting in open sores or scratch marks. These can increase the risk of secondary infections (Stander 2021).

The chronic phase of AD refers to the persistent and long-term nature of the condition beyond the acute flare-ups. It is characterized by a continuous or recurrent cycle of symptoms and skin inflammation, often lasting for months or

years. Typical symptoms of the chronic AD include persistent dry thickened skin, chronic skin infections, continuous itching as well as hyperpigmentation and hypopigmentation. Due to the impaired skin barrier, the skin may appear scaly, thickened, and leathery in the lesional area. The compromised skin barrier in AD can make individuals more susceptible to bacterial, viral, or fungal infections. Recurrent or persistent infections, such as impetigo or herpes simplex virus, may occur during the chronic phase. The itchiness can vary in intensity but is generally present even during periods of relatively low disease activity. Itching can significantly impact the quality of life, leading to sleep disturbances, irritability, and psychological distress. Apart from these, the prolonged inflammation in the skin during the chronic phase can lead to changes in pigmentation, resulting in areas of darkened (hyperpigmentation) or lightened (hypopigmentation) skin (Stander 2021).

1.2.2 Etiology of AD

AD is a multifactorial disease with a complex etiology involving a combination of genetic and environmental triggers. These factors can interact with each other and contribute to the on-set of AD. Genetic factors that cause AD referred to gene mutations and polymorphisms. Recent genome-wide association studies (GWAS) have identified several susceptibility loci associated with AD. Variations in genes involved in skin barrier function, immune response regulation and epidermal differentiation have been linked to an increased risk of AD (Loset, Brown et al. 2019, Nedoszytko, Reszka et al. 2020). AD displays genetic linkage to chromosome 1q21, which contains multiple genes relating to epidermal barrier integrity and function (Loset, Brown et al. 2019). Previous studies revealed Filaggrin (*FLG*) gene null mutations are associated with AD (Palmer, Irvine et al.

2006). The most common gene variants are loss-of-function mutations in *FLG* are R510X and 2282del4, which have been found highly associated with presence of asthma and atopic dermatitis, carried by 9% of people of European origin (Palmer, Irvine et al. 2006). These gene variants reduce Filaggrin protein, which can be further cleaved into natural moisturizing factors and adversely affect the pH balance of the skin barrier.

Apart from *FLG* gene null mutation, other genetic factors related to skin barrier dysfunction are also involved in pathogenesis of AD. Genes with reduced functions in corneodesmosomes like Desmoglein (*DSG*) and Desmocollin (*DSC*) as well as tight junction genes (*Claudins* and *Occludin*s) are found to participate in the development of AD (Martin, Estravis et al. 2020, Nedoszytko, Reszka et al. 2020). The epidermal protease genes and their inhibitors, such as *Kallikreins, Cathepsins and Caspase 14 as well as SPINK5 and Cystatin A,* are also discovered in the GWAS studies (Walley, Chavanas et al. 2001, Martin, Estravis et al. 2020, Nedoszytko, Reszka et al. 2020). The gene that encodes the upstream transcriptional factor of *FLG* regulation, *OVOL1*, was found significantly associated with AD from a meta-analysis of GWAS (Tsuji, Hashimoto-Hachiya et al. 2017).

Except for genes involved in the skin barrier dysfunction, those of the immune system also play a role in the onset of AD. Genes for the innate immune system like Toll-like receptors (*TLR2, TLR4 and TLR6*) and nucleotide-binding oligomerization domain (NOD)-like receptor (*NOD1*) were associated with AD (Loset, Brown et al. 2019, Martin, Estravis et al. 2020, Nedoszytko, Reszka et al. 2020). As for the adaptive immune system, many studies have focused on genes

related to proinflammatory cytokines, such as *IL-4*, *IL-13* and Thymic Stromal Lymphopoietin (*TSLP*). Polymorphisms in gene *IL-13*, which encodes an inflammatory cytokine that promotes skin inflammation, have been demonstrated to associate with the development of AD (Furue, Chiba et al. 2017). Gene polymorphisms affecting IL-4Rα, the common receptor subunit shared by IL-4 and IL-13, also correlate with the onset of AD (Furue, Chiba et al. 2017). Associations between *TSLP* polymorphisms and AD have also been reported (Gao, Rafaels et al. 2010). TSLP, the pro-Th2 cytokine, drives Th2 cell differentiation and promotes Th2-mediated cytokine secretion (Gao, Rafaels et al. 2010). These findings illustrated the correlation between Th2 immune response and AD. Other genes regulating DNA methylation (*KIF3A*) were also showed in the GWAS study (Loset, Brown et al. 2019, Martin, Estravis et al. 2020, Nedoszytko, Reszka et al. 2020).

Environmental factors play a significant role in the development and exacerbation of AD. These factors can influence the skin barrier function, immune response and overall disease severity. That includes allergens, irritants, air pollutions and climate etc. Allergens, such as house dust mites, pollen, pet dander, mold spores and certain foods, can induce an allergic response in susceptible individuals. *Staphylococcus aureus (S. aureus)* was previously reported to be associated with the severity of AD (Kim and Kim 2019). The numerous proteases produced by *S. aureus* not only play a role in the immunological response by releasing toxins, but also impair the skin barrier directly (Kim and Kim 2019). The exogenous proteases like serine and cysteine proteases derived from dust mites could trigger an immune response in AD and allergens connected to dust mites could result in allergic sensitization and disease exacerbation (Mette Deleuran 1998).

Other allergens like pollens can also exacerbate AD. Patients exposed to grass pollens developed significantly increased CCL17, CCL22 and IL-4 in the previous publications (Ridolo, Martignago et al. 2018).

Other environmental factors like irritants also trigger AD. This includes harsh soaps, detergents, fragrances, chemicals and certain fabrics. Soaps, detergents and other chemicals could increase skin pH, which might potentially lead to AD (Tamagawa-Mineoka and Katoh 2020). Previous studies revealed that alkaline pH could result in the hyperactivity of proteases, leading to increased cleavage of corneodesmosomes and impaired skin barrier leading to AD (Kishibe 2019). Prolonged or repeated exposure to these substances can disrupt the skin's natural protective mechanisms, leading to dryness, redness, and itching. Using gentle, fragrance-free products and minimizing contact with irritants is essential for managing AD.

Air pollution, particularly rereferring to matter, vehicle emissions and industrial pollutants, has been recognized as a contributing factor to the development and aggravation of AD. Multiple studies have associated exposure to air pollutants with an increased risk of AD and the worsening of its symptoms. For instance, previous study revealed that mice keratinocytes that persistently expressed Aryl hydrocarbon receptor pathway had skin manifestations similar to AD (Tsuji, Hashimoto-Hachiya et al. 2017, Fadadu, Abuabara et al. 2023). Besides, air pollutions like nitrogen oxides and O_3 can trigger the production of reactive oxygen species. Scientists have observed a notable rise in carbonyl groups, indicative of direct oxidative harm to proteins, within AD lesions (Y.NIWA 2003). These findings suggest that pollutants, such as those present in vehicle

emissions, can directly damage the skin barrier and promote the development or worsening of AD.

Climate and weather conditions can have a significant impact on AD. Cold and dry environments can cause skin dryness, leading to increased itchiness and flares. Similarly, hot and humid conditions can trigger sweating and worsen the symptoms. Extreme temperatures, low humidity, and changes in seasons can disrupt the skin barrier function and exacerbate AD (Tamagawa-Mineoka and Katoh 2020).

The etiology of AD involves intricate interactions between genetic, immunological and environmental factors. The importance of gene-environment interactions has highlighted in AD susceptibility, emphasizing the need for personalized medicine approaches. This includes not only the treatment targeting at AD biological pathogenesis, but also the guidance in daily life like skin care and living habits.

1.2.3 Pathogenesis of AD

Although the pathogenesis of AD is not fully understood, two major components have been identified: skin barrier dysfunction and abnormal immune response. Previously, scientists believed that AD was primarily driven by a hyperactive immunological response, leading to an "inside to outside" process (**Figure 1.4**). In this model, patients with AD would experience infiltration of Th2 cells into the skin barrier, resulting in immune response dysregulation and elevated levels of certain inflammatory immune cytokines, particularly Th2-mediated cytokines. Consequently, skin barrier dysfunction was considered a secondary cause of AD (Leung 2000).

In the context of disrupted skin barrier function, irritants and allergens present in the environment, including S. aureus, can penetrate through multiple layers of the skin. Proteases produced by S. aureus have been shown to degrade AMPs, which play a crucial role in defending against microbial invasion from the environment. Additionally, these proteases can also degrade DSG1, which forms the adhesion proteins known as corneodesmosomes. The degradation of DSG1 impairs the structure of the skin barrier, contributing to skin barrier dysfunction. Moreover, colonization of S. aureus can down-regulate epidermal free fatty acids, which are essential components of lipid lamellae in the skin barrier. The reduction of these lipid molecules can damage the skin barrier and eventually lead to epidermal barrier dysfunction (Cork, Danby et al. 2009, Langan, Irvine et al. 2020).

However, it has been observed that approximately 20% of patients with AD do not exhibit enhanced activity of immunoglobulin E (IgE) and do not display the typical atopic skin phenotype, suggesting that immune response dysregulation may not be the primary cause of AD (Bieber 2008). As a result, the "outside to inside" theory has gained attention in recent years (**Figure 1.4**). According to this theory, skin barrier dysfunction caused by genetic factors is considered the primary cause of AD. The invasion of allergens from the environment can trigger an abnormal immune response, leading to the release of inflammatory cytokines and subsequent skin inflammation.

This outside to inside theory proposes that a compromised skin barrier due to genetic factors allows allergens and irritants to penetrate into the deeper layers of the skin, triggering an immune response and inflammatory cascade. These

allergens can induce an adaptive immune response and activate various immune cells, such as dendritic cells, mast cells, and T cells, leading to the release of pro-inflammatory cytokines, including interleukin IL-4, IL-13 and TNF-α. This cascade of events eventually results in the characteristic features of AD, including erythema, pruritus, and eczematous lesions (Bieber 2008, Yang, Seok et al. 2020).

In this theory, the skin barrier abnormalities tend to be predominant cause of AD. One of the triggers for aberrant skin barrier function is the excessive serine protease activity as they over-degrade the adhesion proteins in SC, leading to over-desquamation. The serine protease activities were enhanced in AD lesions (Voegeli, Rawlings et al. 2009). This could be caused by the imbalance between serine protease and its inhibitor. Lympho-epithelial Kazal-type-related inhibitor (LEKTI) protein is the major serine protease inhibitor produced by keratinocytes (Hovnanian 2013). It was reported in the Netherton Syndrome (NS) that the loss-of function mutations of *SPINK5*, which encodes LEKTI, was found in the patients (Hovnanian 2013). As NS develop similar clinical manifestations with AD in a more severe manner, the LEKTI has been also investigated in AD. The E420K LEKTI variants are found to prevent the formation of LEKTI fragment D6D9 by increasing the furin cleavage rate at the LEKTI linker region D6-D7 (Fortugno, Furio et al. 2012, Nomura, Suganuma et al. 2020). This fragment shows the strongest inhibition against DSG1 degradation by KLK5 (Nomura, Suganuma et al. 2020). The decreased LEKTI activity will boost serine protease activities in the skin, particularly Kallikrein-related peptidases (KLKs), which can further cause overdegradation of corneodesmosomes and lead to skin barrier dysfunction (Nomura, Suganuma et al. 2020). The impaired skin barrier will trigger immune

response due to excessive penetration of allergens and irritants etc. and contribute to the development of AD. This highlighted the importance of serine protease activity in maintaining normal skin barrier functions.

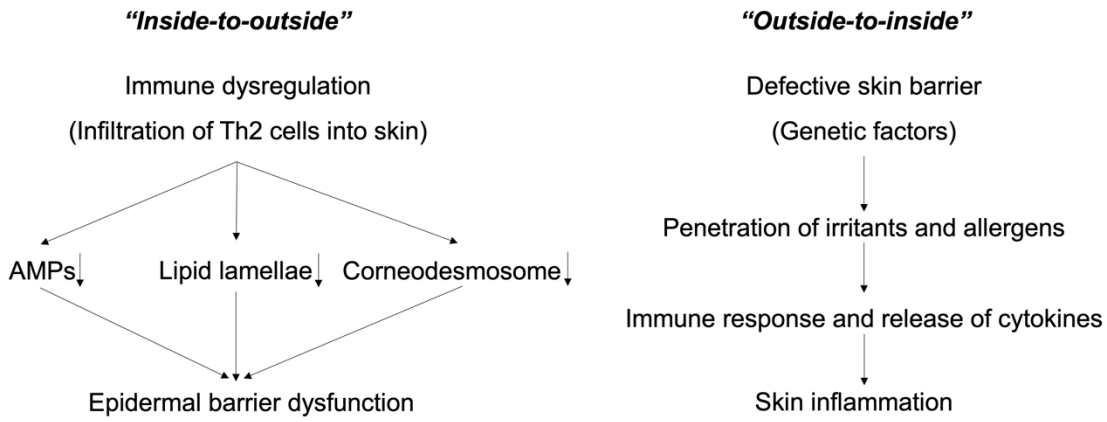

Figure 1.4 Two theories for the pathogenesis of AD

One of the pathological theories of AD believed the immune dysfunction used to be the primary cause of AD, which would trigger the epidermal barrier dysfunction through impaired epidermis. Another theory focused on defective skin barrier as primary cause of AD, which would let external irritants to penetrate through the skin and lead to immune response in vivo.

1.3 Kallikrein family and Atopic Dermatitis

As stated above, epidermal serine proteases play critical roles in various physiological and pathological processes in skin barrier, in particular Kallikrein family (KLKs). Studies revealed trypsin-like KLKs and their inhibitors were found to accelerate or reduce the rate of skin desquamation (Bissett, McBride et al. 1987), (Egelrud, Hofer et al. 1988, Lundstrom and Egelrud 1990, Egelrud and Lundstrom 1991).

1.3.1 Kallikreins

KLKs are the major serine protease in skin. They encompass a group of serine proteases that share structural and functional similarities. These proteases are widely distributed throughout different tissues and body fluids and are the largest

family of trypsin-like or chymotrypsin-like proteases expressed in epidermis. There are 15 family members (KLK1-15) (Kalinska, Meyer-Hoffert et al. 2016). They all map to same chromosomal region (19q13.4) in human genome (Emami and Diamandis 2007) and share similar structural feature like exon and intron distributions etc (Borgono and Diamandis 2004). The kallikrein activation cascade is a proteolytic event involving a series of enzymatic activations, of which the Kallikrein 5 (KLK5) is the main activator of the whole process. KLK5 is not only capable of self-activation, but also activating other KLKs, such as Kallikrein 7 (KLK7) and Kallikrein 14 (KLK14). The activated KLK14 could activate newly formed pro-KLK5, forming an activation loop. Other KLKs, such as pro-KLK1, pro-KLK6 and pro-KLK8 can also be activated by active KLK5 (**Figure 1.5**) (Brattsand, Stefansson et al. 2005, Kishibe 2019, Nauroy and Nystrom 2020). Eight KLKs are mainly expressed in skin at protein level, of which are KLK5, 6, 7, 8, 10, 11, 13 and 14 (Lundwall and Brattsand 2008). Among them, KLK5, 7, 8 and 14 display active form in skin (Komatsu, Saijoh et al. 2005).

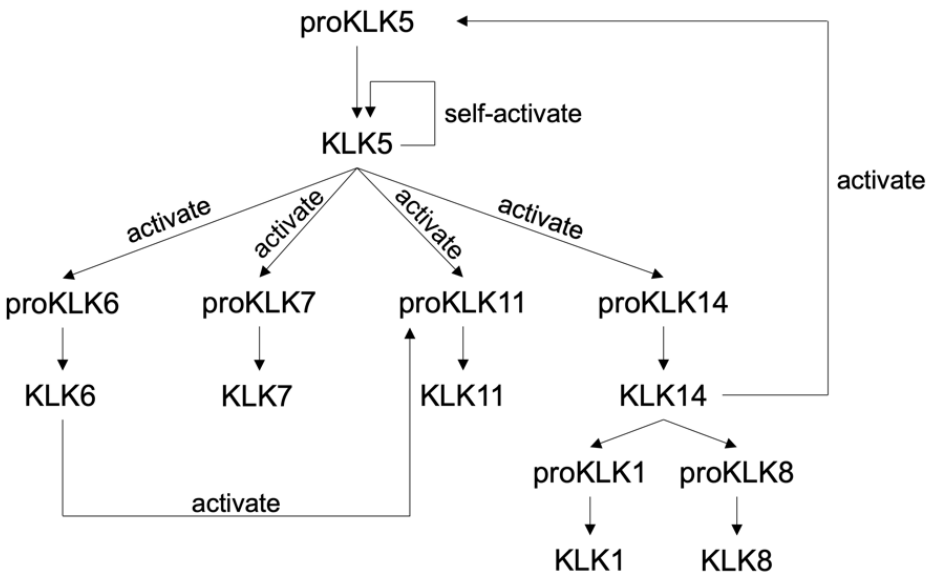

Figure 1.5 KLKs activation cascade

KLK5 is capable of activating proKLK6, proKLK7, proKLK11 and proKLK14 and self-activated. The KLK14 can activate proKLK5 as a feedback loop.

As one of the major KLKs that play an important role in skin, KLK5 is first discovered as stratum corneum tryptic enzyme (SCTE) that performs majority trypsin-like proteolytic activity in the epidermis (Ekholm, Brattsand et al. 2000). The *KLK5* gene is located on chromosome 19q13.4, which spans approximately 9.5 kilobases and consists of 6 exons and 5 introns. 5 among 6 exons are coding exons (Brattsand and Egelrud 1999, Yousef and Diamandis 1999). The encoding KLK5 protein is a serine protease that functions pivotally in skin physiology. The synthesis of KLK5 begins as a pre-pro-KLK5 polypeptide, initially translated in the endoplasmic reticulum. This pre-pro-KLK5 is comprised of 293 amino acids and can be divided into distinct regions. The N-terminal region encompasses a signal peptide consisting of 29 residues. This signal peptide functions as a targeting signal, guiding the newly synthesized KLK5 to the secretory pathway for extracellular secretion. Following the signal peptide, there is a propeptide region comprised of 37 residues. This propeptide region is essential for preserving the inactivity of KLK5 while it is still within the cell. Its main function is to prevent the premature activation of KLK5 and ensures that the enzyme remains inactive until it reaches the appropriate location in the extracellular space. The largest and most critical segment of the pre-pro-KLK5 is the S1 family serine protease domain, encompassing 227 amino acids. This domain serves as the catalytic site of the enzyme, responsible for its proteolytic activity. With the serine protease domain, KLK5 gains the capacity to cleave specific protein substrates in the skin, playing a significant role in processes such as desquamation, inflammation and antimicrobial defense (Brattsand, Stefansson et al. 2005, Goettig and Magdolen 2013). After the synthesis of the pre-pro-KLK5 in the endoplasmic reticulum, the protein is then transported to the Golgi apparatus.

During its journey through the secretory pathway, the N-terminal signal peptide is enzymatically removed, resulting in the mature pro-KLK5 form. The removal of the signal peptide is crucial for enabling KLK5 to be subsequently secreted into the extracellular space. As keratinocytes migrate from the stratum granulosum to the stratum corneum, they release pro-KLK5 into the extracellular space. Once in the extracellular space, KLK5 remains in its pro-KLK5 form. The activation of KLK5 into its active form predominantly occurs in the stratum corneum (Brattsand, Stefansson et al. 2005, Goettig and Magdolen 2013), which is accomplished by KLK5 itself or KLK14, and exhibit multi-functions in the skin.

1.3.2 The functions of Kallikreins

KLKs are involved in wide array of physiological and pathological processes, including the epidermal barrier function, wound healing, inflammation and regulation of skin homeostasis. The major function of KLKs in the skin is involved in skin desquamation, which is predominantly accomplished by KLK5 (trypsin-like serine protease) and KLK7 (chymotrypsin-like serine protease) (Kishibe 2019). KLK5 can degrade corneodesmosome by cleaving the extracellular domain of Desmoglein 1 (DSG1), Desmocollin 1 (DSC1) and Corneodesmosin (CDSN), which are major compartments in corneodesmosomes (Caubet, Jonca et al. 2004) (**Figure 1.6**). This enzymatic activity significantly contributes to the process of desquamation. Besides, DSG1-silenced skin raft cultures displayed disorganized morphology including irregular cell shapes and widen intercellular space, referring to abnormal keratinocyte proliferation and differentiation (Getsios, Simpson et al. 2009). As DSG1 can suppress epidermal growth factor receptor EGFR-Erk1/2 signaling and promote keratinocyte differentiation, DSG1 has

potential to regulate skin morphology (Getsios, Simpson et al. 2009). Thus, by interacting with DSG1, KLK5 might be involved in keratinocyte growth.

In addition, the hyperactivity of KLK5 is believed to be associated with Filaggrin abnormalities in epidermis (**Figure 1.6**). KLK5 has been found to potentially cleave pro-elastase 2 (pro-ELA2) and activate elastase 2 (ELA2), which is a novel epidermal protease (Bonnart, Deraison et al. 2010). ELA2 has the direct proteolytic ability to lysis profilaggrin and filaggrin monomers (Bonnart, Deraison et al. 2010). Filaggrin enhances the integrity of the epidermal barrier by bundling keratin intermediate filaments and forming cornified envelope (Manabe, Sanchez et al. 1991, Candi, Schmidt et al. 2005, Kim and Lim 2021). Filaggrin could also be cleaved into small amino acids such as NMF to provide support to hydration in epidermis (IAN R. SCOTT 1982, Rawlings and Harding 2004). Thus, upregulation of KLK5 could result in enhanced activity from ELA2, leading to filaggrin deficiency and impairing epidermal integrity (Bonnart, Deraison et al. 2010). As a result, this would be attributive to excessive epidermal water loss and immune response caused by external antigens stimulation, which will further feedback to skin barrier dysfunction and skin inflammation. However, most of these findings were discovered in NS disease model. More research needs to be conducted in AD model.

Moreover, Kallikreins have been associated with the processes involved in wound healing in the skin. When the skin undergoes repair following a wound, kallikreins play a role in the formation of granulation tissue, re-epithelialization and remodeling of the extracellular matrix. They facilitate the activation of proteolytic cascades, which lead to the breakdown of injured tissue and subsequent

generation of new tissue. Kallikreins actively participate in regulating cell migration, proliferation, and differentiation, which are crucial for the successful healing and rejuvenation of the skin (Nauroy and Nystrom 2020).

Kallikreins play a role in inflammatory skin diseases, such as psoriasis and rosacea. In these diseases, KLKs are marked upregulated. It has been reported that KLKs function in the activation of the kallikrein-kinin system, leading to the release of inflammatory mediators, vasodilation and increased permeability of blood vessels. These mechanisms facilitate the infiltration of immune cells and the production of pro-inflammatory cytokines, ultimately contributing to the initiation and persistence of skin inflammation (Kishibe 2019). The kallikrein family members also interact with other proteins and enzymes within the skin, contributing to the skin inflammation. KLK5 has been implicated in the regulation of inflammation and the immune response by activating proteinase-activated receptor 2 (PAR2), a member of transmembrane G-coupled receptor superfamily, which can regulate skin inflammation (Briot, Deraison et al. 2009). Upon the proteolytic activity of KLK5, this serine protease targets the extracellular domain of PAR-2, cleaving it at a specific site, typically on the receptor's N-terminus (**Figure 1.6**). As a result of this cleavage, a new N-terminal sequence is exposed, acting as a tethered ligand. This tethered ligand enables the N-terminus to bind within the receptor's own structure, leading to a conformational change. Consequently, the intracellular domains of the receptor become exposed and gain the ability to interact with G proteins (Steinhoff, Buddenkotte et al. 2005, Oikonomopoulou, Hansen et al. 2006, Stefansson, Brattsand et al. 2008, Briot, Deraison et al. 2009). Once PAR2 is activated, it initiates NF-κB signaling and transduces the signals from the activated receptor to downstream effector

molecules, triggering various cellular responses associated with epidermal growth as well as inflammation and immune activation (Steinhoff, Buddenkotte et al. 2005). The PAR2 activation also displays non-responsive activity to other activating proteases. The activated PAR2 can couple with G-proteins and trigger intracellular calcium mobilization (Kawabata 2002, Oikonomopoulou, Hansen et al. 2006, Stefansson, Brattsand et al. 2008).

Previous study revealed KLK5 can upregulate TSLP and pro-inflammatory molecules via PAR2-mediated NF-κB signaling pathway in human keratinocytes (Briot, Deraison et al. 2009), which will further drive to Th2-skewed inflammation. Besides, PAR2 activated by KLK5 is also capable of inducing the release of pro-inflammatory/inflammatory cytokines/chemokines, such as IL-8 (Chin, Lee et al. 2008). IL-8 could recruit neutrophils and play a part in the innate immunity (Chin, Lee et al. 2008). However, Zhu. et al found that in the chronic conditions of AD with overexpression of KLK5, there was PAR2 desensitization, indicating there might be alternative pathways compensating for PAR2 desensitization in the immune response in AD (Zhu, Underwood et al. 2017). Elevated levels of some inflammatory cytokines such as IL-8, IL-10 and TSLP were still detected in the disease model, implying the presence of an unknown pathway between the overexpression of KLK5 and immune response in AD (Zhu, Underwood et al. 2017). This is the pathway we are interested in studying.

Apart from PAR2, KLK5 could participate in skin immunity by activating antimicrobial peptides, such as human cathelicidin (Morizane 2019). The inactive human cathelicidin consists of cathelin domain at N-terminal and C-terminal domain encoding mature cathelicidin peptide LL-37 (Yamasaki, Schauber et al.

2006). KLK5 cleaves cathelicidin precursor hCAP18 to generate mature peptides LL-37 (Yamasaki, Schauber et al. 2006). Hence, LL-37 acts like natural antibiotics and regulates leukocyte recruitment (Zanetti 2005). These findings revealed that KLK5 plays a role in skin inflammatory pathways.

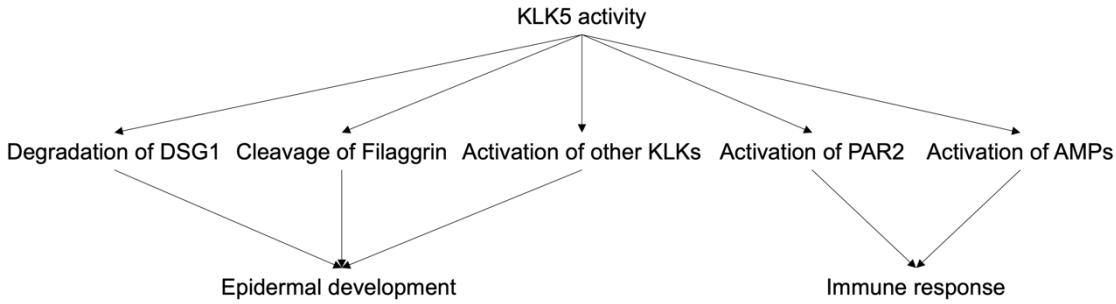

Figure 1.6 The function of KLK5 activity

The flow chart showed the functions of KLK5 activity, which involved in the epidermal development and immune response.

1.3.3 The effects of upregulated KLKs in AD

The activities of KLKs can be influenced by various factors, including pH level and their inhibitors like metal ions and proteins (Masurier, Arama et al. 2018). As mentioned above, the balance between serine proteases and their inhibitors is essential for skin homeostasis. KLK activity has been implicated in the disruption of the skin barrier and the generation of pro-inflammatory mediators in AD. Several studies have demonstrated increased expression and activity of KLKs in AD lesional skin (Komatsu, Saijoh et al. 2007, Voegeli, Rawlings et al. 2009, Zhu, Underwood et al. 2017, Morizane, Sunagawa et al. 2022). Up-regulated KLKs have been implicated in the pathogenesis of AD through the disruption of skin barrier that illustrated previously (Christian Jobin 1999, Caubet, Jonca et al. 2004, Briot, Deraison et al. 2009, Cork, Danby et al. 2009, Sakabe, Yamamoto et al. 2013, Zhu, Underwood et al. 2017, Kim and Lim 2021). The over-degradation of corneodesmosomes (Caubet, Jonca et al. 2004, Descargues, Deraison et al.

2006) and Filaggrin (Bonnart, Deraison et al. 2010, Sakabe, Yamamoto et al. 2013) could lead to the compromised skin barrier in AD, which not only increases vulnerability to environmental irritants but also facilitates the entry of allergens and pathogens into the skin, triggering an exaggerated immune response in PAR2-independent manner. However, the alternative signaling pathway that links KLK5 overexpression and immune response remains unclear and requires further investigations.

1.4 Aim of the study

Previous research showed up-regulation of KLK5 expression in AD (Komatsu, Saijoh et al. 2007, Voegeli, Rawlings et al. 2009) and further laboratory studies demonstrated that increased KLK5 could impair the skin barrier and result in skin barrier dysfunction (Zhu, Underwood et al. 2017). This is due to the overexpression of KLK5 over-degrading adhesion proteins like DSG1 between corneocytes and disrupting the cornified layer (Descargues, Deraison et al. 2005, Descargues, Deraison et al. 2006). Apart from this, the data in our lab also revealed that overexpression of KLK5 was found to increase the expression of some inflammatory molecules including IL-8, IL-10 and TSLP, suggesting a link between KLK5 activity and immune response (Zhu, Underwood et al. 2017). PAR2 was believed to regulate the immune response in LEKTI-deficient keratinocytes previously (Briot, Deraison et al. 2009). However, studies carried out in our lab showed that PAR2 activity was desensitized with constant overexpression of KLK5 in keratinocytes (Zhu, Underwood et al. 2017). But the elevated pro-inflammatory/inflammatory molecules like IL-8, IL-10 and TSLP were still detected. As in the chronic AD, patients tend to develop long-term KLK5 overexpression with inflammatory symptoms not the transient expression. This

suggested that PAR2 may not be the only key molecule triggering immunological dysregulation in AD. Alternative immune regulatory pathway might exist due to the overexpression of KLK5.

1.4.1 Hypothesis

The hypothesis of this project was that KLK5 overexpression in keratinocytes could regulate immune response by influencing keratinocytes themselves or interacting with immune cells (**Figure 1.7**).

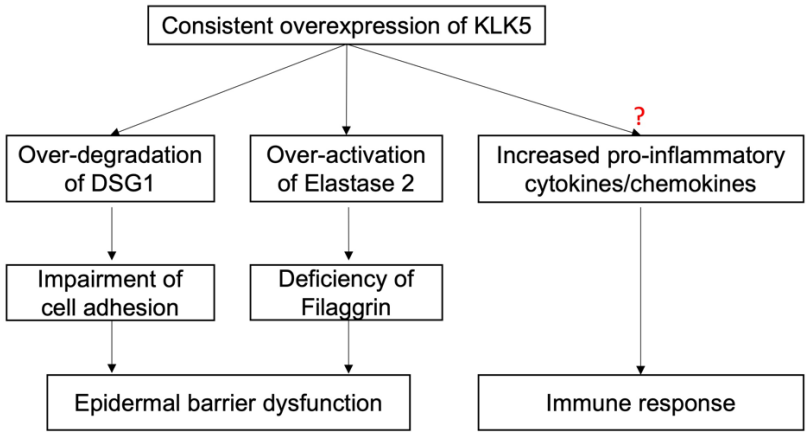

Figure 1.7 The hypothesis of KLK5 overexpression in AD

The flow chart shows that the role of KLK5 overexpression in the skin. The overexpression of KLK5 might regulate gene and protein expressions involved in immune response and epidermal development, causing abnormal immune response, inflammation and skin barrier dysfunction. The defective skin barrier could allow external irritants to penetrate through skin barrier and further contribute to skin inflammation.

1.4.2 Objectives

To investigate the hypothesis listed above, primary keratinocyte model with KLK5 overexpression was re-established to study the following objectives:

1. To find whether there were differentially expressed genes related to immune response in keratinocytes overexpressing KLK5

2. To examine whether there were abnormal pro-inflammatory/inflammatory cytokine secretions from keratinocytes with KLK5 overexpression

3. To check whether the conditional medium collected from keratinocytes with KLK5 overexpression could drive Th2 differentiation among naïve $CD4^+$ T cells

4. To generate a keratinocyte model with inducible KLK5 overexpression for studying the reversible effect of KLK5 overexpression

Chapter 2: Methods and Materials

2.1 Donor recruitment

Clinical samples were obtained from healthy donors attending the Department of Dermatology at Great Ormond Street Hospital with written consent form from their guardians. Ethical approval was granted from local research ethics committee with REC reference 12/LO/1522. Details of each donor were listed in the Table 2.1 below.

Donor	Gender	Age (years)	Sample	Usage
1	Female	13	Skin biopsy	RNA-seq; RT-qPCR
2	Female	16	Skin biopsy	RNA-seq
3	Female	13	Skin biopsy	RNA-seq
4	Male	9	Skin biopsy	RT-qPCR
5	Female	12	Skin biopsy	RT-qPCR
6	Female	9	Skin biopsy	RT-qPCR
7	Male	30-50	Peripheral blood	Th2 assay optimisation
8	Female	30-50	Peripheral blood	Th2 assay optimisation
9	Female	30-50	Peripheral blood	Th2 assay optimisation
10	Female	30-50	Peripheral blood	Th2 assay using conditional media
11	Female	30-50	Peripheral blood	Th2 assay using conditional media
12	Female	30-50	Peripheral blood	Th2 assay using conditional media
13	Female	30-50	Peripheral blood	Th2 assay using conditional media
14	Male	30-50	Peripheral blood	Th2 assay using conditional media
15	Female	30-50	Peripheral blood	Th2 assay using conditional media

Table 2.1 Details of donor recruitment

2.2 Lentivirus production

HEK293T cells were seeded in T175 flask one day before the transfection and cultured in Dulbecco's Modified Eagle Medium (DMEM, Gibco, Horsham, UK) supplied with 10% fetal bovine serum (FBS), 100 U/ml penicillin and 100 μg/ml streptomycin (Pen/Strap) (Invitrogen, Paisley, UK). Cells were maintained at 37°C and 5% CO_2. On the second day, 25μg of expression vector containing transgene with 17.5μg of pMD2.G VSV-G envelope expressing plasmid and 32.5μg of 2nd generation lentiviral packaging plasmid pCMVR8.74 were mixed in 5ml Opti-Mem reduced serum medium (Gibco, Horsham, UK) and filtered through a 0.22μm polyethesulfone membrane filter (Millipore, Watford, UK). 1μl

of a 10mM stock of Polythylenimine (Merck, Dorset, UK) is added to 5ml Opti-Mem media and filtered through a 0.22μm polyethesulfone membrane filter. These two solutions were then mixed at 1:1 ratio and stabilized for 20 minutes at room temperature. HEK293T cells were incubated in the mixed solutions for 5 hours and then changed back to DMEM media. The lentiviruses were produced and harvested 48-hour and 72-hour post-transfection. The cultured media were collected and centrifuged at 2000 rpm for 10 minutes to remove the debris, followed by filtering through 0.45μm polyvinylidene difluoride membrane filter (Millipore, Watford, UK). The filtered supernatants were concentrated by ultracentrifuge at 23000 rpm for 2 hours. The viral pellets were resuspended in Opti-Mem for 30 minutes on ice and aliquoted and stored at -70°C for further use.

2.3 Titrations of lentivirus titers

$1x10^5$/well 293T cells were seeded in a 24-well plate. 24 hours post seeding, viral stocks were added into cells in a range of 0μl, 0.032μl, 0.16μl, 0.8μl, 4μl and 20μl followed by Doxycycline induction if for inducible lentivirus 72 hours post-transduction. Then the positive transduced cells were assessed by flow cytometry based on GFP^+ cells. Virus titers were calculated based on the formula: virus titer (IU/ml) = [(cell number at seeding point) x (percentage of transduced cells)] / (volume of virus added in ml).

2.4 Primary keratinocyte isolation

Primary keratinocytes and fibroblasts were isolated from the skin biopsy and the isolation protocol was adopted from Di, Melleio (Di, Mellerio et al. 2013). The skin biopsies obtained from healthy donors were immersed in phosphate buffered saline (PBS, ThermoFisher Scientific, Horsham, UK) at room temperature and

cut into small pieces. Neutral protease NB (1U/ml, Nordmark Biochemical GmBH) was applied on skin at 37ºC for three hours. After digestion, the epidermis was peeled off from dermis and transferred to a 50ml falcon. Further digestion was carried out in 0.25% Trypsin-EDTA to get single cell suspension with physical dissociation. Cells were pelleted by centrifuge at 500g for 10 minutes (room temperature). Cells were then resuspended in the culture media following discarding of the supernatant. Irradiated murine 3T3 cells were co-cultured with keratinocytes to support cell growth. Collagenase NB6 (0.45U/ml, Nordmark Biochemical GmBH) was used for dermis digestion. After 2-hour digestion, residue tissue and cell suspension were transferred to a 50ml falcon with physical dissociation and centrifuged at 500g for 10 minutes. Both isolated keratinocytes and fibroblasts were resuspended in the culture media and cultured in 37°C, 10% CO_2.

2.5 Cell culture and harvest for primary keratinocytes persistently overexpressing KLK5

The primary keratinocytes were cultured as described by Di, Mellerio (Di, Mellerio et al. 2013). Briefly, $6x10^5$ primary keratinocytes were seeded in T25 one day before transduction. Cells were cultured in RM+ media, which is made of equal amount of DMEM and DMEM/Ham F12 (DMEM/F12, 3:1 mixture) (ThermoFisher Scientific, Horsham, UK) supplemented with 10% FBS, 10% Pen/Strep (Invitrogen, Paisley, UK) and human keratinocyte growth supplement and maintained at 37°C and 5% CO_2. The final concentrations of each component from human keratinocyte growth supplement in the culture media were: 10 ng/ml human epidermal growth factor, 0.4 μg/ml hydrocortisone, 5 μg/ml transferrin, 5 μg/ml insulin, $2x10^{-11}$M Liothyronine sodium salt and $1x10^{-10}$M cholera toxin.

Keratinocytes were transduced with lentiviruses containing KLK5-GFP transgene (KC-KLK5) or GFP transgene (KC-GFP) alone on the second day at Multiplicity of infection (MOI) 30 overnight. Cells were washed with normal keratinocyte media on the following day and irradiated murine 3T3 cells were added to support primary keratinocyte growth. Cells were then monitored until it reached to confluent under the fluorescent microscope. Images of cells were taken and processed by ImageJ (National Institutes of Health, USA) and Adobe Photoshop (Version 22.4.2, California, USA). The cultured media were collected, aliquoted and stored at -70°C. One aliquot of the cultured media from untransduced keratinocytes (KC-UT), KC-GFP and KC-KLK5 of Donor 4, 5 and 6 were pooled together and prepared for T cell work. A small portion of cells were transferred to another tube and digested with 0.25% trypsin to obtain single cell suspension for flow cytometry detection using CyAn ADP flow cytometer (Beckman Coulter, High Wycombe, UK). The rest of cells were scraped and collected into two portions: one for RNA detection and another one for protein detection.

2.6 RNA extraction

0.3-0.4ml of TRIzol Reagent (ThermoFisher Scientific, Horsham, UK) was added per $1x10^6$ cells and pipetted up and down to homogenize. The lysate was incubated for 5 minutes to permit nucleoproteins complex to dissociate. 0.2ml of chloroform was added per 1ml of TRIzol Reagent used for lysis and incubated for 2-3 minutes. Samples were centrifuged at 12,000g, 4°C for 15 minutes. After centrifuge, the aqueous phase containing RNA was transferred to new tube. 0.5ml of isopropanol was added to the aqueous phase per 1ml of TRIzol reagent used for lysis and incubated for 10 minutes. Samples were centrifuged again at 12,000g, 4°C for 10 minutes and the supernatant was discarded. RNA formed

gel-like pellet at the bottom. 1ml of 75% ethanol was used per 1ml of TRIzol used for lysis to resuspend the pellet. Samples were vortexed briefly and centrifuged at 7500g, 4°C for 5 minutes. Supernatant was discarded and the pellet was dried at room temperature for 5-10 minutes. The dry pellet was resuspended in RNase-free water and the concentration of RNA was measured by Nanodrop.

2.7 RNA-seq

The quality of RNA samples was examined on Aligent RNA ScreenTape System (Agilent, Cheadle, UK) before proceeding to RNA-seq following manufacturer's instructions. cDNA library was prepared and sequence was performed with 75 base-pair paired-end run by NextSeq instrument (Illumina) in UCL Genomics (UCL Genomics, London, UK). Data analysis was reported by UCL Genomics using DESeq2 Bioconductor package including Read data quality test, mapping, normalization, modeling and differential expression analysis. Genes with negligible expression levels (Raw read counts<100) were excluded to reduce sample errors. Statistical analysis was performed to find differentially expressed genes in KC-KLK5 compared to KC-UT and KC-GFP and each P value given by multiple testing was corrected using the Benjamini-Hochberg method to generate an adjusted P value (P_{adj}). 0.05 was used as a significant difference level for adjusted P value during potential gene candidate selection. In terms of individual data analysis, $|\log_2 \text{fold change}|>1$ was applied to select gene candidates. An online tool, iDEP, was used for data analysis. The protein interactions among gene candidates were analyzed using String software and the differentiated pathways were matched with KEGG database (Minoru Kanehisa 2000, Kanehisa 2019, Kanehisa, Furumichi et al. 2023, Szklarczyk, Kirsch et al. 2023). Details of softwares can be found in **Section 2.18**.

2.8 RT-qPCR

The total RNA extracted by Trizol (ThermoFisher Scientific, Horsham, UK) were reverse transcribed to form cDNA using High Capacity cDNA Reverse Transcription kit (Applied Biosystems, Warrington, UK) based on manufacturer's instructions. Quantitative gene expressions in these samples were measured by quantitative polymerase chain reaction (qPCR) using the primers listed in the **Appendix 1**. CT values of target genes were normalised to GAPDH and $\Delta\Delta$RQ ($2^{\Delta\Delta CT}$) values and fold changes of target gene expressions in KC-KLK5 compared to KC-GFP cells were collected for statistical tests (**Section 2.18**).

2.9 Protein quantification

Cells were lysed in ice-cold lysis buffer pH 8.0 containing 50 mmol/L Tris-HCl, 150 mmol/L NaCl, 5 mmol/L EDTA, 1x protease inhibitor cocktail (Roche, Hertfordshire, UK), 1mmol/L phenylmethanesulfonylfluoride (Merck, Dorset, UK) and 1% Triton. Samples were kept on ice for 15 minutes and then centrifuged at 12000 rpm 4°C for 10 minutes. 5µL of cell lysates were transferred to a new tube and further 1:2 diluted for further quantification. The protein concentration was measured using Pierce 660nm Protein assay reagent kit (ThermoFisher Scientific, Horsham, UK). The ready-made protein standards were 1:1 diluted in the same lysis buffer to make a standard curve. 5µl of each 1:1 diluted standard and 1:2 diluted cell lysate was added into individual wells in a 96-well plate followed by adding 150µl of the protein assay reagent to each well. The plate was centrifuged at 1100rpm for 1 minute to get rid of bubbles. The absorbance was detected at the wavelength of 660nm and protein concentration was calculated according to the standard curve and dilution factor.

2.10 Western blotting

Cell lysates and culture supernatant were diluted in 5x sample buffer containing 10% Sodium Dodecyl Sulfate (SDS, Merck, Dorset, UK), 30% Glycerol, 0.001% Bromphenol blue, 0.5M Tris/HCl buffer, pH 6.8. Dithiothreitol was added to stabilize samples. Samples were heated at 95°C for 5 minutes. SDS-PAGE gels were made according to the recipe (**Table 2.2**). 30μg of samples and 5μl of full range rainbow marker were loaded to the SDS-PAGE gel and run at 200V for 1.5 hours. After electrophoresis, gels were transferred to 0.2μm Nitrocellular membrane using Trans-Blot Turbo Transfer system (Bio-Rad, Hertfordshire, UK). After transfer, the membrane was stained with Ponceau S solution (Merck, Dorset, UK) to view the loading of protein and confirm the protein transfer. The membrane was then blocked with 5% milk (ThermoFisher Scientific, Horsham, UK) at room temperature for 1 hour followed by 5 minutes wash 3 times using PBS solution with 0.2% Tween 20 (Santa Cruz, Texas, USA). Primary antibodies were applied to the membrane and incubated on a shaker overnight at 4°C. On the next day, primary antibodies were removed and the blot was washed for 5 minutes 3 times. Secondary antibody was applied to the blot. After 1 hour incubation at room temperature on a shaker, the blot was washed 3 times with 15 minutes interval. Pierce Enhanced chemiluminescence kit (ThermoFisher Scientific, Horsham, UK) was applied to the blot and the blot was visualized by ChemiDoc (Bio-Rad, Hertfordshire, UK). The images were exported to ImageLab (Bio-Rad, Hertfordshire, UK) for further analysis and densitometry was performed using ImageJ software. The membrane was then stripped by the stripping buffer (ThermoFisher Scientific, Horsham, UK) for 7 minutes and washed with PBS for 10 minutes twice. It was proceeded to the blocking and used for application of

other antibodies. All the antibodies and their usage conditions were listed in the **Appendix 2**. Densitometry was performed to quantify expressions. The expressions of target proteins in cell lysates were normalised to internal loading standards Actin, GAPDH or Vinculin and Ponceau S solution for culture media. The statistical test was listed in **Section 2.18**.

Component	Company	Cat No.	6% Separating gel	10% Separating gel	Stacking gel
H_2O	-	-	5.3ml	4ml	6.1ml
30% Bis Acrylamide	Sigma Aldrich	A3699-100ml	2ml	3.33ml	1.3ml
Tris–HCl (1.5 M, pH 8.8)	Bio-Rad	1610798	2.5ml	2.5ml	-
Tris–HCl (0.5 M, pH 6.8)	Bio-Rad	1610799	-	-	2.5ml
10% Sodium Dodecyl Sulfate (SDS)	Sigma Aldrich	75746-1KG	100ul	100ul	100ul
10% Ammonium persulfate (APS)	VWR Chemicals	K833-100TABS	100ul	100ul	100ul
TEMED	Sigma Aldrich	T9281-25ml	10ul	10ul	20ul

Table 2.2 SDS-PAGE gel recipe

2.11 Multi-spot V-PLEX and S-PLEX assays

Expressions of pro-inflammatory/inflammatory molecules secreted by KC-UT, KC-GFP and KC-KLK5 cells were tested by Multi-Spot assays (Meso Scale Discovery, Rockville, USA) in three donors with high KLK5 overexpression level, including IL-1β, IL-2, IL-4, IL-6, IL-8, IL-10, IL-12p70, IL-13, IFN-γ and TNF-α by V-PLEX Proinflammatory Panel 1 Human kit and TSLP by S-PLEX Human TSLP kit. The assay was performed based on manufacturer's instructions in Inflammation and Rheumatology Section in the Institute of Child Health. For the V-PLEX assay, briefly, the highest calibrator was reconstituted with 1000μl of Diluent 2 and 100μl of the highest calibrator was diluted with 300μl of diluent 2. Seven calibrators and diluent 2 alone as zero calibrator were prepared after repeating 4-fold serial dilutions 5 additional times. Cultured supernatants from KC-UT, KC-GFP and KC-KLK5 cells were collected and 1:1 diluted for the assay. The 96-well plate pre-coated with antibodies for these cytokines were washed three times with 150μl/well of wash buffer, which referred to PBS containing 0.05% Tween-20. 50μl of prepared calibrators and samples were added to the 96-well

plate and the plate was sealed and incubated at 4°C with shaking overnight. The plate was washed three times again prior to the addition of 25μl of the detection antibody solution to each well. The plate was sealed and shaked at room temperature for 2 hours. After 2-hour shaking, the plate was washed three times again and 150μl of 2x read buffer T was added to each well. The plate was then read and data was collected.

For the S-PLEX assay, the 96-well plate was washed three times with 150μl/well of wash buffer followed by the addition of 50μl/well of coating solution. The plate was then sealed and shaked at 700rpm at 4°C overnight. The highest calibrator was prepared by adding 20μl of the reconstituted calibrator to 180μl of Diluent solution and repeating another time. The 40μl was taken and added to 260μl of Diluent solution to generate Standard 1. Then Standard 2 was prepared by adding 50μl of Standard 1 to 150μl of Diluent solution. This was repeated 4-fold serial dilutions five additional times to generate Standard 3-7. In total, 8 standards including Diluent alone as a zero standard were used in the study. Cultured supernatants from KC-UT, KC-GFP and KC-KLK5 cells were collected and 1:1 diluted for the assay. The plate was washed three times with 150μl/well of wash buffer after the coating completed. The plate was blocked by adding 25μl of blocking solution to each well. Then 25μl of calibrators or diluted samples were added to each well. The plate was sealed again and shaked at 700rpm at room temperature for 1.5 hours. After the incubation, the plate was washed three times and 50μl of Turbo-Boost antibody solution was added to each well. The sealed plate was then shaked again under the same condition followed by the 50μl of the enhancer added to each well after three washes. The enhancer was

incubated at room temperature for 30 minutes during shaking at 700 rpm and washed three times again. 50μl of Turbo-Tag detection solution was added and incubated at 27°C for 1 hour during shaking. The plate was washed three times again prior detection and data was collected for analysis.

Results were standardized based on protein quantification of each cell lysate and normalized by expressions in KC-GFP samples to obtain ratios for statistical analysis (**Section 2.18**).

2.12 PBMC extraction

Healthy donors were recruited in the study to extract human peripheral blood mononuclear cells (PBMCs) by using Lymphoprep density gradient medium following manufacturer's instructions (Stemcell Technologies, Cambridge, UK). Basically, 20ml peripheral blood was taken from each donor and 1:1 diluted with normal T cell Roswell Park Memorial Institute (RPMI, Gibco, Horsham, UK) media supplied with 10% Pen/Strep. The diluted blood was then gently added to two 50ml falcons containing 10ml of Lymphoprep density gradient medium equally and respectively. Both were centrifuged at 800g at room temperature for 20 minutes with acceleration set to 2 and brake set to 1. The PBMC layer was transferred by a sterile pasteur pipette to a 15ml falcon containing 1ml of RPMI media supplied with 10% FBS. The falcon was topped up to 15ml and pelleted at 699g at room temperature for 10 minutes with acceleration set to 9 and brake set to 9. The cell pellet was resuspended in RPMI media with 10% FBS and washed again. A small portion of cells were taken to record the cell count at this stage. The rest of cells were pelleted at 552g at room temperature for 7 minutes. The

cells were resuspended again in the RPMI media with 10% FBS and proceeded to naïve $CD4^+$ T cell isolation after the centrifugation.

2.13 Human naïve $CD4^+$ T cell isolation

Human naïve $CD4^+$ T cells were isolated from PBMCs using EasySep Human naïve $CD4^+$ T cell isolation kit II (Stemcell Technologies, Cambridge, UK). According to manual, PBMCs were dilated to the concentration of $5x10^7$ cells/ml in the isolation buffer, which consisted of PBS and 2% FBS and 1mM Ethylenediaminetetraacetic acid. The diluted cells were added to 5ml polystyrene round-bottom tube and bound with 50μl/ml of isolation cocktails. The complex was then mixed properly and incubated at room temperature for 5 minutes. The RapidSpheres, which referred to magnetic beads, was vortexed to mix properly and added to the samples at the concentration of 50μl/ml. The tube was then inserted into the magnet and incubated at room temperature for 3 minutes. After 3-minute incubation, the magnet was tilted to pour the enriched cell suspension into a new tube. Remove the original tube in the magnet and repeat this procedure once to purify the cells again. The enriched cells after the second separation were ready to be used for further investigations. The purity of isolated cells was checked by staining with $CD4^+CD45RA^+CD45RO^-$ cell markers and detected using flow cytometry (**Section 2.15**).

2.14 Cell activation and culture for human naïve CD4+ T cells

Anti-CD3 (Life Technologies, Horsham, UK) and anti-CD28 antibodies (Cambridge Bioscience, Cambridge, UK) were used to activate naïve $CD4^+$ T cells. One day prior T cell isolation, a round-bottom 96-well plate was pre-coated with 1μg/ml anti-CD3 and anti-CD28 antibodies at 37°C overnight. On the second

day, the plate was washed with PBS three times followed by the addition of isolated cells. The isolated naïve $CD4^+$ T cells were divided equally and cultured in seven different conditions: normal T cell RPMI media, normal T cell RPMI media with positive stimuli IL-4 (20ng/ml, Bio-techne, Abingdon, UK), normal keratinocyte media RM+, normal keratinocyte media RM^+ with IL-4 as well as cultured media from KC-UT cells, KC-GFP cells and KC-KLK5 cells. Recombinant IL-2 (100U/ml, Peprotech, London, UK) and anti-IFN-γ (2.5μg/ml, Life Technologies, Horsham, UK) were supplied in all cultures. After 4-day culture, cells were expanded in same conditions and re-activated again by anti-CD3 and anti-CD28 antibodies on Day 7 for 16 hours. Cells from seven different conditions were then collected on Day 8 and proceeded to staining. Cells expressed non-$CD25^-CD69^-$ were defined as activated cells and Th2 cells expressed $GATA3^+$. The staining protocol refers to **Section 2.15**.

2.15 Cyto-immunofluorescence staining

Two types of staining methods were used in the study. For the surface staining, cell markers of $CD4^+CD45RA^+CD45RO^-$ were used to check the purity of isolated human naïve $CD4^+$ T cells (**Appendix 2**). After the isolation of naïve $CD4^+$ T cells, a small portion of isolated cells were washed with staining buffer, which was PBS with 2% FBS, in a round-bottom 96-well plate. Then, the plate was centrifuged and cells were incubated with antibody cocktails, including anti-CD4, anti-CD45RA and anti-CD45RO antibodies as well as their isotype controls on ice for 1 hour in dark. After 1 hour incubation, the plate was centrifuged at 500g for 5 minutes and discarded the waste. The pellet cells were washed with staining buffer again and resuspended in the same buffer. Then the cells were ready to be examined by CytoFLEX flow cytometer (Beckman Coulter, High Wycombe,

UK). Apart from checking the purity of the isolated cells, the surface staining was also applied to check the activation rate among human $CD4^+$ T cells by anti-CD25 and anti-CD69 antibodies. Same staining protocol was applied. Details of antibodies used for staining were listed in **Appendix 2**.

Apart from the surface staining, the intracellular staining was also used to check the differentiation rate among $CD4^+$ T cells by specific Th2 cell markers GATA3. Cells were washed by staining buffer prior to the intracellular staining and then fixed by Fixation/Permeabilization working solution (ThermoFisher Scientific, USA) based on manufacturer's instructions on ice for 20 minutes in dark. The wash was performed by following the equilibrium for the fixed cells with 1x Permeabilization buffer (ThermoFisher Scientific, Horsham, UK). The cells were then stained with anti-GATA3 antibody on ice for 1 hour in the dark. Cells were then washed again with 1x permeabilization buffer after 1 hour incubation and resuspended in the staining buffer. They were proceeded to flow cytometry detection using CytoFLEX flow cytometer (Beckman Coulter, High Wycombe, UK). The antibodies were listed in Appendix 2. Expressions were analysed using percentage of desired cell population, followed by statistical tests (**Section 2.18**).

2.16 Construction of inducible lentiviral vectors

The KLK5 transgene linked to GFP reporter gene (KLK5-GFP) with an internal ribosome entry site (IRES) in between was amplified from the LV-KLK5 vector using CloneAmp amplification kit (Takara Bio, London, UK) according to manufacturer's instructions. The GA-TetOne-KLK5 forward primer and GA-TetOne-GFP reverse primer were used for Polymerase chain reaction (**PCR, Appendix 1**). The GFP reporter gene was amplified from LV-GFP vector using

Q5 amplification kit (New England BioLabs, Hitchin, UK) according to the instruction from the manufacture. The Infusion-TetOne-GFP forward primer and Infusion-TetOne-GFP reverse primer were used for PCR (**Appendix 1**). The amplified products were checked in 1% Agarose gel and the bands of 2291bp and 720bp were cut and PCR products were purified using NucleoSpin Gel and PCR Clean-up kit (Macherey-Nagel, Loughborough, UK). The concentration of purified products were measured using Nanodrop (DeNovix, Cambridge, UK). The KLK5-GFP fragment and GFP fragment were then run in the 1% agarose gel again to check the size and purity.

The Tet-One-Puro vector was obtained from the company Takara (Takara Bio, London, UK) and digested with BamHI-HF and EcoRI-HF. The digested vector was then run through 1% agarose gel and purified using NucleoSpin Gel and PCR Clean-up kit (Macherey-Nagel, Loughborough, UK). The purified linearized Tet-One-Puro vector was ligated with GFP by Infusion cloning kit (Takara Bio, London, UK) or KLK5-GFP fragment using Gibson assembly kit (New England BioLabs, Hitchin, UK). The ligated products was then transformed into E.coli competent cells JM109 (Promega, Hampshire, UK). Clones were screened by growing in the Ampicillin plate and some clones were picked up to further culture in Luria Bertani medium (Merck, Dorset, UK). The plasmid DNAs were extracted using Maxiprep kit (Qiagen, Manchester, UK). The size of the vectors was then checked by running in 1% agarose gel following the restriction digestion using KpnI and XbaI enzymes. Clones with correct digestion fragment were further proceeded to confirm the sequence by Sanger sequencing (DNA sequencing services, Crick Institute, London, UK). The sequences were analyzed using

Sequencher v5.2 (Gene Codes Corporation, USA). The maps of generated vectors were listed in **Appendix 5**.

The details of primers designed for sequencing reactions were listed in **Appendix 1**. BigDye Terminator v3.1 Cycle Sequencing kit was used for sequencing reactions (ThermoFisher Scientific, Horhsam, UK). The products from sequencing reactions were purified by precipitating at 1500rpm centrifugation and 1μl of 3M sodium acetate and 25μl of 100% ethanol were added in each well. The plate was then incubated at room temperature for 15 minutes and centrifuged at 3000rpm for 30 minutes. After the centrifugation, the plate was flipped immediately and spun again at 185g for 1 minute to remove the supernatant. Then 35μl of 70% ethanol was added to each well and centrifugated at 3000 rpm for 15 minutes. The plate was inverted immediately after centrifugation and then spun again at 185g for 1 minute. It was air-dried for 5-10 minutes and covered with aluminium foil and stored at -20°C until assay.

2.17 Cell culture and harvest for inducible KLK5 overexpression system

$4x10^5$ primary keratinocytes were seeded in 6-well plate one day before transduction followed by the same transduction protocol as stated in **Section 2.5**. 3 days post-transduction, 1μg/ml of doxycycline was added to induce the expression of transgene and monitored for 48 hours under the fluorescent microscope. Images of cells were taken and processed by ImageJ (National Institutes of Health, USA) and Adobe Photoshop (Version 22.4.2, California, USA). 48 hours later, supernatants were collected from half of the samples and cells were scraped for further protein detection. A small portion of cells were collected to further digest with trypsin for flow cytometry detection. The other half of

samples were continuously cultured without doxycycline induction for a week. All samples and supernatants were collected after a week's cultured using the same method stated above.

The same protocol of cell transduction and induction was applied to $1x10^5$ HEK293T cells in 6-well plate at MOI of 10. The rest remained the same.

2.18 Statistical tests and softwares

The statistical tests used in the study were listed below (**Table 2.3**). The normality was checked by Shapiro-Wilk test prior statistical significance tests. The significance level was set to 0.05 ($p \leq 0.05$).

Test used in experiments	Test
Normality test	Shapiro-Wilk
RT-qPCR	T test or Mann-Whitney
Densitometry for Western blotting	T test
Multi-spot assay	T test or Mann-Whitney
Activation rates for Th2 assay	T test
Th2 differentiation for Th2 assay	T test

Table 2.3 Statistical tests

Details of the softwares used for analysis were showed in **Table 2.4**.

Software	Version	Source	Usage
Prism	9.5	GraphPad Software	Statistical tests and figures
Flowjo	10.8.2	BD Biosciences	Analysis for flow cytometry
Photoshop	2021	Adobe systems	Figure preparation
Snapgene	7.0	GSL Biotech	Vector sequence
CFX Manager	3.1	Bio-Rad	RT-qPCR
ImageLab	6.1.0	Bio-Rad	Western blot image visualisation
String	11.5	https://string-db.org	Analysis for protein network
KEGG	106.0	https://www.genome.jp/kegg/	Analysis for pathways
Primer Blast	-	https://www.ncbi.nlm.nih.gov/tools/primer-blast/index.cgi	Primer design
iDEP	0.96	http://bioinformatics.sdstate.edu/idep96/	RNA-sequence

Table 2.4 Softwares used in the study

Chapter 3: KLK5-overexpressed keratinocyte transcriptome revealed down-regulated TGF-β signaling and FLG2-mediated epidermal development

Upregulation of KLK5 protein has been reported in patients with AD (Komatsu, Saijoh et al. 2007, Voegeli, Rawlings et al. 2009, Zhu, Underwood et al. 2017, Nomura, Suganuma et al. 2020). Studies have demonstrated that the KLK5 protein could degrade the adhesion protein Desmoglein 1 (DSG1), one of corneodesmosomes in the skin (Celine Deraison 2007). Studies also found that the recombinant KLK5 could activate the PAR2, causing nuclear factor kappa B (NF-κB) mediated pro-inflammatory cytokine regulations in cells ectopically expressing PAR2 (Stefansson, Brattsand et al. 2008). However, a further study found that PAR2 could be desensitized if it was constantly stimulated by KLK5 in a keratinocyte model with persistent KLK5 overexpression, but there were still upregulated pro-inflammatory/inflammatory cytokines including IL-8 and TSLP (Zhu, Underwood et al. 2017). This study suggested that up-regulated KLK5 may link to immune response in an alternative or indirect pathway but not through PAR2. Several potential candidate targets were investigated previously to check whether increased KLK5 was associated to immune response, such as Toll-like Receptor 2 (Yamasaki, Kanada et al. 2011). Results showed there was a co-localisation of toll-like receptor 2 and KLK5 in keratinocytes and increased toll-like receptor 2 could lead to elevated KLK5 expression. However, whether and how toll-like receptor interacts KLK5 regulation is unclear. I proposed to examine whole transcriptomes in keratinocytes with sustained KLK5 overexpression to identify candidate genes related to immune response.

In this study, primary keratinocytes from normal donors overexpressing KLK5 by the lentiviral vector containing *KLK5-GFP* transgene under the control of Spleen focus-forming virus (SFFV) promoter (LV-KLK5) were used. The whole transcriptome was examined by bulk RNA sequencing (RNA-seq). Differentially

expressed genes (DEGs) between normal keratinocytes and keratinocytes overexpressing KLK5 identified by RNA-seq were further checked by RT-qPCR.

3.1 Primary keratinocyte overexpressing *KLK5*

Keratinocytes overexpressing KLK5 were generated using the lentivirus LV-KLK5. The lentivirus containing *GFP* reporter gene alone (LV-GFP) was used as negative control. Pseudo-lentiviruses were produced and titrated in 293T cells (**Section 2.2**). The ranges of the virus titers were from $8.5x10^7$ to $5.7x10^8$ IU/ml ($3.5\pm2.2x10^8$ IU/ml, n=6) for LV-KLK5 and $1.9x10^9$ to $3.4x10^9$ ($2.4\pm0.9x10^9$IU/ml, n=3) for LV-GFP. The lentiviruses with titers $\geq10^8$ IU/ml were used in the study. Primary keratinocytes isolated from healthy donors' skin samples were transduced with LV-KLK5 or LV-GFP at MOI of 30 (**Section 2.5**) and transduced cells were named as KC-KLK5 and KC-GFP, respectively. Untransduced primary keratinocytes (KC-UT) were run in parallel.

The expression of GFP and morphological changes in transduced cells were monitored under the microscope. KC-KLK5 had lower intensity of green fluorescence than that in KC-GFP (**Figure 3.1**). This might be that in the LV-KLK5 vector, the *GFP* gene was linked to the *KLK5* gene by an internal ribosome entry site sequence (IRES), an RNA element allowing the coordinated co-expression of two genes under the same promoter. As IRES is not a promoter and may have a weaker gene regulation effect compared to a promoter, resulting in low GFP expression in cells transduced with LV-KLK5 vector than that in cells transduced with LV-GFP vector. There was no change in cell morphology between KC-GFP, KC-KLK5 and KC-UT (**Figure 3.1**). The transduction efficiencies were assessed

by measuring GFP positive cells using flow cytometry. Cells with the transduction efficiency more than 45% were used for further study (**Figure 3.1b**).

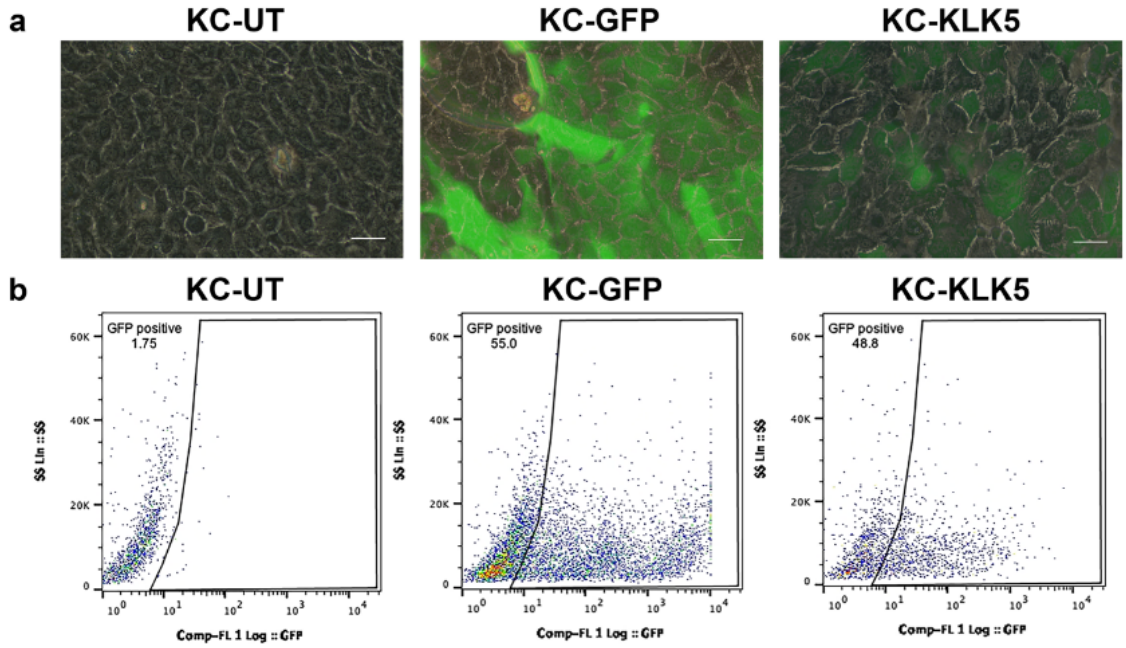

Figure 3.1 Transduction efficiency in primary keratinocytes

Primary keratinocytes were transduced with the viruses of LV-GFP or LV-KLK5. GFP expression and cell morphologies with and without transduction are shown in the images (a). Representative dot plots of flow cytometry showed the transduction efficiency as assessed by GFP^+ cells (b). The images were representative from 6 experiments. Scale bar =200μm. KC-UT= untransduced keratinocytes. KC-GFP=keratinocytes transduced with LV-GFP. KC-KLK5=keratinocytes transduced with LV-KLK5.

The overexpression of *KLK5* was confirmed at transcriptional level by RT-qPCR (**Section 2.8**). A significant increase in the expression of *KLK5* in KC-KLK5 cells was observed compared to KC-GFP and KC-UT cells (**Figure 3.2a**). GAPDH served as an internal reference for RT-qPCR. The protein level of KLK5 was further checked by Western blotting (**Section 2.10**). Full length KLK5 was detected at the expected size of 38 kDa in all cell lysates but with a higher intensity in the cells transduced with LV-KLK5. Comparing to the media collected from KC-GFP and KC-UT cultures, a higher intensity band for KLK5 was detected in the culture media collected from KC-KLK5 cell culture, indicating increased

secretion of active KLK5 in keratinocytes transduced with LV-KLK5 (**Figure 3.2b and c**) (Brattsand, Stefansson et al. 2005). β-actin and Ponceau S served as a loading control for cell lysates and cell culture media, respectively.

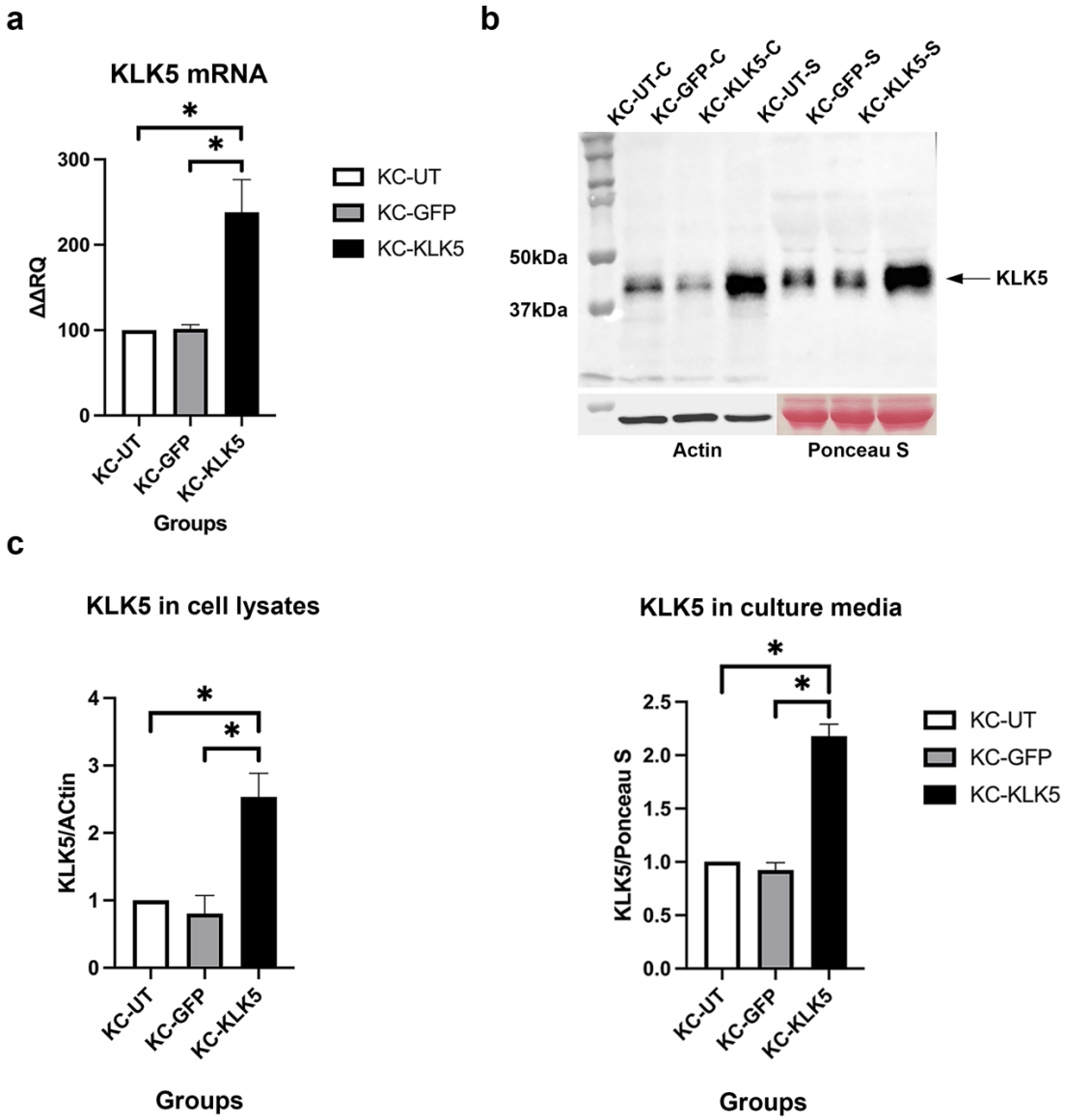

Figure 3.2 Confirmation of overexpression of KLK5 in primary keratinocytes

*Primary keratinocytes were transduced with LV-KLK5 or LV-GFP. There was increased KLK5 mRNA (a) and increased KLK5 protein in cell lysates and culture media (b) in cells transduced with LV-KLK5. The quantification of KLK5 protein was confirmed by densitometry (c). The images were representative from 3 experiments. *p≤0.05, n=4. Error bar=standard error. C=cell lysates. S=culture supernatants. KC-UT=untransduced keratinocytes. KC-GFP=keratinocytes transduced with LV-GFP. KC-KLK5=keratinocytes transduced with LV-KLK5.*

3.2 Transcriptomic changes in keratinocytes overexpressing *KLK5*

The genome-wide transcriptome in primary keratinocytes transduced with LV-KLK5 at passage 2 and cultured for 7 days was examined by RNA-seq (**Section 2.5 and 2.7**). Cells transduced with LV-GFP and untransduced cells were used as negative controls. Primary keratinocytes from three healthy donors (Donor 1, 2 and 3, **Table 2.1**) were used in the study.

3.2.1 The pipeline of RNA-seq data analysis

The quality of total RNA was evaluated before RNA-seq. All RNA samples passed quality control with RNA integrity number (RIN) more than 8.5 and clear bands at 18S and 28S (**Figure 3.3**). 26,485 genes with raw sequence reads ranging from 19 to 23 million per sample for KC-UT, 16-18 million per sample for KC-GFP and 13-16 million per sample for KC-KLK5 were collected. 6840 genes had null read counts (25.83%) and were excluded from further analysis, leaving 19,645 genes taken to data process. Genes with low expression levels (raw read counts<100) were further excluded in the analysis to reduce errors. Therefore, a total of 8133 genes were analysed with batch correction.

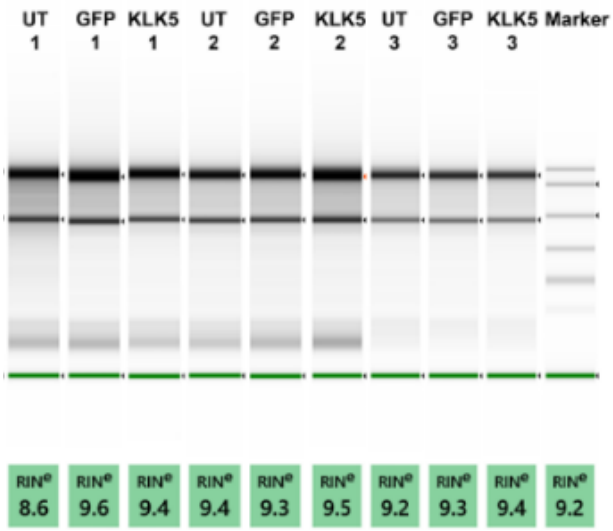

Figure 3.3 Quality of RNA extracted from keratinocytes

The qualities of RNA samples from three different experiments were assessed using RNA ScreenTape and results showed high RIN value (>8.5) in all samples.

3.2.2 Differentially expressed genes in keratinocytes with overexpression of *KLK5*

Genes that passed the pipeline screening with adjusted P value less than 0.05 were defined as DEGs. There were no DEGs between KC-UT and KC-GFP (**Figure 3.4a**), indicating the lentiviral backbone with reporter gene GFP alone did not affect transcriptomes in cells and the KC-GFP cells could be used as negative controls. Comparing the transcriptomes between KC-KLK5 cells and KC-GFP cells, there were 126 DEGs with 11 up-regulated genes and 115 down-regulated genes in KC-KLK5 cells (**Appendix 3**). Among the 126 genes, the *KLK5* gene showed an average increase of 2.3-fold in KC-KLK5 cells (Log_2FoldChange=1.2) compared to KC-GFP, confirming the overexpression of KLK5 in KC-KLK5 cells. All other genes had fold changes ranging from -1.9 to 1.7 (0.5<|Log_2FoldChange|<0.8). They were statistically differentially expressed but the expression changes were relatively low, less than 2-fold (**Figure 3.4**).

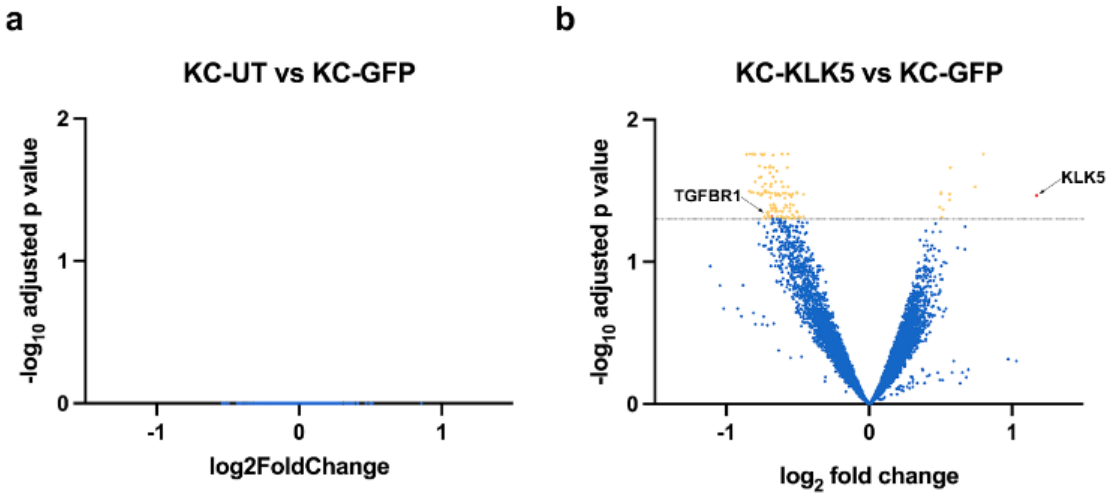

Figure 3.4 Differentially expressed genes (DEGs) in KC-UT, KC-GFP and KC-KLK5 cells

No significant differences in gene expressions were observed between KC-UT and KC-GFP (a). 11 significantly upregulated genes and 115 down regulated genes were detected in KC-KLK5 compared to KC-GFP cells (b). The dotted line indicates the level of statistical significance ($P_{adj} \leq 0.05$). KC-UT= untransduced keratinocytes. KC-GFP=keratinocytes transduced with LV-GFP. KC-KLK5=keratinocytes transduced with LV-KLK5.

The potential interaction between the 126 DEGs' corresponding proteins were further studied using the String network and KEGG pathway analysis (**Section 2.7**). Results showed 70 out of 126 genes potentially involved in some interaction pathways (**Figure 3.5**).

The top 10 protein interaction pathways were listed in **Table 3.1** and TGF-β signaling was at the top of the list (p=0.0003). Seven DEGs were involved in the TGF-β pathway including *TGFBR1*, *PPP1CB*, *XPO1*, *CDK6*, *CCNC*, *DBAP1* and *UBE2D1*. It was reported that the decreased TGFBR1, PPP1CB and XPO1 could negatively control TGF-β receptor signaling, attenuating TGF-β signaling in cells and resulting in cell proliferation, inflammation and fibrosis (Lodyga and Hinz 2020).

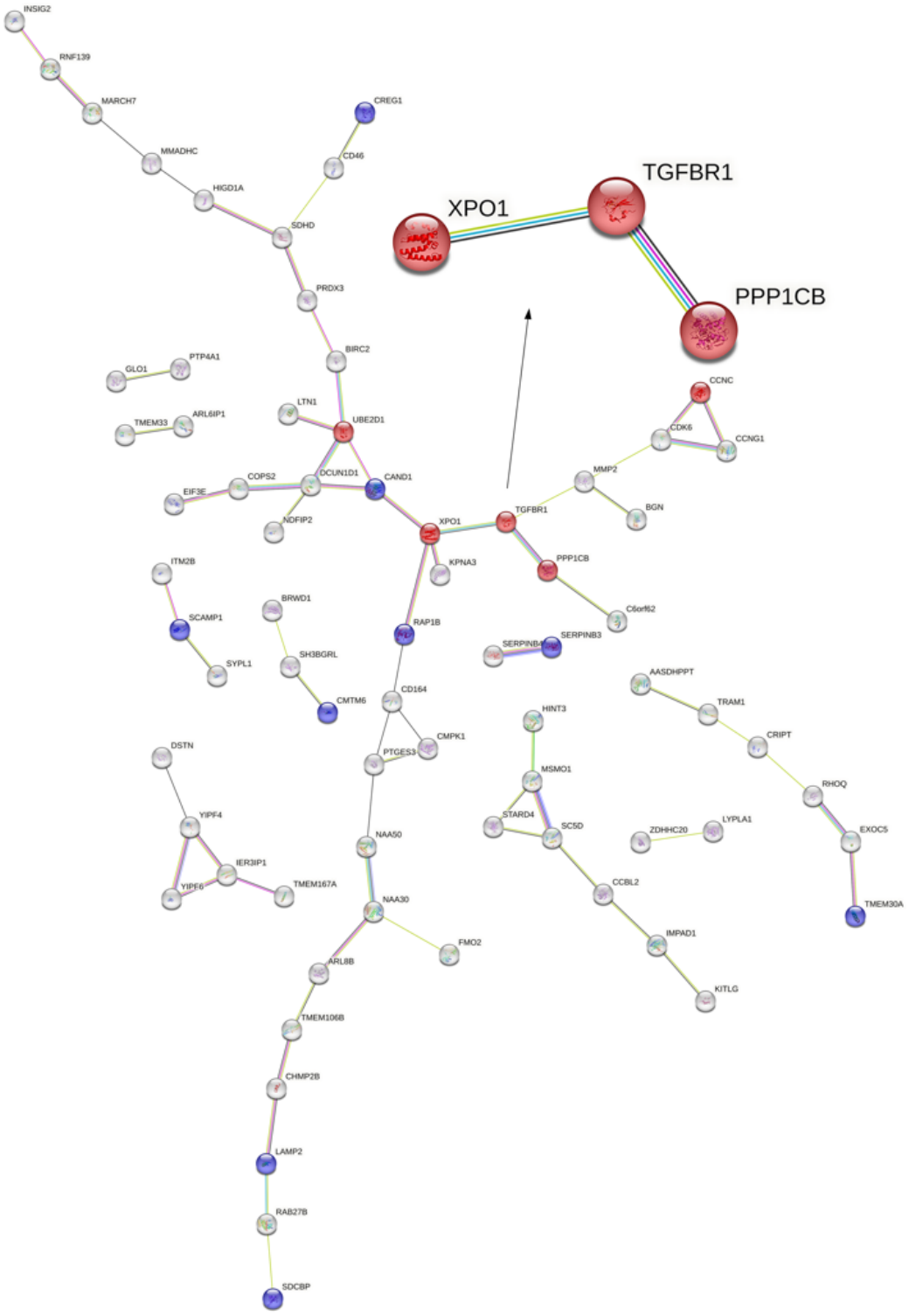

Figure 3.5 Protein interactions of differentially expressed genes

Corresponding protein interactions of 126 differentially expressed genes were analysed using String and 72 genes were engaged in central signaling pathways. The genes highlighted in red nodes were related to TGF-β signaling. The arrow at the up part of the figure showed an enlarged image of the pathway. The blue nodes showed the proteins involved in neutrophil degranulation. Filled nodes represent protein known or predicted 3D structures, whereas empty ones stand for

proteins of unknown 3D structures. Green line = neighborhood gene. Blue line = known interactions from curated databases. Black line = co-expression. Light purple = protein homology.

Pathway name	Genes involved	p-value	FDR
Signaling by TGFB family members	7/136	0.0003	0.129
Signaling by TGF-beta receptor complex	6/107	0.0005	0.129
TICAM1, RIP1-mediated IKK complex recruiment	3/19	0.0008	0.129
IKK complex recruiment mediated by RIP1	3/24	0.0020	0.188
Downregulation of TGF-beta receptor signaling	3/28	0.0020	0.233
RUNX1 regulates transcription of genes involved in differentiation of keratinocytes	2/11	0.0050	0.364
Regulated necrosis	4/76	0.0060	0.364
Regulation of necroptotic cell death	3/39	0.0060	0.364
RIPK1-mediated regulated necrosis	3/45	0.0090	0.411
Regulation of gene expression by Hypoxia-inducible Factor	2/15	0.0090	0.411

Table 3.1 Top 10 pathways affected by DEGs in keratinocytes overexpressing KLK5

Pathway analysis was matched with KEGG database to find top 10 differential pathways influenced by KLK5 overexpression in keratinocytes. FDR=false discovery rate.

3.2.3 Transcriptomes in individuals

During data analysis, it was noticed that there were baseline differences of transcriptome among individuals (**Figure 3.6**). As only three donors were used for RNA-seq, the accuracy of analysis using pooled data from three individuals might be affected. In addition, it was noticed that the overexpression levels of KLK5 in three donors varied with 3.4-fold increase in the Donor 1, but 1.9-fold and 1.7-fold increase in Donor 2 and 3.

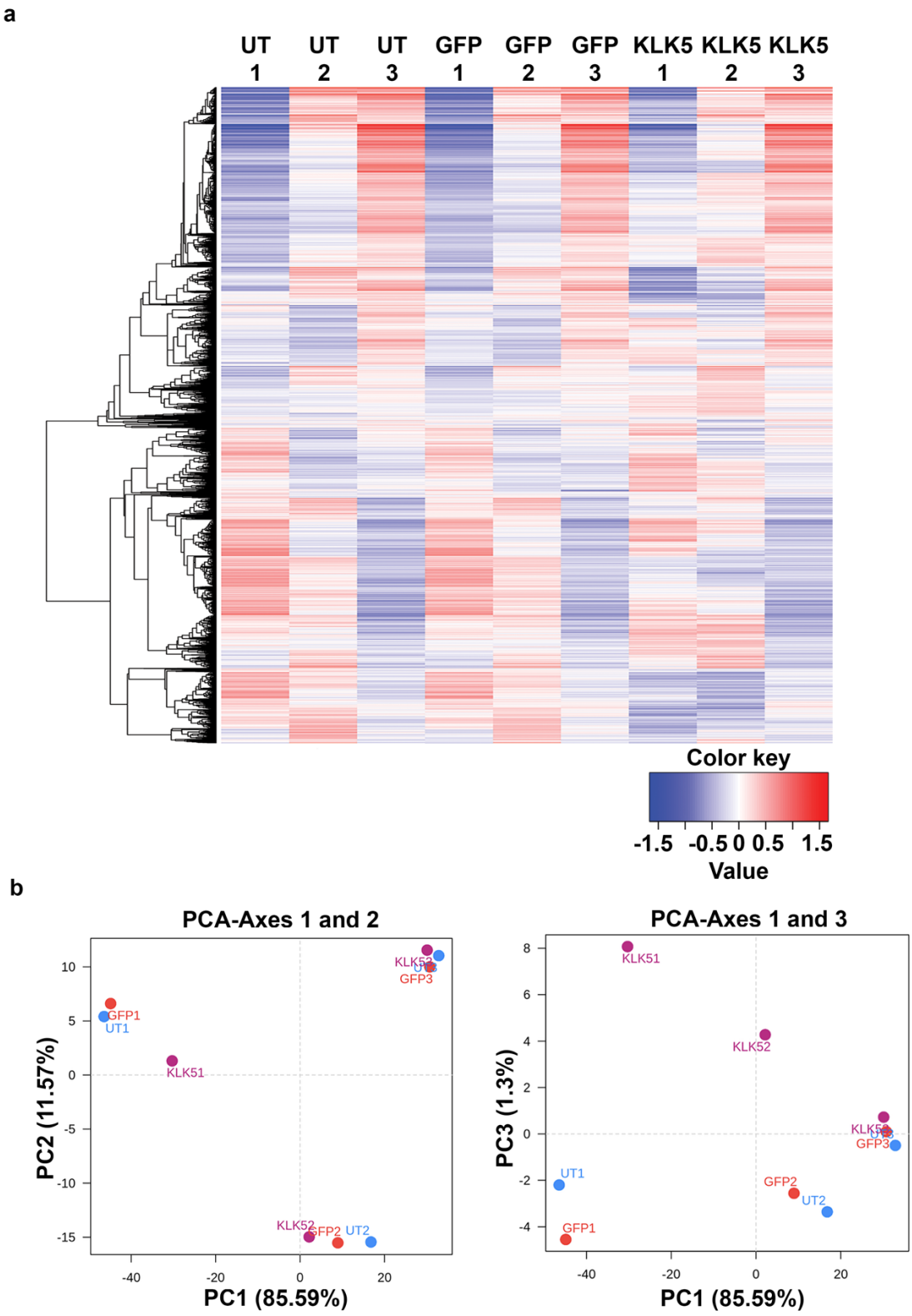

Figure 3.6 The baseline of transcriptomes in individual donors

Heatmap of transcriptomes analysed using the software iDEP showed individual variations of baseline transcriptomes in three donors (a). This was further confirmed by principal component analysis by detangling different factors (b). UT=untransduced keratinocytes. KC-GFP=keratinocytes transduced with LV-GFP. KC-KLK5=keratinocytes transduced with LV-KLK5. PCA=Principal component analysis.

Based on this, individual datasets were further checked. A cut-off of equal to or more than 2-fold changes ($|Log_2FoldChange| \geq 1$) of gene expression was used to identify DEGs between KC-UT, KC-GFP and KC-KLK5 in individuals. This was because mean value and statistical significance could not be analysed in individual dataset. The first comparison was conducted between KC-UT and KC-GFP cells to check the effect of lentiviral backbone with *GFP* reporter gene on transcriptome. The results showed that apart from one up-regulated DEG called X-inactive specific transcript (*XIST*) in the Donor 2, there was no other DEGs between KC-UT and KC-GFP cells in all three individual datasets. The *XIST* gene showed a 3-fold upregulation in KC-GFP cells compared to KC-UT cells but only 1.4-fold up-regulated expression in KC-KLK5 compared to KC-UT cells in Donor 2. This change was not observed in Donor 1 and 3. *XIST* is a non-coding RNA on the X chromosome of the placental mammals that acts as a major effector of the X-inactivation process, which might be less related to KLK5 regulation. The outcome of KC-UT and KC-GFP comparison revealed that there was no significant difference of transcriptome in the cells transduced with LV-GFP, indicting a neglected effect of lentiviral backbone. In contrast, there were 143 DEGs in Donor 1 and 102 DEGs in Donor 2 between KC-GFP and KC-KLK5 cells (**Appendix 4**). However, there was no DEGs in the Donor 3. This might be due to the lower level of KLK5 overexpression in the Donor 3 (only 1.7-fold change). The protein interactions among these DEGs in Donor 1 and 2 were also analysed (**Section 2.7**). Results showed the TGF-β signaling was on the top of the list in both donors. Apart from the TGF-β signaling, the genes related to p53 signaling were listed at the 3rd position with up-regulated expressions in the Donor 1 but

not in Donor 2 (**Table 3.2**). This result suggested that the TGF-β signaling might be the most affected pathway in keratinocytes with overexpressed KLK5.

Donor	Pathway name	Genes involved	p-value	FDR
1	Downregulation of TGF-beta receptor signaling	3/28	0.003	0.409
1	Interferon alpha/beta signaling	6/129	0.003	0.409
1	TP53 regulates metabolic genes	5/126	0.011	0.433
2	RAB GEFs exchange GTP for GFP on RABs	4/94	0.005	0.293
2	Circadian Clock	4/105	0.008	0.293
2	Downregulation of TGF-beta receptor signaling	2/28	0.018	0.293

Table 3.2 Pathways affected by DEGs in KC-KLK5 cells from each individual

Differential pathways in each individual were analyzed by KEGG database. FDR=false discovery date.

3.3 The confirmation of DEGs by RT-qPCR

As the DEGs found in RNA-seq datasets were from small sample size (n=3), DEGs selected from RNA-seq analysis (**Appendix 3 and 4**) were further confirmed in more donors using RT-qPCR. The *TGFBR1* was selected since it is the key gene in the TGF-β pathway. Apart from this, the top five genes in the DEG list (**Appendix 3 and 4**) related to epidermal barrier formation were selected (**Table 3.3**).

Genes	Log_2Fold change between KC-KLK5 vs KC-GFP	Gene ontology	Source of dataset
TGFBR1	-0.7	Epidermal formation; Immune response	Pooled dataset
LCE3D	3.6	Epidermal formation	1st donor
FLG2	2.2	Epidermal formation	1st donor
ASPRV1	2.1	Epidermal formation	1st donor
CRCT1	1.7	Epidermal formation	1st donor
SPRR2E	1.6	Epidermal formation	1st donor

Table 3.3 Candidate genes selected for RT-qPCR

Four healthy donors were used for this study (Donor 1, 4, 5 and 6, **Table 2.1**). Primary keratinocytes isolated from these donors were transduced with LV-GFP or LV-KLK5, cultured for 7 days and harvested for RNA (**Section 2.5**). UT-KC cells were run in parallel. The overexpression of KLK5 in transduced cells were

confirmed by RT-qPCR and Western blotting (**Figure 3.7**). Both mRNA and protein levels of KLK5 showed more than 3-fold increase in all four donors.

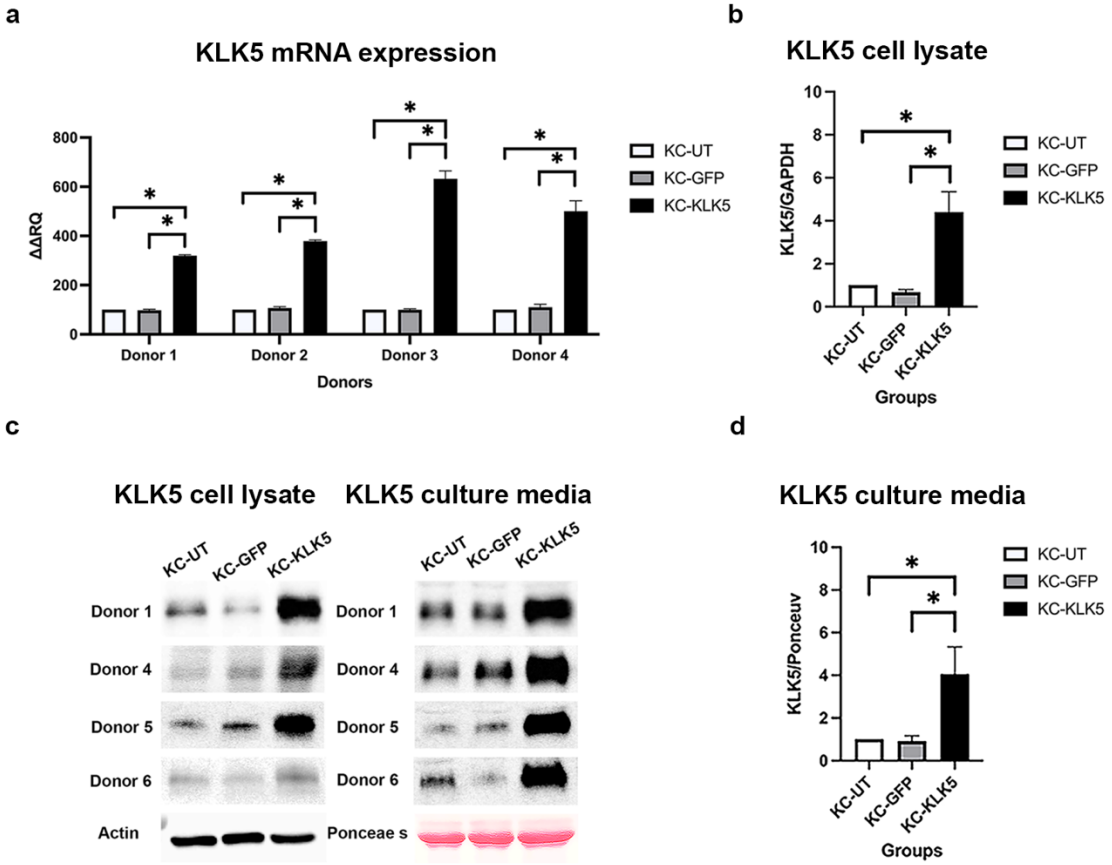

Figure 3.7 mRNA and protein expressions of KLK5 in cells transduced with LV-KLK5

*Primary keratinocytes obtained from 4 donors were transduced with LV-GFP or LV-KLK5 or without transduction. The expression of KLK5 in all cells was confirmed at mRNA level (a) and protein level (c). The densitometry analysis showed significant increase of KLK5 expression in KC-KLK5 cells (b and d). *p≤0.05, n=4. Error bar=standard error. KC-UT=untransduced cells. KC-GFP=keratinocytes transduced with LV-GFP. KC-KLK5=keratinocytes transduced with LV-KLK5.*

As the sample from the 1st donor were used in both RNA-seq and RT-qPCR test, the levels of DEG expressions measured by RNA-seq and RT-qPCR were firstly compared to check the correlation between two assays. The results showed that there were similar trends of gene expressions between two methods (**Figure 3.8**). *TGFBR1* showed a downregulation in KC-KLK5 compared to KC-GFP cells in

both assays. *LCE3D, ASPRV1, CRCT1* and *SPRR2E* showed upregulations in both tests. However, there was no change of *FLG2* gene between KC-KLK5 and KC-GFP cells by RT-qPCR, although it was increased in RNA-seq assay (**Figure 3.8**). These results suggest that two methods have different sensitivities, but similar trends of gene expressions were still observed.

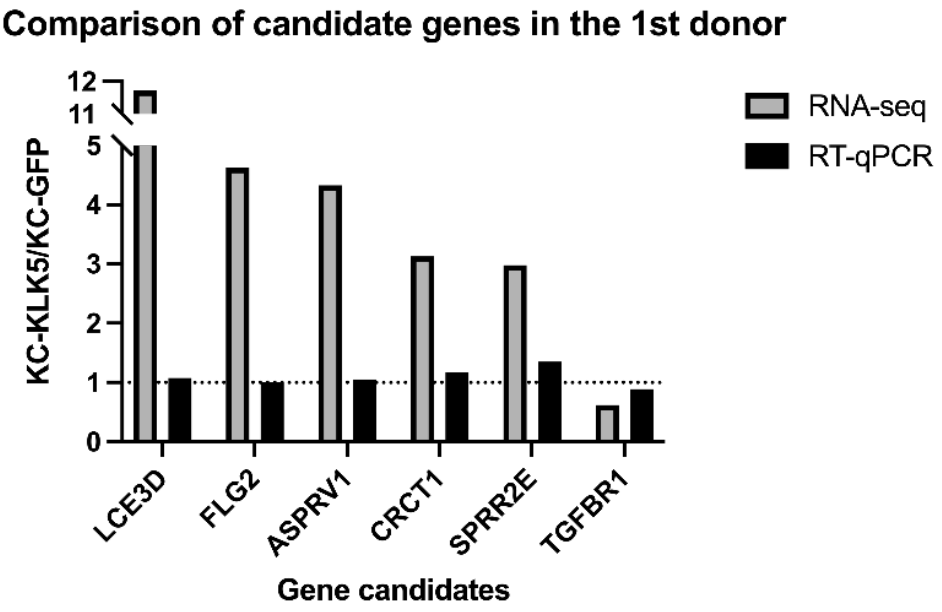

Figure 3.8 The comparison of candidate gene expressions in the Donor 1 using RNA-seq and RT-qPCR

The expressions of selected genes in the 1st donor measured by RNA-seq and RT-qPCR were compared. The fold change of each gene mRNA level in KC-KLK5 cells was calculated against KC-GFP. The dash line showed the unchanged level as 1. Genes with the fold change over the line were upregulated, while the ones under the line were downregulated genes.

Next, the expressions of the six candidate genes in four donors were analysed. *TGFBR1* and *FLG2* expressions significantly decreased in KC-KLK5 compared to KC-GFP cells (**Figure 3.9, Section 2.18,** $p \leq 0.05$, n=4). This result was partially consistent with previous RNA-seq data as *TGFBR1* expression in both methods declined. Although FLG2 was up-regulated in KC-KLK5 cells from RNA-seq data, its expression decreased in KC-KLK5 cells compared to KC-GFP cells in RT-

qPCR where more than 4 donors were tested. There were no significant changes in other four gene expressions, *ASPRV1, CRCT1, LCE3D* and *SPRR2E*, in KC-KLK5 compared to KC-GFP cells (**Figure 3.9, Section 2.18,** p>0.05 n=4).

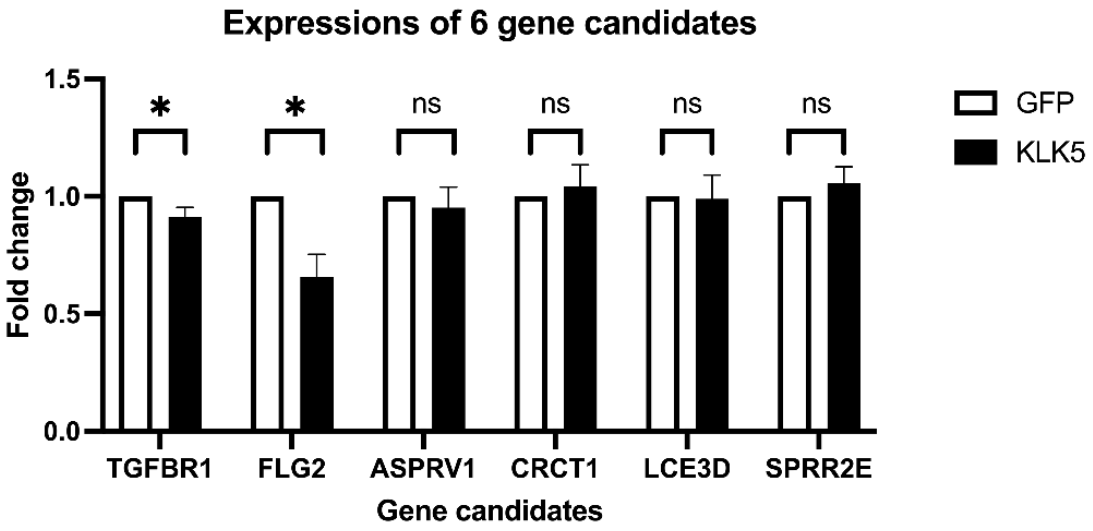

Figure 3.9 Six candidate genes expressions assessed by RT-qPCR

*Expressions of gene candidate genes were measured using RT-qPCR. TGFBR1 and FLG2 expressions were significantly reduced in KC-KLK5 compared to KC-GFP cells, while other four genes did not change significantly. *p≤0.05. NS=non-significant. n=4. Error bar=standard error.*

3.4 Summary

To investigate the influence of overexpressed KLK5 in primary keratinocytes, the transcriptome in cells with overexpressed KLK5 was examined and compared to those in cells transduced with LV-GFP and untransduced cells. Results showed TGF-β signaling was on the top list of protein interactions. Further checking using qRT-PCR with more donors showed significantly down-regulated *TGFBR1* expression. The decreased expression of TGF-β 1 receptor was reported to attenuate the binding of TGF-β 1 cytokine, potentially causing reduced phosphorylation of downstream factors like SMAD2/3 and inactivating the TGF-β signaling, consequently resulting in regulations of cell proliferation and differentiation (Vander Ark, Cao et al. 2018). A study in immortalized human

keratinocyte cell line HaCaT cells revealed that increased TGF-β 1 was associated with the elevation of calcium concentration in culture medium, which could drive HaCaT keratinocytes differentiation. This suggested that there might be a relation between TGF-β 1 signaling and keratinocytes differentiation (Hang-Rae Cho 2004). In addition, it was also noticed that the loss of function mutation in *TGFBR1* gene enabled rapid development of cutaneous squamous cell carcinoma through the aberrant canonical SMAD signaling (Cammareri, Rose et al. 2016). Previous studies also reported that the TGF-β signaling was a crucial regulator for inflammatory response (Tzavlaki and Moustakas 2020). It could inhibit IL-2 production and hinder naïve T cell activation and differentiation (Das and Levine 2008, Liarte, Bernabe-Garcia et al. 2020).

Apart from *TGFBR1*, the result also revealed a reduction of *FLG2* expression in keratinocytes with KLK5 overexpression using RT-qPCR. However, FLG2 showed an upregulation in RNA-seq in Donor 1, which could be donor variation as only one out of four donors was up-regulated and *FLG2* expression in other three donors was down-regulated as assessed by RT-qPCR. Studies showed *FLG2* gene sequence and protein structure are similar to *FLG*, an early differentiated protein involved in stratum corneum development. Based on these, it was suspected that the function of *FLG* and *FLG2* might be similar, specifically the role in skin barrier (Wu, Hansmann et al. 2009, Margolis, Gupta et al. 2014). Studies have shown that the terminal part of FLG2 was one of the components in cornified envelopes, suggesting a role of FLG2 in epidermal barrier formation (Alberola, Schroder et al. 2019). FLG and FLG2 also co-localized and both proteins were found decreased in the AD lesional skin (Wu, Hansmann et al. 2009, Pellerin, Henry et al. 2013). As KLK5 could indirectly process Profilaggrin via

Elastase 2 or potentially directly cleave Profilaggrin (Bonnart, Deraison et al. 2010, Sakabe, Yamamoto et al. 2013), KLK5 might also affect FLG2 protein processing. *FLG2* may be a potential target influenced by KLK5 overexpression in keratinocytes, but more donors are required to confirm this.

Chapter 4: KLK5 overexpression-induced pro-inflammatory cytokines mildly facilitate Th2 differentiation in $CD4^+$ T cells

Th2 skewed immune response is one of the characteristics in AD. It is defined by the activation and differentiation of Th2 cells in response to specific antigens, which orient from $CD4^+$ T cells, a type of T cells. As a vital coordinator of adaptive immune response, $CD4^+$ T cells can differentiate into various subsets upon encountering antigens and processing ligands provided by the antigens, and then initiate downstream signaling, including Th2 cells by pro-inflammatory/inflammatory cytokines such as TSLP and IL-4 (He, Oyoshi et al. 2008, Tatsuno, Fujiyama et al. 2015, Wallmeyer, Dietert et al. 2017). Th2 cells play a pivotal role in orchestrating the immune response and drive antibody-mediated immune defensive system by releasing cytokines such as IL-4, IL-5 and IL-13, which were found in patients with AD (Langan, Irvine et al. 2020, Stander 2021). A previous study reported that there were increased pro-inflammatory cytokines such as TSLP and IL-8 in primary keratinocytes with KLK5 overexpression (Zhu, Underwood et al. 2017, Das, Mounika et al. 2022). I speculated that increased pro-inflammatory cytokines and chemokines in keratinocytes with KLK5 overexpression might facilitate $CD4^+$ T cells differentiating to Th2.

In this study, a $CD4^+$ T cell differentiation assay (Yanez, Lau et al. 2019) was used to evaluate whether keratinocytes overexpressing KLK5 could derive Th2 differentiation. Naïve $CD4^+$ T cells from human peripheral blood mononuclear cells (PBMCs) were isolated from healthy donors' blood and activated *in vitro* by antibodies. Instead of culturing activated T cells in Roswell Park Memorial Institute 1640 medium (RPMI), the conditional medium collected from KC-KLK5 cells were used to assess whether pro-inflammatory cytokines and chemokines secreted from keratinocytes with overexpression KLK5 affect T cells

differentiation. The specific Th2-cell differentiation marker GATA3 was used to assess the differentiation (**Figure 4.1b**).

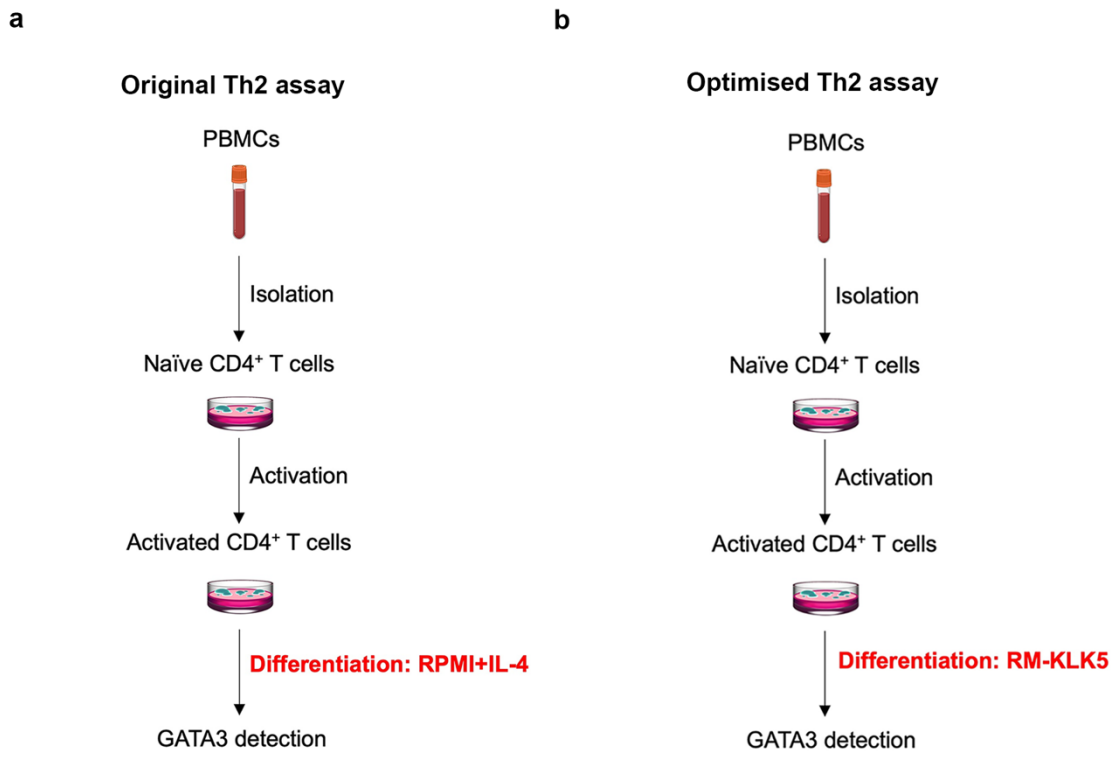

Figure 4.1 The workflow of Th2 differentiation assay

In the original Th2 assay, naïve $CD4^+$ T cells were isolated from peripheral blood and activated by anti-CD3/CD28 antibodies. Cells were then cultured in RPMI media with IL-4 for T cell differentiation (a). Instead of RPMI medium, the conditional media collected from KC-KLK5 cells were used for assessing Th2 differentiation in naïve $CD4^+$ T cells (b).

4.1 Naïve $CD4^+$ T cells were activated and differentiated in RM^+ medium

Naïve $CD4^+$ T cells from healthy donors 7,8 and 9 (**Table 2.1**) were isolated and purified from PBMCs (**Section 2.12 and 2.13**). The mean purity of naïve $CD4^+$ T cells evaluated by cell markers $CD4^+CD45RA^+CD45RO^-$ was 90.1%±4.1% (**Figure 4.2 a and c, Table 4.1**). The Th2 differentiation cell marker GATA3 was also checked in purified cells to ensure there was few or no Th2 cells in the purified cells. The mean percentage of GATA3 was 0.6%±0.3% (**Figure 4.2b and d, Table 4.1**).

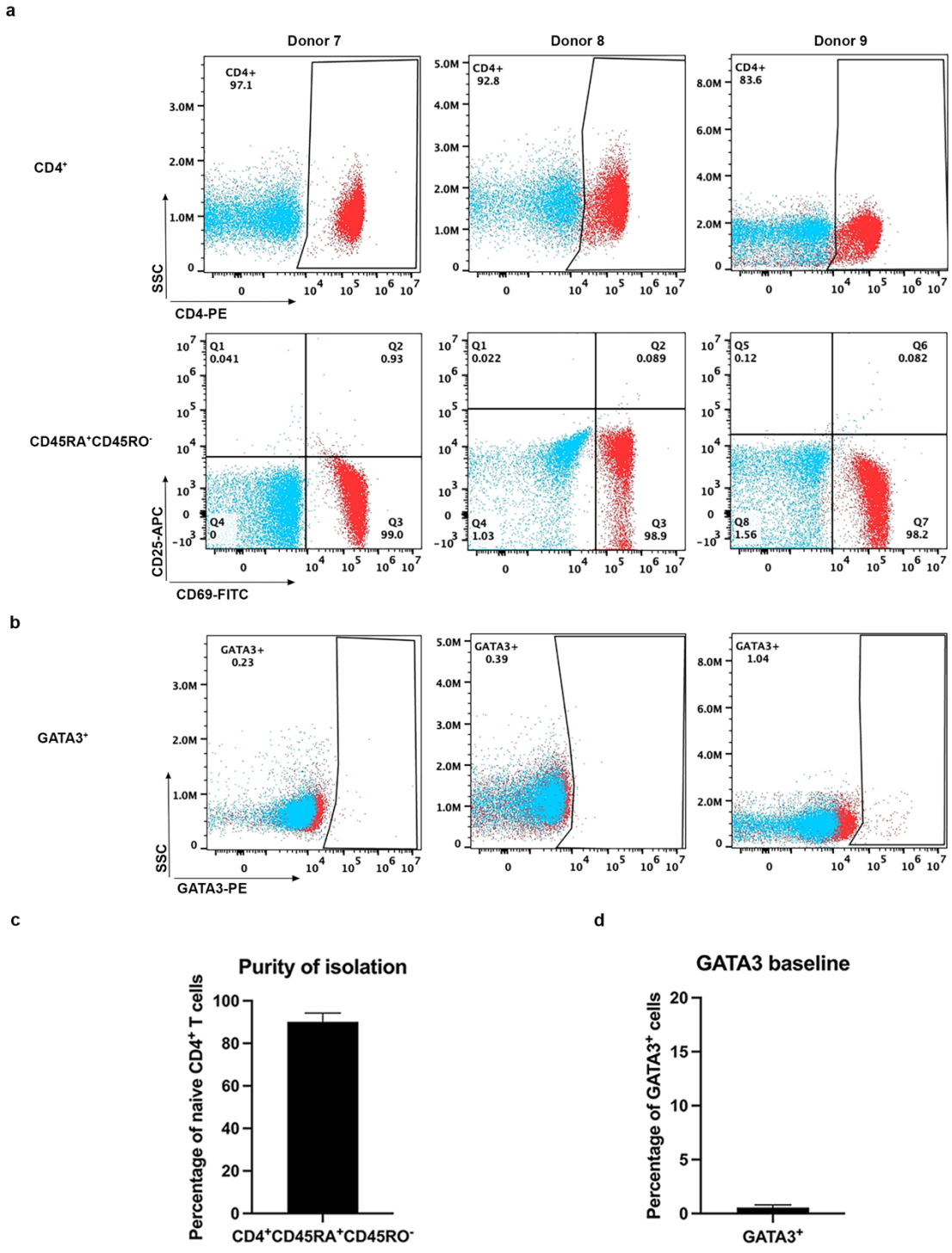

Figure 4.2 The purity of isolated naïve CD4$^+$ T cells

Positively stained naïve CD4$^+$ T cells confirmed by CD4$^+$CD45RA$^+$CD45RO$^-$ were showed in a (red dots). High purification rate in isolated CD4$^+$ cells was achieved in all three donors (c). The population of Th2 differentiated cells were checked by Th2 cell marker GATA3 (b) and few or no GATA3$^+$ cells were detected among the isolated cells (d). The isotypes were used as negative control (blue dots). Error bar=standard error.

Donor	Purity of isolation ($CD4^+CD45RA^+CD45RO^-$)	GATA3 baseline ($GATA3^+$)
7	96.1%	0.2%
8	91.9%	0.4%
9	82.3%	1.0%
Mean±SE	90.1%±4.1%	0.6%±0.3%

Table 4.1 Purity of naïve $CD4^+$ T cells

Purified naïve $CD4^+$ T cells were cultured in RPMI or RM^+ media, activated using anti-CD3 and anti-CD28 antibodies and differentiated by adding IL-4, which was used as positive control (**Section 2.14**). Media without IL-4 were used as negative control. Cell viability was checked once by Propidium Iodide (PI) staining and detected by flow cytometry. The cell deaths in all conditions were less than 10%, indicating human $CD4^+$ T cells could be cultivated in RM^+ media (**Figure 4.3f**). The activation rate detected by the $CD25^+$ and $CD69^+$ populations in naïve $CD4^+$ T cells was similar among cells cultured in RPMI+IL-4 medium and in RPMI alone (71.8%±2.2% vs 56.4%±4.0%, $p>0.05$, n=3, **Figure 4.3e, Table 4.2**). Similarly, the activation rate in cells cultured in RM^++IL-4 condition was also close to cells cultured in RM^+ media alone (58.8%±5.4% vs 35.4%±16.2%) **(**$p>0.05$, n=3, **Figure 4.3e, Table 4.2**). All these suggested that cells cultured in different media had the same activation capacity.

Donor	Activation (Non $CD25^-CD69^-$)			
	RPMI	RPMI+IL-4	RM^+	RM^++IL-4
7	56.0%	74.2%	16.0%	52.2%
8	49.7%	66.8%	22.6%	54.6%
9	63.6%	72.5%	67.6%	69.5%
Mean±SE	56.4%±4.0%	71.2%±2.2%	35.4%±16.2%	58.8%±5.4%

Table 4.2 Percentages of activated $CD4^+$ T cells

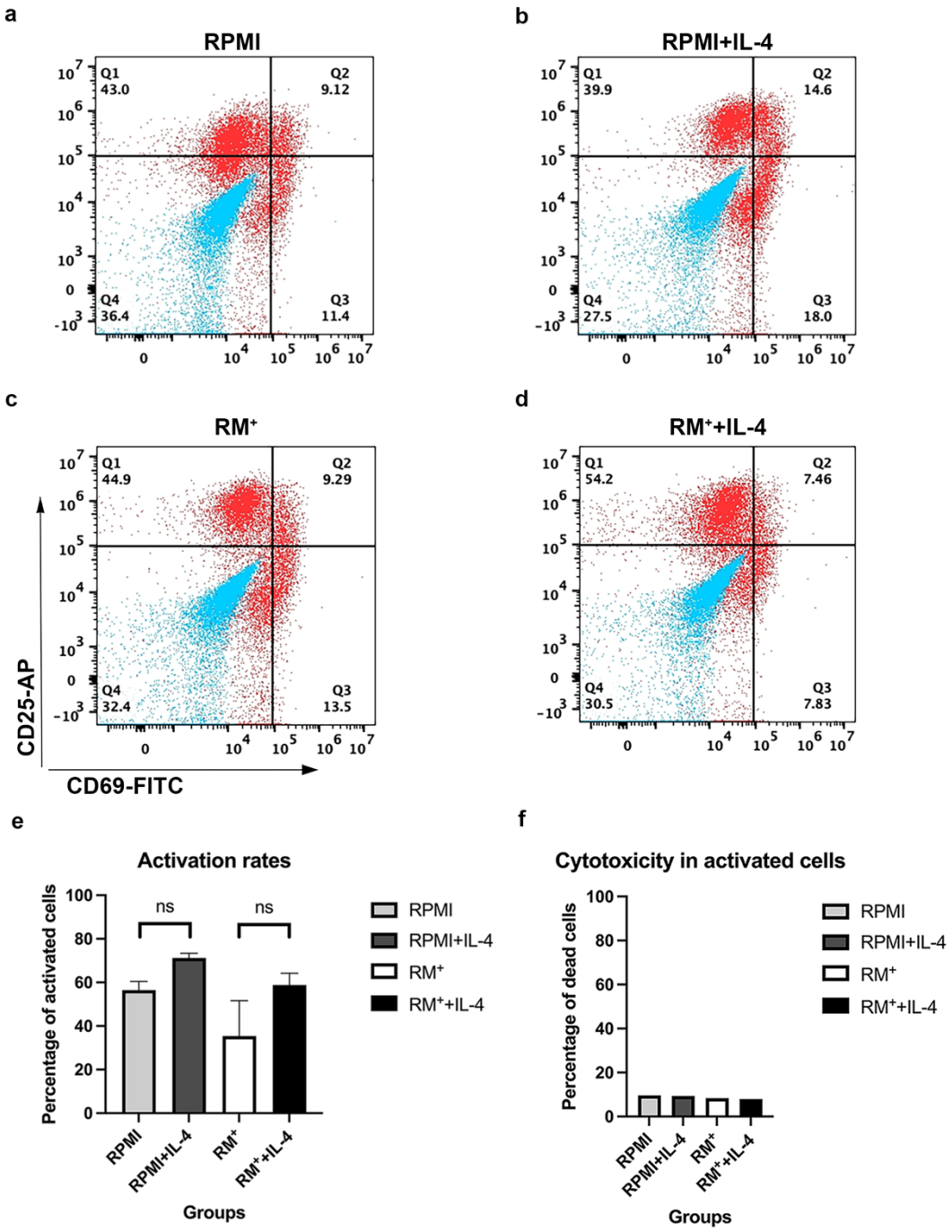

Figure 4.3 Activation rates of naïve CD4$^+$ T cells

Naïve CD4$^+$ T cells were activated by anti-CD3/CD28 antibodies and activation rates were measured by the markers CD25, CD69 and CD25+CD69 using flow cytometry. The representative positively stained cells (red dots) were showed in a-d with the isotype controls (blue dots). The activation rates were increased in cells with RPMI+IL-4 and RM$^+$+IL-4 compared to their controls (i). The cell deaths which were only assessed once were less than 10% (j). P=0.05, n=3. NS=no significant difference. Error bar=standard error.

Differentiation rate in activated $CD4^+$ T cells was further evaluated by measuring $GATA3^+$ cells. There was significant increase of $GATA3^+$ cells in cells cultured with RPMI+IL-4 medium compared to those in RPMI medium (30.6%±0.9% vs 7.5%±3.7%, p≤0.05, n=3, **Figure 4.4** and **Table 4.3**). Similarly, the percentage of $GATA3^+$ in cells cultured in RM^++IL-4 medium was significantly higher than that in RM^+ medium (52.0%±9.9% vs 28.7%±1.9%, p≤0.05, n=3, **Table 4.3**). It was noticed that the percentage of GATA3 positive cells in RM^+ medium was higher than that in RPMI medium. This was due to RM^+ medium contained six supplements (**Section 2.5**). Some supplements, for example, epidermal growth factor could induce Th2 differentiation in activated $CD4^+$ T cells (Zeboudj, Maitre et al. 2018). Considering this, RM^+ medium was used as baseline medium for assay control.

Donor	Differentiation ($GATA3^+$)			
	RPMI	RPMI+IL-4	RM^+	RM^++IL-4
7	4.0%	32.5%	29.3%	40.6%
8	15.0%	29.8%	25.0%	71.8%
9	3.4%	29.7%	31.7%	43.6%
Mean±SE	7.5%±3.8%	30.6%±0.9%	28.7%±1.9%	52.0%±9.9%

Table 4.3 Details of optimised Th2 differentiation

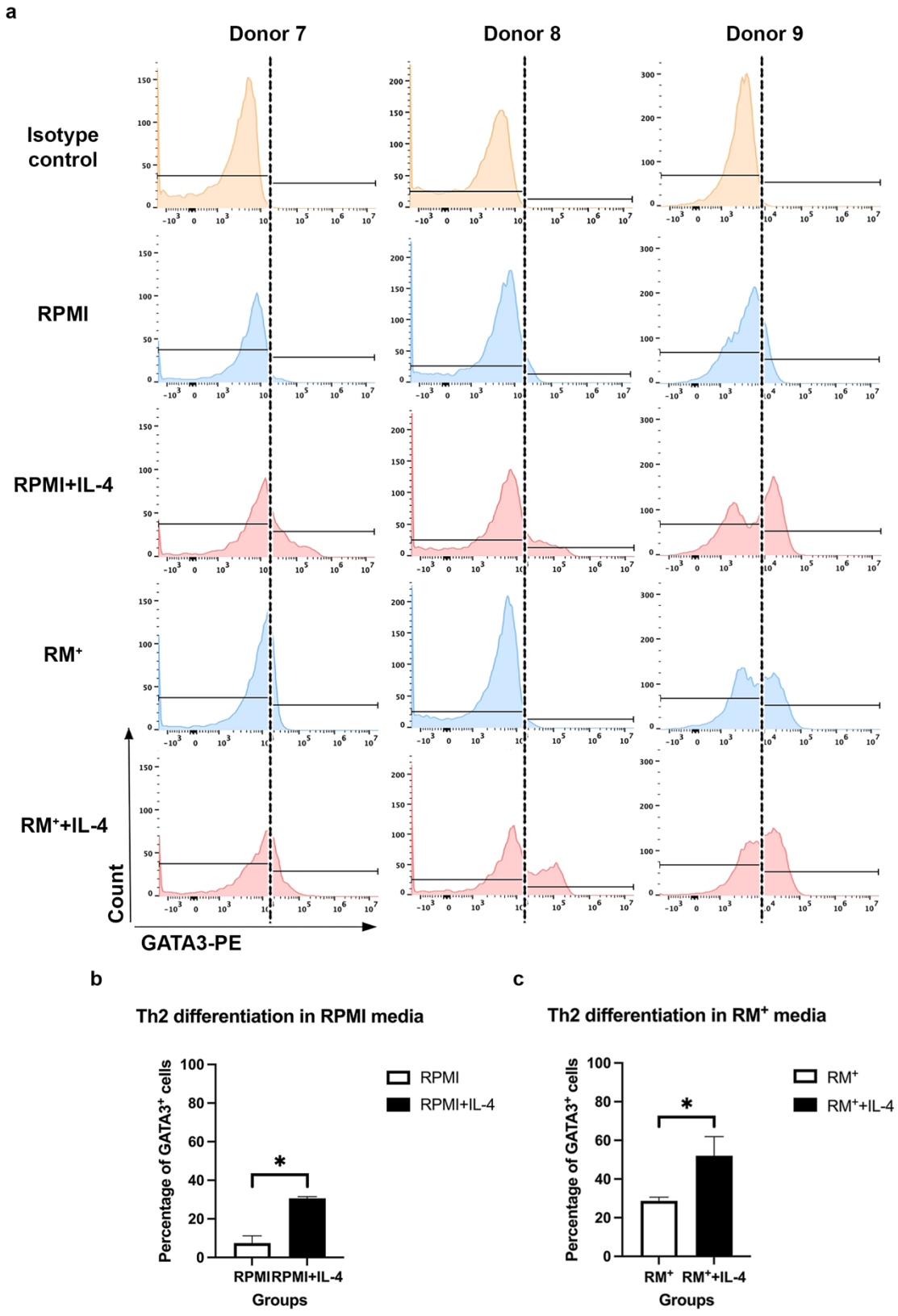

Figure 4.4 Th2 population in activated CD4$^+$ T cells in RPMI and RM$^+$ cultures

*Histograms for differentiated CD4$^+$ T cells assessed by GATA3$^+$ T cells in three donors using flow cytometry were shown in a. Results showed significantly increased Th2 differentiated cells in RPMI+IL-4 compared to cells cultured in RPMI culture (b) and in RM$^+$+ IL-4 medium compared to those cultured in RM$^+$ (c). *p≤0.05. n=3. Error bar=standard error.*

4.2 Increased cytokines in the conditional medium from KC-KLK5 cell culture

To evaluate whether keratinocytes with overexpressed KLK5 secreted cytokines/chemokines that might interact with T cells, the multi-spot assay kits (**Section 2.11**) which contained antibodies detecting IL-1β, IL-2, IL-4, IL-6, IL-8, IL-10, IL12p70, IL-13, IFN-γ, TNF-α and TSLP were used to check pro-inflammatory cytokines/chemokines in the conditional media collected from KC-KLK5 cultures (**Section 2.5**) from Donor 4, 5 and 6. There were significantly increased IL-6 and decreased TSLP expression in the RM-KLK5 conditional media compared to RM-GFP and RM-UT media (**Figure 4.5**). Although IL-2 expression was not found elevated with statistical difference, its expression in RM-KLK5 conditional media was slightly higher than that in RM-GFP and RM-UT media (**Figure 4.5**). It has been reported that IL-2 and IL-6 could regulate immune response, especially in facilitating Th2 differentiation among $CD4^+$ T cells and priming IL-4 production (Doris A. Morgan, Francis W. Ruscetti et al. 1976, Diehl, Chow et al. 2002, Ross and Cantrell 2018). It was also reported up-regulated TSLP in AD lesional skin (Soumelis, Reche et al. 2002), eczematous-like skin in transgenic mice with induced TSLP and elevated TSLP in keratinocytes with the overexpression of KLK5 (Zhu, Underwood et al. 2017). However, my results showed a decreased TSLP expression in keratinocytes overexpressing KLK5, which was controversial with these fundings. There were no significant changes of IL-1β, IL-4, IL-8, IL-10, IL-13 and TNF-α expressions in RM-KLK5 medium compared to RM-GFP and RM-UT media (**Figure 4.5**). The level of IL-12p70 and IFN-γ expression were undetectable in all groups.

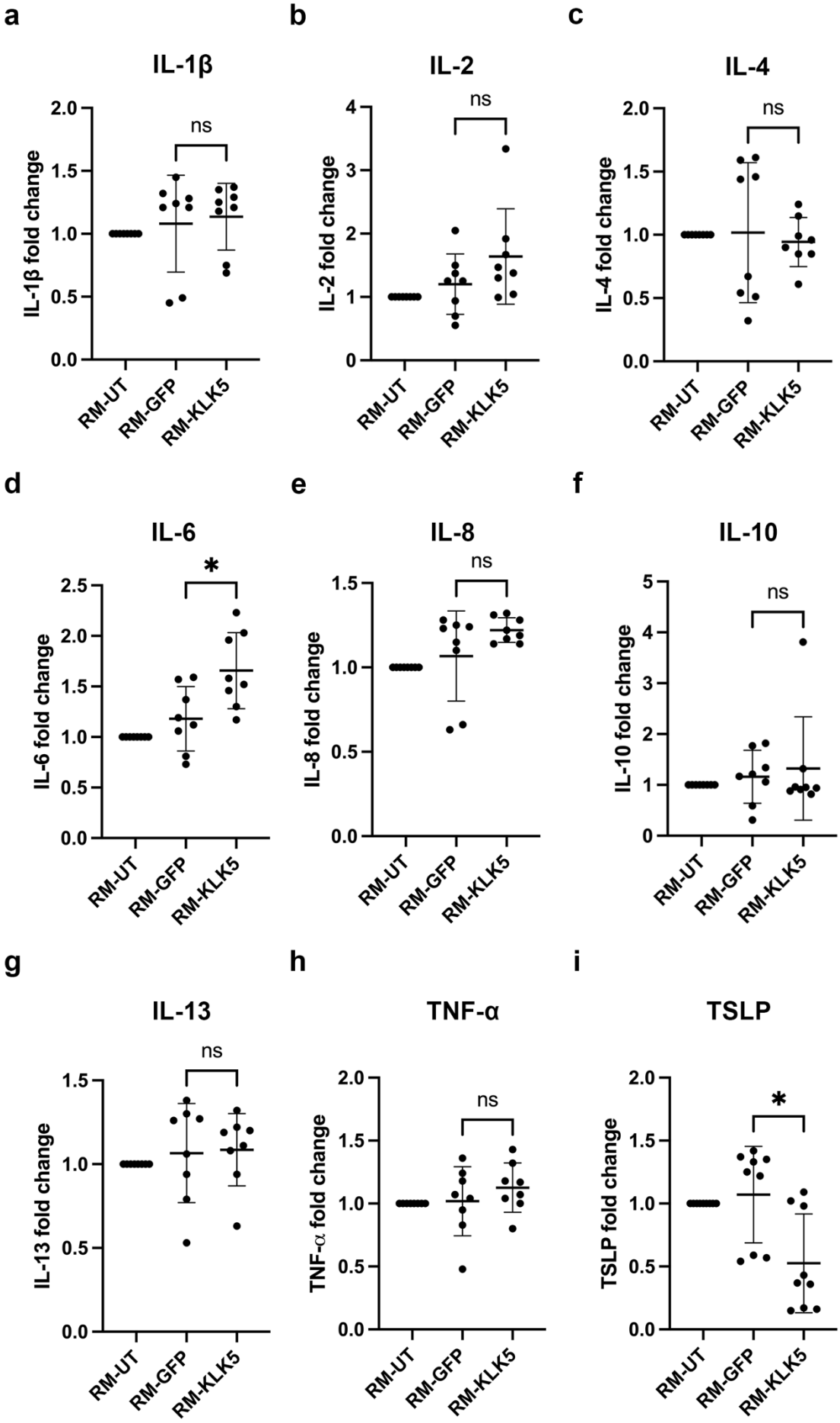
a
IL-1β
IL-1β fold change
2.0
1.5
1.0
0.5
0.0
ns
RM-UT
RM-GFP
RM-KLK5
b
IL-2
IL-2 fold change
4
3
2
1
0
ns
RM-UT
RM-GFP
RM-KLK5
c
IL-4
IL-4 fold change
2.0
1.5
1.0
0.5
0.0
ns
RM-UT
RM-GFP
RM-KLK5
d
IL-6
IL-6 fold change
2.5
2.0
1.5
1.0
0.5
0.0
*
RM-UT
RM-GFP
RM-KLK5
e
IL-8
IL-8 fold change
1.5
1.0
0.5
0.0
ns
RM-UT
RM-GFP
RM-KLK5
f
IL-10
IL-10 fold change
5
4
3
2
1
0
ns
RM-UT
RM-GFP
RM-KLK5
g
IL-13
IL-13 fold change
1.5
1.0
0.5
0.0
ns
RM-UT
RM-GFP
RM-KLK5
h
TNF-α
TNF-α fold change
2.0
1.5
1.0
0.5
0.0
ns
RM-UT
RM-GFP
RM-KLK5
i
TSLP
TSLP fold change
2.0
1.5
1.0
0.5
0.0
*
RM-UT
RM-GFP
RM-KLK5

Figure 4.5 Cytokine expressions in the conditional media collected from keratinocytes overexpressing KLK5

*A panel of cytokines were examined for the culture media from KC-UT, KC-GFP and KC-KLK5 cells. IL-6 was significantly increased in RM-KLK5 group, while TSLP showed significant decrease in RM-KLK5 group. There is a slightly elevated IL-2 expression in RM-KLK5 conditional media compared to RM-GFP and RM-UT group. No significant differences of IL-1β, IL-4, IL-8, IL-10, IL-13 and TNF-α were noticed among RM-KLK5, RM-GFP and RM-UT group. *p≤0.05. NS=non-significant difference. n=3. Error bar=standard deviation. RM-UT=conditional media from untransduced keratinocytes. RM-GFP=conditional media from keratinocytes transduced with LV-GFP. RM-KLK5=conditional media from keratinocytes transduced with LV-KLK5.*

4.3 RM-KLK5 conditional media did not significantly drive naïve CD4+ T cells to Th2 differentiation

The conditional media from KC-KLK5 cells were collected and pooled (RM-KLK5). In the meantime, the media from KC-UT and KC-GFP cells were also collected as RM-UT and RM-GFP for controls (**Section 2.5**). The activated KLK5 level in the media was confirmed by Western blotting and RT-qPCR after normalised to Ponceau S and GAPDH respectively. There was a 5.4-fold increase of KLK5 in the RM-KLK5 compared to RM-GFP (**Figure 4.6**). These media were used for T cell cultures.

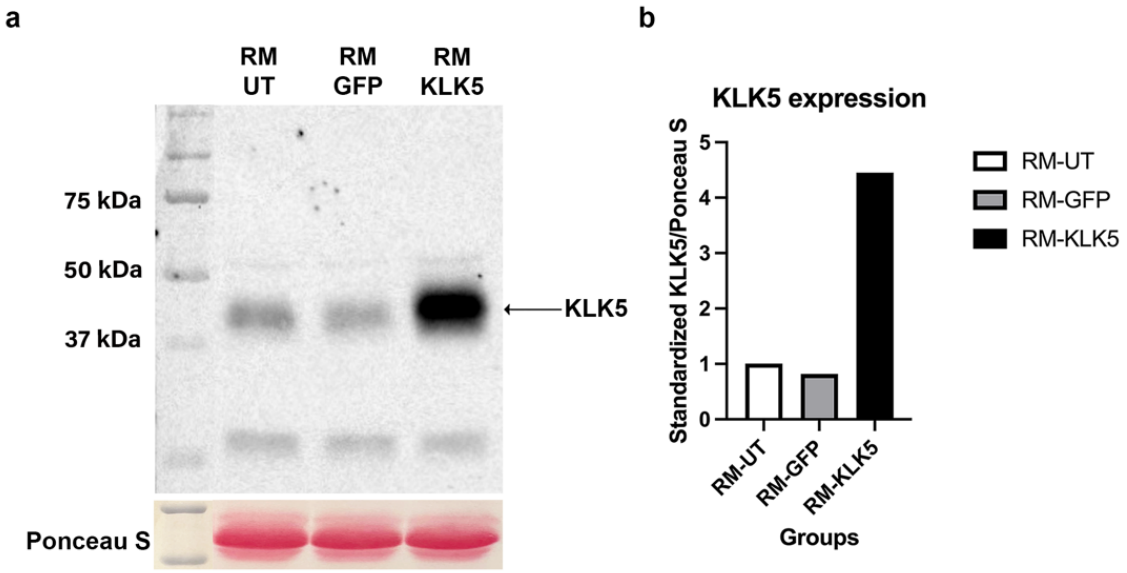

Figure 4.6 The secreted KLK5 level in the conditional media

The level of KLK5 in the conditional media from KC-KLK5 cells was examined by Western blotting (a). It showed increased expression in RM-KLK5 group compared to RM-UT and RM-GFP groups. The KLK5 expression level was quantified by densitometry (b). RM-UT= conditional media from untransduced keratinocytes. RM-GFP=conditional media from keratinocytes transduced with LV-GFP. RM-KLK5=conditional media from keratinocytes transduced with LV-KLK5.

Naïve $CD4^+$ T cells from six healthy donors were isolated (**Section 2.1 and 2.13**) with the average purity of 87.6%±3.0% (**Figure 4.7, Table 4.4**).

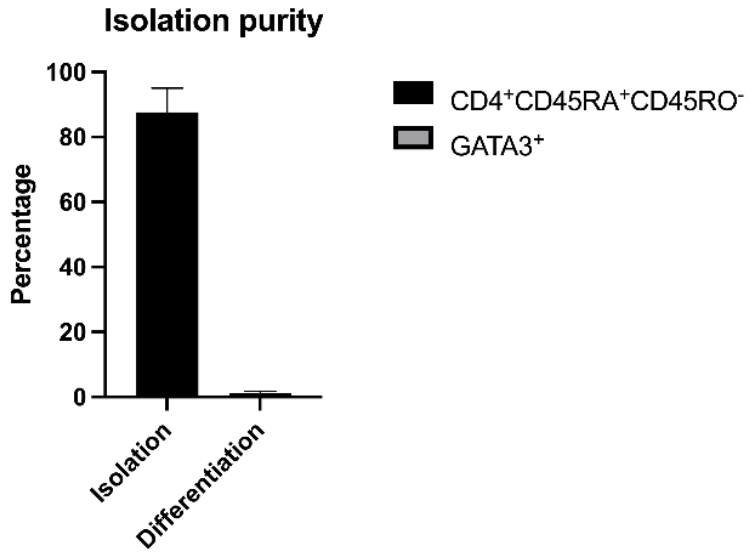

Figure 4.7 The purity of isolated naive $CD4^+$ T cells

The high purity of isolated naïve $CD4^+$ T cells was confirmed by the cell markers $CD4^+CD45RA^+CD45RO^-$ using flow cytometry. Low percentage of differentiated Th2 cells was confirmed by $GATA3^+$ marker in isolated T cells from 6 healthy donors.

Donor	Purity of isolation ($CD4^+CD45RA^+CD45RO^-$)	GATA3 baseline ($GATA3^+$)
10	90.2%	0.7%
11	82.3%	1.0%
12	90.4%	1.3%
13	88.6%	0.5%
14	97.9%	1.7%
15	76.5%	1.8%
Mean±SE	87.6%±3.0%	1.2%±0.2%

Table 4.4 Isolation purity in 6 donors

The isolated naïve $CD4^+$ T cells activated by anti-CD3/anti-CD28 antibodies were cultured in pooled RM-KLK5 conditional medium or RM-UT or RM-GFP conditional media. The average activation rate in naïve $CD4^+$ T cells cultured in RM-KLK5, RM-UT and RM-GFP were similar, which was 62.6%±10.6%, 66.0%±10.7% and 63.1%±11.4% respectively (**Figure 4.8, Table 4.5,** p>0.05, n=6).

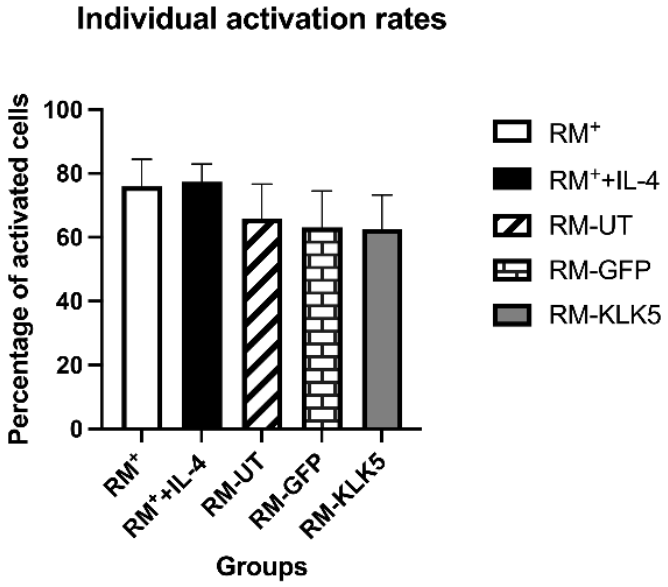

Figure 4.8 The activation rates in isolated naïve $CD4^+$ T cells

The activation among $CD4^+$ T cells following anti-CD3/CD28 antibodies treatment was assessed by $CD25^+$ or $CD69^+$ markers. Results showed more than 60% of cells could be activated in the conditional media. RM^+=normal keratinocyte media. RM^++IL-4=normal keratinocyte media with IL-4. RM-UT=conditional media from untransduced keratinocytes. RM-GFP=conditional media from keratinocytes transduced with LV-GFP. RM-KLK5=conditional media from keratinocytes transduced with LV-KLK5.

Donor	RM^+	RM^++IL-4	RM-UT	RM-GFP	RM-KLK5
Donor 10	83.1%	80.9%	77.2%	71.4%	68.9%
Donor 11	67.7%	69.5%	29.5%	51.6%	42.3%
Donor 12	70.7%	77.7%	59.3%	59.2%	58.2%
Donor 13	96.9%	95.2%	94.3%	94.8%	94.0%
Donor 14	41.8%	55.7%	43.9%	16.3%	26.1%
Donor 15	95.8%	85.4%	91.7%	85.4%	86.1%
Mean±SE	76.0%±8.5%	77.4%±5.6%	66.0%±10.7%	63.1%±11.4%	62.6%±10.6%

Table 4.5 Activation rates in 6 donors

The $GATA3^+$ cells for Th2 cell differentiation were further checked and results showed that the $GATA3^+$ cells were significantly increased in positive controls cultured in RM^++IL-4 medium, indicating the assay worked (**Figure 4.9,** $p \leq 0.05$ n=6). In the cells cultured with RM-KLK5 conditional medium, there was also an increase of $GATA3^+$ T cell population compared to those cultured in the RM-GFP and RM-UT conditional media (54.5%±8.3% vs 49.3%±8.7% and 44.6%±5.5%, **Figure 4.9).** However, this increase was not significantly different (**Table 4.6,** $p \geq 0.05$, n=6). Some donors had increased differentiation rates while others showed minor increase (**Table 4.6**). From the results of positive controls (RM^++IL-4 vs RM^+), it was noticed that there were individual variations of T cell response stimulated by IL-4. Nevertheless, these results suggested that increased pro-inflammatory cytokines/chemokines in keratinocytes induced by KLK5 overexpression could influence Th2 differentiation in naïve $CD4^+$ T cells to some extent.

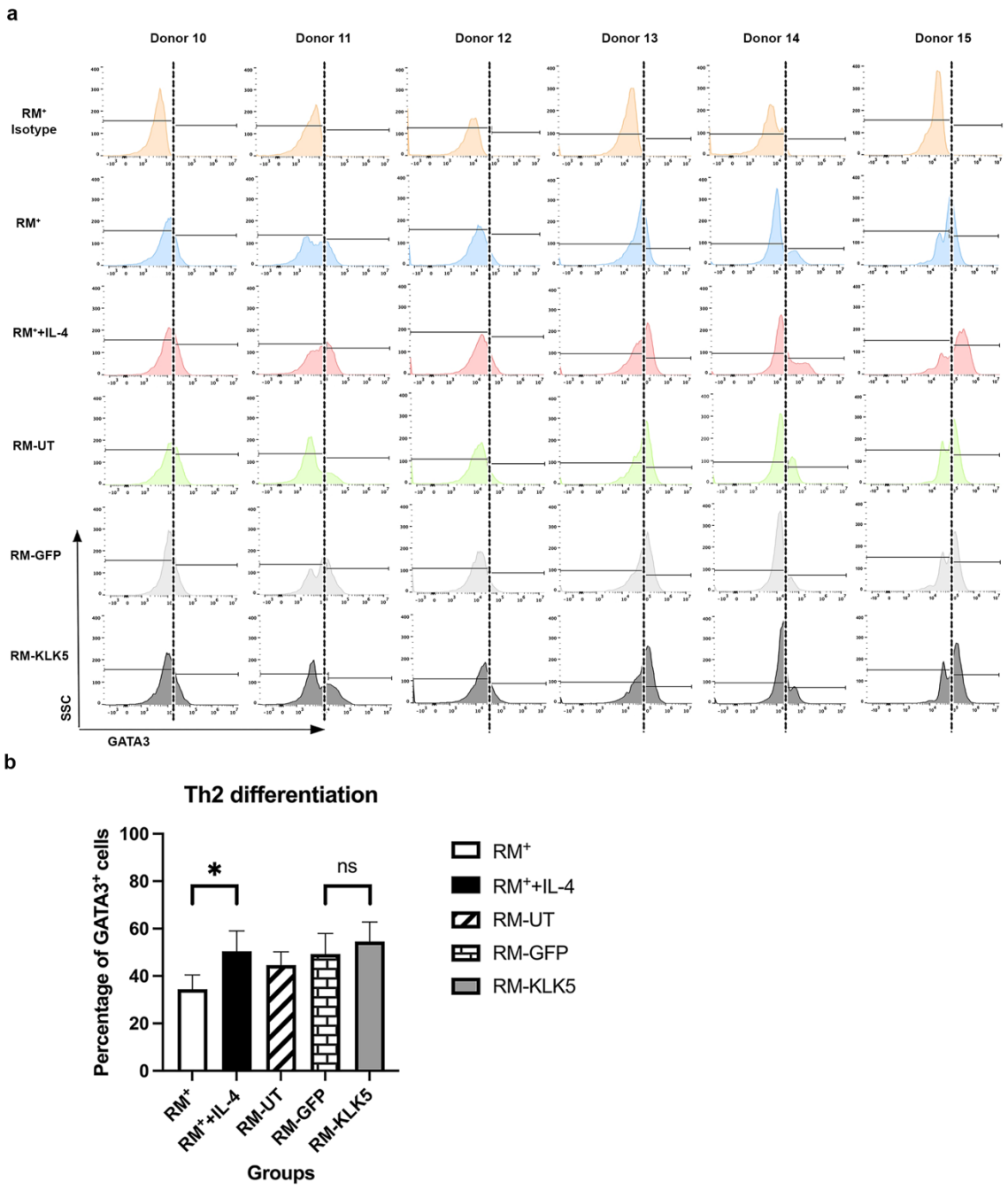

Figure 4.9 Th2 differentiation in naïve CD4$^+$ T cells treated with conditional media

*Th2 differentiation response in conditional media from six donors was assessed by GATA3$^+$ marker. Significantly enhanced Th2 differentiation was detected in positive controls (a). The bar chart showed the percentages of GATA3$^+$ T cells among CD4$^+$ T cells cultured in conditional media from KC-KLK5 (RM-KLK5) (b). *p≤0.05. NS=Non-significant difference. n=6. RM-UT=conditional media from untransduced keratinocytes. RM-GFP=conditional media from keratinocytes transduced with LV-GFP. RM-KLK5=conditional media from keratinocytes transduced with LV-KLK5.*

Donor	RM^+	RM^++IL-4	RM-UT	RM-GFP	RM-KLK5
Donor 10	25.7%	35.4%	39.0%	31.0%	31.4%
Donor 11	31.7%	43.6%	51.9%	61.4%	61.2%
Donor 12	15.8%	26.1%	20.9%	18.1%	30.8%
Donor 13	30.0%	46.4%	43.9%	51.8%	52.7%
Donor 14	52.5%	69.5%	53.3%	76.1%	79.7%
Donor 15	51.2%	81.7%	58.5%	57.4%	71.2%
Mean±SE	34.5%±5.9%	50.5%±8.6%	44.6%±5.5%	49.3%±8.7%	54.5%±8.3%

Table 4.6 Th2 differentiation rates in 6 donors

The differentiation rates were calculated as the ratio of differentiated cells in activated cells.

4.4 Summary

The interactions between keratinocytes overexpressing KLK5 and human CD^+ T cells were studied to reveal the potential role of KLK5 overexpression on a Th2 immune response. The optimised Th2 assay was used for human naïve $CD4^+$ T cells cultured in the conditional media collected from keratinocytes overexpressing KLK5. The pro-inflammatory cytokines/chemokines expressions were checked in conditional media. Results showed significantly increased IL-6 and slightly elevated IL-2. The binding activity of IL-2 and its receptor on $CD4^+$ T cells could initiate IL-2 dependent JAK1/3-STAT cell signaling as well as the IL2-STAT5 mediated IL-4Rα axis to prime Th2 differentiation (Javier Cote-Sierra 2004, Liao, Schones et al. 2008). IL-6 is known to facilitate Th2 differentiation in $CD4^+$ T cells and boost IL-4 production via NFATc2-mediated transcription and the upregulation of Th1 suppressor SOCS1 (Sean Diehl and Rinco 2000). Thus, the elevation of IL-2 and IL-6 detected in the keratinocytes overexpressing KLK5 suggested the potential contributions to prime Th2 differentiation and boost IL-4 production in $CD4^+$ T cells, possibly via Jak1/3-STAT-NFκB pathway.

Apart from the upregulations of cytokines/chemokines detected above, the TSLP expression was downregulated. Enhanced TSLP expression in AD-skin lesions and keratinocytes overexpressing KLK5 has been reported and my result was

controversial to the results of others (Soumelis, Reche et al. 2002, Yoo, Omori et al. 2005, Zhu, Underwood et al. 2017). Many factors could cause this difference, such as, different cell models and the assay sensitivity etc. As increased KLK5 was the only experimental factor in my study, it is likely that the overexpression of KLK5 did not directly cause increased TSLP in keratinocytes *in vitro*.

An increase of Th2 cell differentiation was detected when naïve $CD4^+$ cells were cultured in RM-KLK5 conditional media in most donors. However, the pooled dataset showed no statistical significance of Th2 differentiation between RM-KLK5 and RM-GFP group, indicating KLK5 overexpression-induced pro-inflammatory cytokine secretions had mild effect on Th2 differentiation in human $CD4^+$ T cells.

Chapter 5: Primary keratinocyte model with inducible KLK5 overexpression was established

The primary keratinocyte model ectopically overexpressing KLK5 was used for my previous studies (**Chapter 3 and 4**). However, based on the phenotypes of AD skin, the expression level of KLK5 was different in non-lesional and lesional skin (Soumelis, Reche et al. 2002, Zhu, Underwood et al. 2017), which seemed the overexpression of KLK5 was located within the affected area. To further understand the dynamic influence of KLK5 overexpression in keratinocytes/skin, I proposed to create an inducible cell model for KLK5 expression. This could allow to study KLK5 activity in keratinocytes/skin by controlling KLK5 expression. In this chapter, the inducible KLK5 expression system was generated and characterised. *KLK5-GFP* transgene controlled by TRE3GS promoter was subcloned into a lentiviral vector and transduced into primary keratinocytes. The expression of *KLK5-GFP* could be induced by treating transduced cells with doxycycline, where doxycycline forms a complex with Tet-On 3G protein. The complex then binds to TRE3GS promoter constructed in the vector to initiate the transcription of the transgene *KLK5-GFP*. The same vector but containing *GFP* transgene alone was used as control.

5.1 Generation of inducible lentiviral vector containing *KLK5-GFP* transgene

KLK5-GFP or *GFP* sequences obtained from the previous vector LV-KLK5 and LV-GFP vectors were subcloned into the vector Tet-One Puro and named as Tet-KLK5 and Tet-GFP (**Figure 5.1**). The confirmed lentiviral vectors (**Section 2.16**) were then used for lentivirus productions in HEK 293T cells (293T) (**Section 2.2**). 72 hours post-transduction, doxycycline was added into cells to induce transgene expression and the titers of LV-Tet-KLK5 and LV-Tet-GFP were assessed by the expression of reporter protein GFP 48 hours post-addition of doxycycline. The

titers of lentivirus ranged from $1.8x10^7$IU/ml to $1.5x10^8$IU/ml for LV-Tet-KLK5 ($5.3x10^7 \pm 5.5x10^7$IU/ml, n=7) and $5.6x10^7$IU/ml to $1.5x10^8$IU/ml for LV-Tet-GFP ($9.6x10^7 \pm 4.2x10^7$IU/ml n=5).

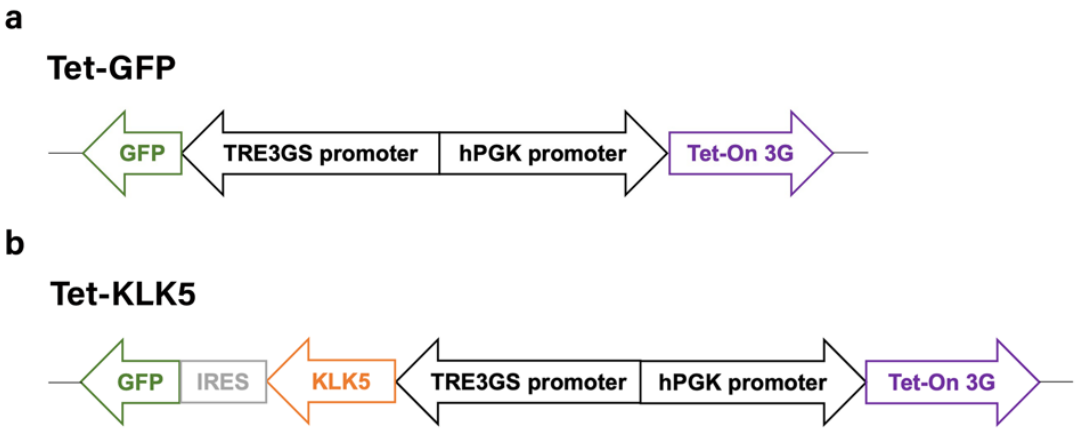

Figure 5.1 The diagrams of the constructs for lentiviral vectors with inducible KLK5 or GFP transgenes

Lentiviral vectors with inducible KLK5 or GFP were constructed by cloning GFP (a) or KLK5-GFP (b) transgenes into the Tet-One-Puro vector.

5.2 Characterization of the inducible vectors in 293T cell line

293T cells were used for vector characterization as there were no detectable endogenous KLK5 expression. Firstly, the time point of peak GFP expression following doxycycline treatment was assessed. $2x10^5$ 293T cells were seeded in 6-well plate and transduced with Tet-GFP and Tet-KLK5 lentivirus at MOI 10. 72-hour post-transduction, 1μg/ml doxycycline was added to induce transgene expression. GFP signal was monitored at 8, 24, 48 and 72 hours under microscope and quantified by flow cytometry. GFP^+ cells were observed at 8 hours after doxycycline addition. The percentage of GFP^+ cells increased and reached to the peak at 48 hours post-doxycycline induction, then declined at 72 hours (**Figure 5.2a**). The peak level of GFP expression monitored by mean fluorescence intensity (MFI) was at 72 hours after cells were treated with

doxycycline (**Figure 5.2b**). Based on these results and also considering the usage of the vectors in primary keratinocytes which have limited live span, 48-hour post-transduction was selected for further study.

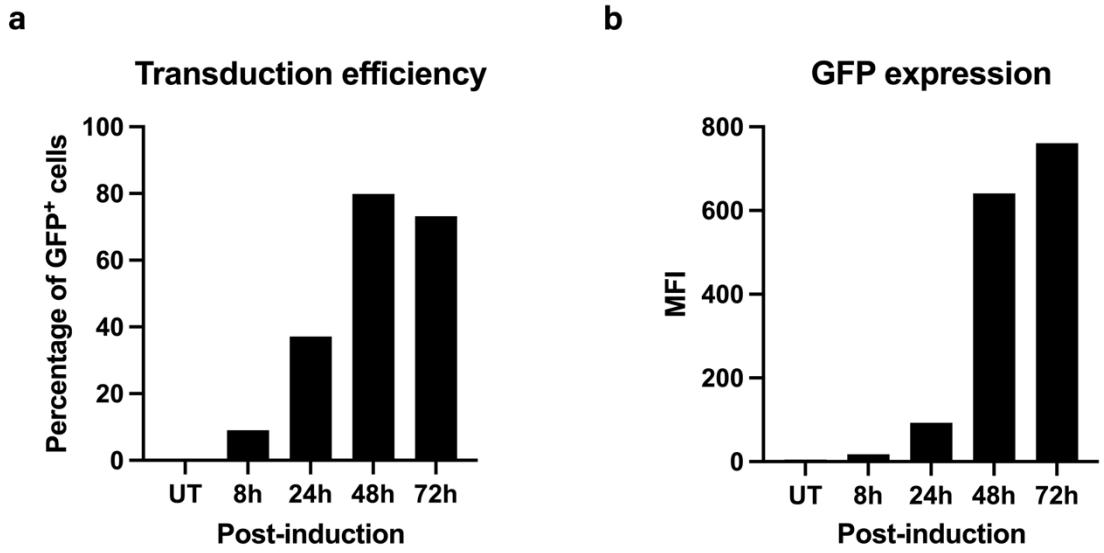

Figure 5.2 GFP signal in transduced cells following doxycycline administration

293T cells were transduced with LV-Tet-GFP or LV-Tet-KLK5 and GFP expression was induced by doxycycline. Untransduced 293T cells (UT) were used as negative control. The GFP^+ cell population as well as GFP expression level recorded by mean fluorescence intensity (MFI) were shown in a and b respectively.

Secondly, the potential 'leakage' of transgene in these lentiviral vectors was tested. 293T cells were transduced with LV-Tet-GFP or LV-Tet-KLK5 with/without doxycycline induction. Untransduced cells were used as negative control. The GFP signal was monitored under microscope 48 hours post doxycycline treatment. The GFP signal was undetectable in untransduced cells and transduced cells without doxycycline treatment. In contrast, the GFP signal was observed in transduced cells with doxycycline treatment. This suggested that transgene expression could only be induced by doxycycline (**Figure 5.3**).

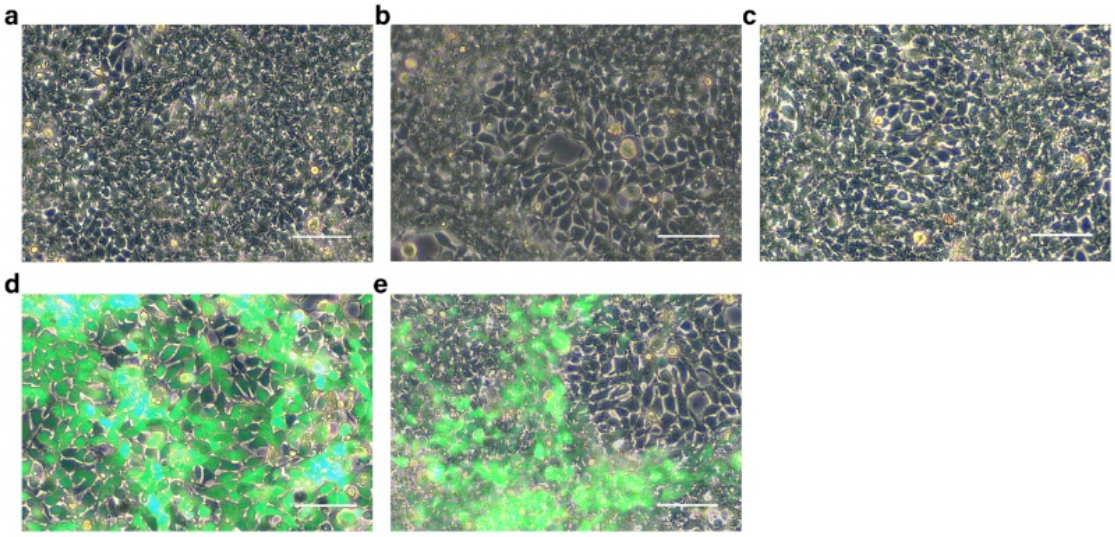

Figure 5.3 GFP signal in transduced 293T cells with and without induction of doxycycline

293T cells were transduced with LV-Tet-GFP or LV-Tet-KLK5. GFP signal was monitored under the fluorescent microscope. No GFP signal was observed in the cells containing GFP gene (b) or KLK5-GFP gene (c) without doxycycline induction. GFP signal was observed in doxycycline treated 293T cells transduced with either LV-Tet-GFP (d) or LV-Tet-KLK5 (e). Untransduced 293T cells without doxycycline were run in parallel as negative control (a). Scale bar=200μm.

The transgene expression and leakage were further confirmed by flow cytometry and Western blotting. There was low background of GFP signal (MFI=$9.9x10^4$) in untransduced cells and transduced cells without doxycycline induction. Following doxycycline treatment, the MFI was increased to $3.1x10^6$ and $9.0x10^5$ in the cells transduced with LV-Tet-GFP or LV-Tet-KLK5, respectively (**Figure 5.4a**). In Western blotting, both expressions of GFP and KLK5 protein in cell lysates and culture medium increased in transduced cells with doxycycline induction after normalised to internal loading control GAPDH or Ponceau S, but not in transduced cells without doxycycline induction (**Figure 5.4b-d**).

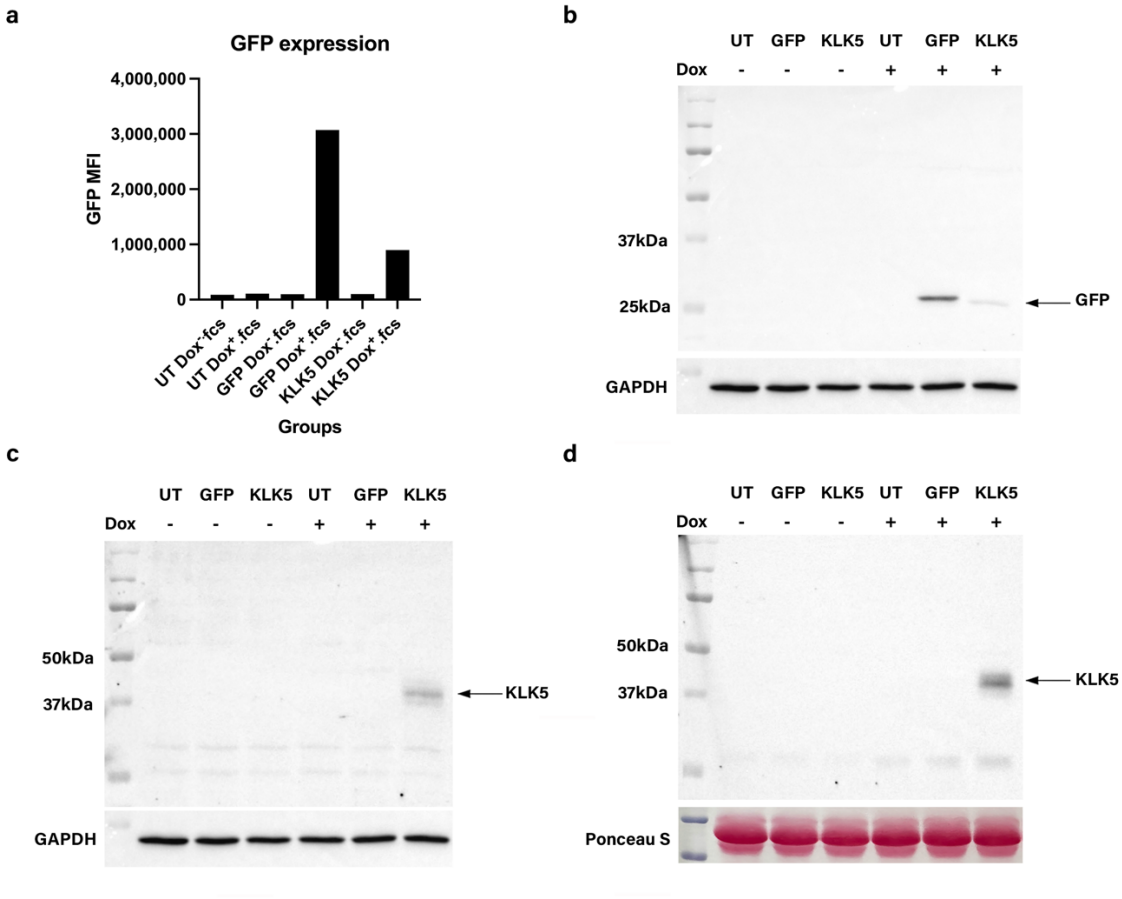

Figure 5.4 Transgene GFP and KLK5 expression in transduced 293T cells

The GFP expression in 293T cells transduced with LV-Tet-GFP or LV-Tet-KLK5 and induced by doxycycline were assessed by flow cytometry and Western blotting. Untransduced 293T cells with/without doxycycline were used as negative control. Increased MFI of GFP fluorescence was detected in LV-Tet-KLK5 transduced cells after doxycycline induction compared to that in cells without doxycycline (a). A positive GFP band was found in the induced 293T cells transduced with LV-Tet-GFP or LV-Tet-KLK5 and induced by doxycycline (b). The KLK5 band was detected in both cell lysate (c) and culture media (d) from cells transduced with LV-Tet-KLK5 and induced by doxycycline, and negative GFP and KLK5 expression were shown in untransduced cells or transduced cells without doxycycline induction. UT=untransduced keratinocytes. GFP=keratinocytes transduced with LV-Tet-GFP. KLK5=keratinocytes transduced with LV-Tet-KLK5. Dox=doxycycline. $^{-}$=without doxycycline. $^{+}$=with doxycycline.

These results further confirmed that the inducible lentivirus containing *KLK5-GFP* or *GFP* transgene could induce transgene expression in cells transduced with LV-Tet-KLK5 or LV-Tet-GFP by doxycycline without leakage.

5.3 Optimization of inducible protocol in primary keratinocytes overexpressing KLK5

To establish the inducible KLK5 overexpression in keratinocytes, the transduction and induction protocols were optimised. A series of MOI for primary keratinocyte transduction was tested to achieve higher transduction efficiency. $4x10^5$ primary keratinocytes were seeded in 6-well plate and transduced with LV-Tet-GFP (KC-Tet-GFP) or LV-Tet-KLK5 (KC-Tet-KLK5) at MOIs of 20, 30, 40, 50 and 60. 72-hour post-transduction, the expressions of transgenes were induced by 1μg/ml doxycycline, and cell viability and GFP expression were examined by flow cytometry. Results showed an increased percentage of GFP^+ cells with the elevation of MOIs. The transduction efficiencies were increased ranging from 37.4% to 53.6% in KC-Tet-GFP cells and 22.0% to 36.2% in KC-Tet-KLK5 cells with MOI of 20 to 50, but slightly dropped to 33.8% at MOI of 60 (**Figure 5.5**). No GFP^+ cells were detected in untransduced cells with/without doxycycline induction (**Figure 5.5a**). The percentage of dead cells were less than 0.2% at different MOIs (**Figure 5.5b**), illustrating that the transduction and induction processed in cells had minimum cytotoxicity. Based on these results, MOI 30 was used for further investigations.

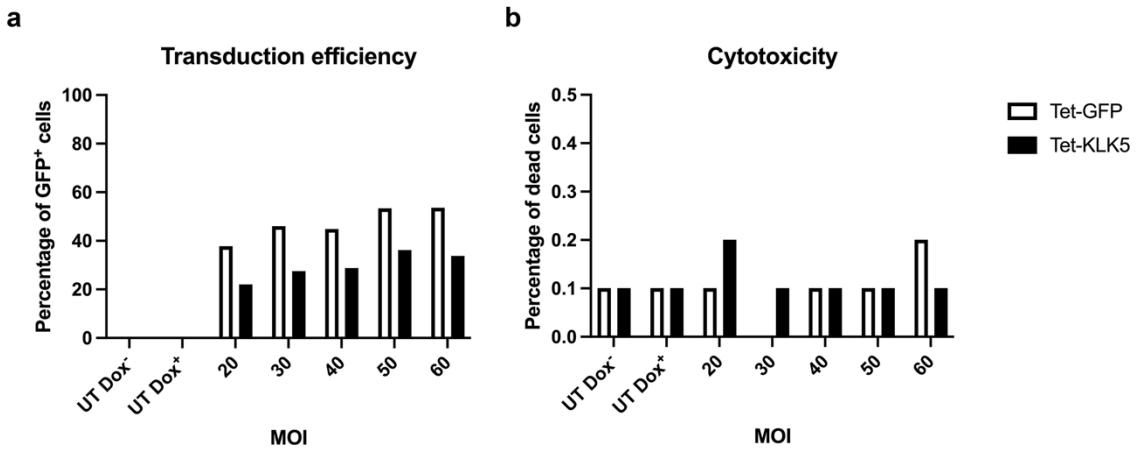

Figure 5.5 Optimization of MOI for LV-Tet lentivirus transduction

Primary keratinocytes were transduced with LV-Tet-GFP or LV-Tet-KLK5 at a series of MOI from 20 to 60 followed by Doxycycline induction. The transduction efficiency assessed by GFP^+ cells and cell death detected by PI^+ cells were detected by flow cytometry. The elevated percentage of GFP^+ cells were noticed with the increased MOI (a). The percentage of dead cells remained less than 0.2% at different tested MOIs (b). UT=untransduced keratinocytes. Dox=doxycycline. $^-$ =without doxycycline. $^+$=with doxycycline.

The dose regimen of doxycycline induction was then tested in cells transduced with LV-Tet-GFP at MOI of 30. 72-hour post-transduction, a series of doxycycline ranging from 0μg/ml, 0.25μg/ml, 0.5μg/ml, 1μg/ml, 2μg/ml and 4μg/ml were added. Untransduced cells with/without doxycycline induction were used as negative control. The GFP signal and cell death were examined 48-hour post-induction. Results showed that untransduced cells and transduced cells without doxycycline treatment did not show any GFP signal. In contrast, there was GFP signal in doxycycline-challenged transduced cells and the intensity of GFP was increased with the elevation of doxycycline concentrations (**Figure 5.6a**). The cell viability showed increased deaths with higher doxycycline dosage in the culture with the maximum dead cells less than 15% (**Figure 5.6b**). After balancing between GFP signal and cell death in transduced cells treated with doxycycline, 1μg/ml of doxycycline was selected for further study.

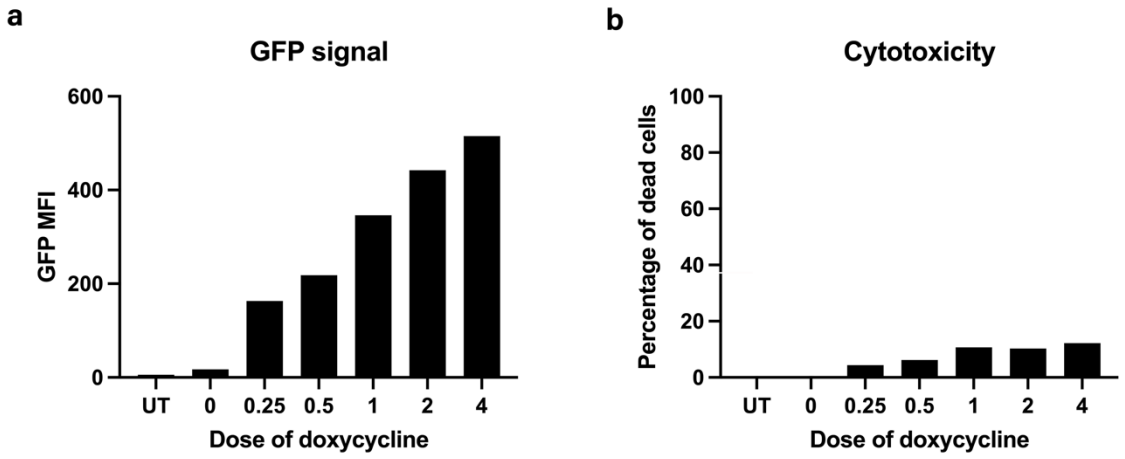

Figure 5.6 Assessment of GFP signal and cell viability after transduction of lentivirus and induction by doxycycline

GFP signal (a) and cytotoxicity (b) were assessed to optimize doxycycline dosage. Results showed 1μg/ml of doxycycline could achieve higher transduction efficiency but low cell death rate. UT=untransduced keratinocytes.

5.4 Reversable expression of KLK5 overexpression and restoration of DSG1 in the inducible cell model

Primary keratinocytes transduced with inducible LV-Tet-KLK5 vector were examined for KLK5 expression following doxycycline treatment and withdrawal. $4x10^5$ primary keratinocytes in 6-well plate from healthy donors were transduced with LV-Tet-KLK5 or LV-Tet-GFP at MOI of 30. Three days post transduction, 1μg/ml doxycycline was added and cultured for 4 days with the replacement of new doxycycline every other day, and then fresh media were replaced without doxycycline. The KLK5 protein expression was checked by Western blotting with and without withdrawal of doxycycline and its expression in cell lysates was normalized to GAPDH and the one in culture media to Ponceau S solution. KLK5 expression in the transduced cells without doxycycline treatment had similar to endogenous KLK5 level in untransduced cells (**Figure 5.7a-d**). There was increased KLK5 expression in cell lysates from cells transduced with LV-Tet-KLK5 and stimulated by doxycycline, indicating full length KLK5 was induced (**Figure 5.7a and b**). When doxycycline was removed from the culture, the overexpressed KLK5 was reversed to the level comparable to the endogenous level showing in untransduced and KC-Tet-GFP cells (**Figure 5.7a and b**).

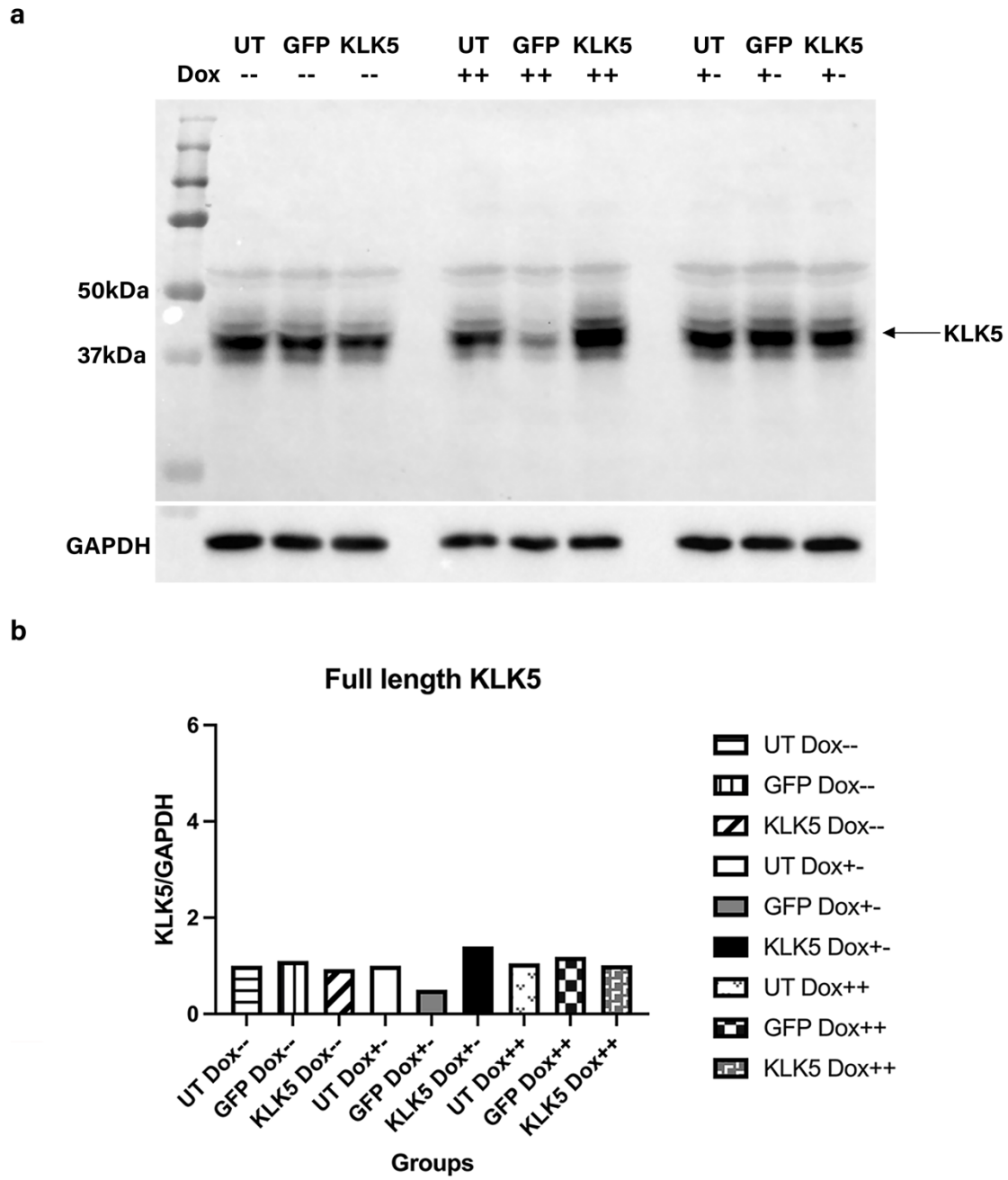

Figure 5.7 Full length KLK5 detected in the induced keratinocyte cell lysates with KLK5-GFP transgene and reversed to normal level after doxycycline removal

Full length KLK5 protein expression was checked in cell lysates from transduced keratinocytes with KLK5-GFP transgene with/without doxycycline induction by Western blotting. Untransduced cells and KC-Tet-UT and KC-Tet-GFP cells without doxycycline treatment were used as negative controls. KLK5 protein was overexpressed in cell lysates from transduced keratinocytes treated with doxycycline and reduced to endogenous level after doxycycline withdrawal (a). Densitometry quantified the results in cell lysates (b). UT=untransduced keratinocytes. GFP=keratinocytes transduced with LV-Tet-GFP. KLK5=keratinocytes transduced with LV-Tet-KLK5. Dox=doxycycline. $^{--}$=without doxycycline. $^{++}$=with doxycycline. $^{+-}$=withdraw doxycycline after the addition.

The active form of KLK5 which was secreted to the extracellular space was also checked by Western blotting. An enhanced level of active KLK5 was found in the culture media collected from stimulated KC-Tet-KLK5 cells (**Figure 5.8a and b**). KLK5 expression reduced to the similar level to ones in the culture media from untransduced and KC-Tet-GFP cells after doxycycline removal as observed in full length KLK5 detection (**Figure 5.8a and b**).

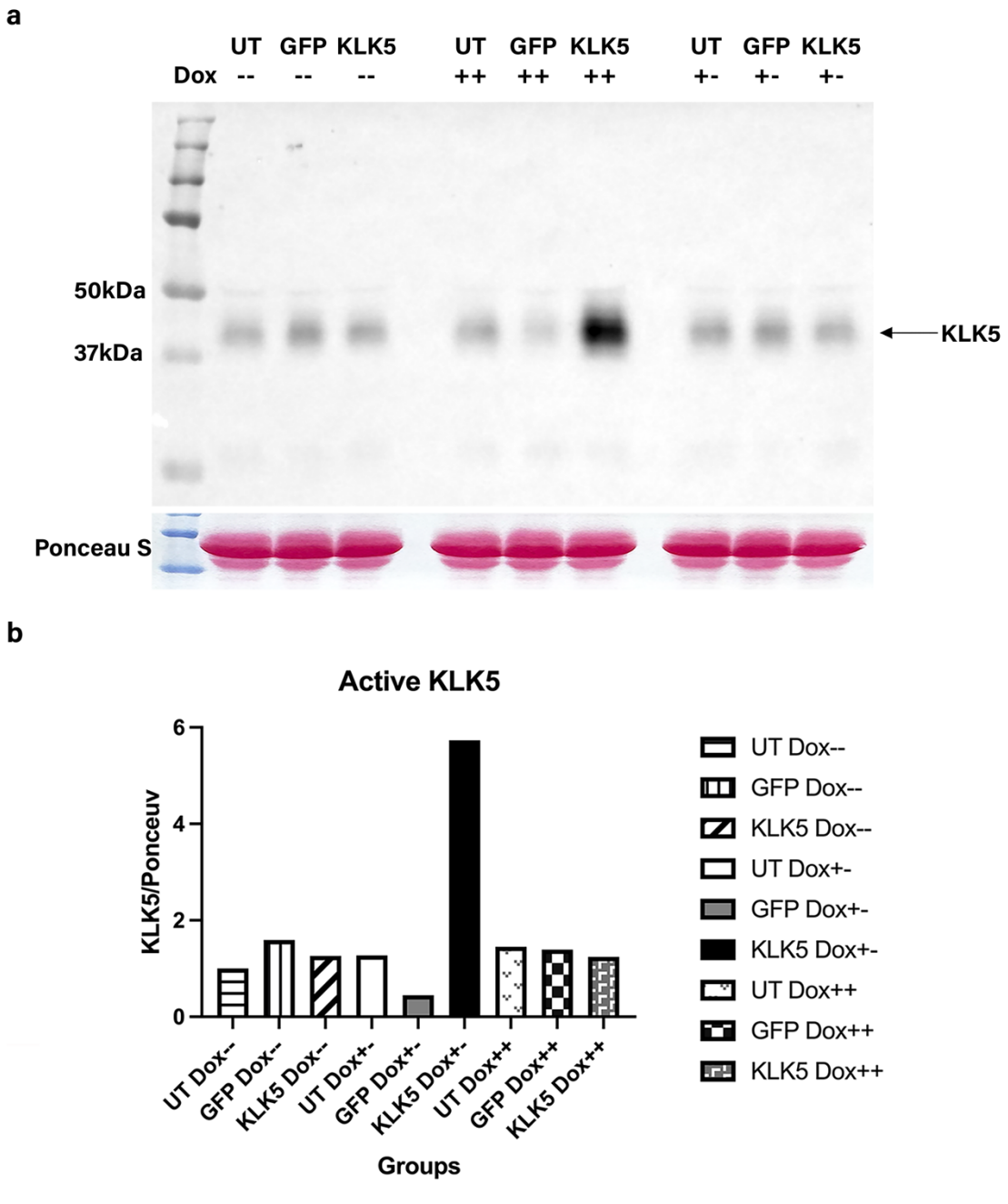

Figure 5.8 Active KLK5 form was detected in the culture media from induced keratinocyte with KLK5-GFP transgene and reduced after doxycycline removal

Active KLK5 form was detected in the culture media from transduced keratinocytes with KLK5-GFP transgene with/without doxycycline induction by Western blotting. Untransduced cells and KC-Tet-UT and KC-Tet-GFP cells without doxycycline treatment were used as negative controls. There was an elevated KLK5 expression in the culture media collected from induced keratinocytes transduced with KLK5-GFP transgene (a). The expression restored to endogenous level after doxycycline removal (a). Densitometry also confirmed the same result (b). UT=untransduced keratinocytes. GFP=keratinocytes transduced with LV-Tet-GFP. KLK5=keratinocytes transduced with LV-Tet-KLK5. Dox=doxycycline. $^{--}$=without doxycycline. $^{++}$=with doxycycline. $^{+-}$=withdraw doxycycline after the addition.

The expression of GFP was also checked by Western blotting to confirm transgene expression. GFP bands showed in both KC-Tet-GFP and KC-Tet-KLK5 cells treated with doxycycline and were not observed after doxycycline removal (**Figure 5.9**). All these results indicated that in this cell model, the KLK5 overexpression could be induced by doxycycline treatment and reversed to the endogenous level after doxycycline withdrawal. In addition, there was no change of KLK5 level in control cells, demonstrating no leakage of transgene in the constructed inducible system.

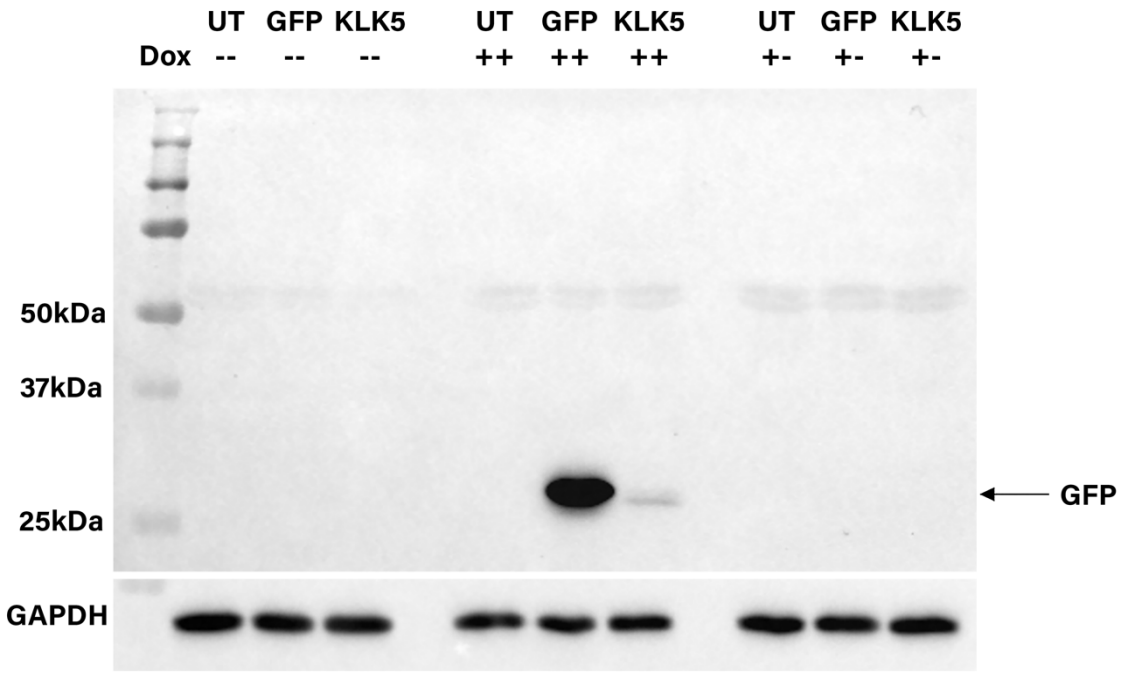

Figure 5.9 GFP expression was induced in the keratinocytes with GFP/KLK5-GFP transgene and declined after doxycycline removal

GFP expression was also checked in the transduced cells with doxycycline induction by Western blotting. Results showed detectable GFP bands in doxycycline-treated transduced cells only. GFP bands disappeared after doxycycline withdrawal. UT=untransduced keratinocytes. GFP=keratinocytes transduced with LV-Tet-GFP. KLK5=keratinocytes transduced with LV-Tet-KLK5. Dox=doxycycline. $^{--}$=without doxycycline. $^{++}$=with doxycycline. $^{+-}$=withdraw doxycycline after the addition.

The expression of downstream molecule DSG1 was also checked by Western blotting and expression was normalized to Vinculin. There was reduced expression in induced KC-Tet-KLK5 cells compared to that in induced KC-Tet-UT cells (**Figure 5.10**), indicating the induced KLK5 overexpression over-degraded DSG1 in keratinocytes. Once doxycycline induction was removed followed by KLK5 level reversed to endogenous level, the DSG1 expression was increased, showing the restoration of DSG1 in KC-Tet-KLK5 cells (**Figure 5.10**). It was noticed that the DSG1 expression was decreased in the induced KC-Tet-GFP cells (**Figure 5.10**). This could be due to abundant GFP expression in the induced KC-Tet-GFP cells, resulting in relatively low amount of DSG1 protein portion in

cell lysate. As this was a single donor sample, repeats are needed to confirm this result.

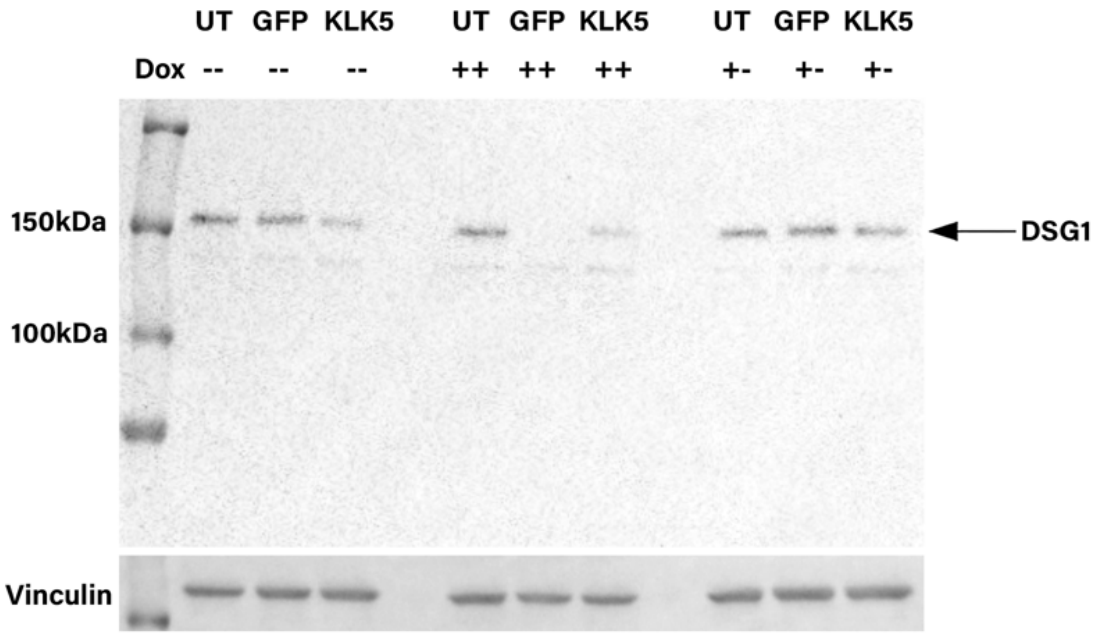

Figure 5.10 DSG1 expression in the transduced keratinocytes with or without doxycycline treatment

The influence of KLK5 overexpression on DSG1 was checked by assessing DSG1 expression using Western blotting. DSG1 expression reduced in the induced KC-Tet-KLK5 cells compared to that in the induced KC-Tet-GFP cells, and the expression was restored after doxycycline removal. UT=untransduced keratinocytes. GFP=keratinocytes transduced with LV-Tet-GFP. KLK5= keratinocytes transduced with LV-Tet-KLK5. Dox=doxycycline. $^{--}$=without doxycycline. $^{++}$=with doxycycline. $^{+-}$=withdraw doxycycline after the addition.

5.5 Summary

It was noticed that although the non-lesional and lesional AD skin share the same genetic background, the protein characteristics remained various, including KLK5 expression. In this study, an inducible KLK5 expression system was generated in keratinocytes, aiming for investigating the influence of dynamic changes of KLK5 overexpression on keratinocytes/skin. In addition, by regulating KLK5 expression, it could also be possible to study the potential influence of reversible KLK5

overexpression in keratinocytes, which could provide more information for the development of therapeutic strategy. The constructed inducible system containing *KLK5-GFP* or *GFP* transgene was validated and characterized in the study. By using 1μg/ml of doxycycline for induction, the KLK5 and GFP expressions could be induced, presenting KLK5 overexpression in keratinocytes without noticeable cytotoxicity. There was no 'leakage' of transgenes without doxycycline induction in this inducible cell model. The induced KLK5 overexpression was also functional to cleave Desmoglein 1 in keratinocytes. The overexpression of KLK5 was reversible when removing doxycycline induction, suggesting the manipulation of KLK5 expression could be achieved in keratinocytes. The Desmoglein 1 expression could also be restored together with KLK5 expression back to the endogenous level after doxycycline removal in the culture.

Apart from induced KLK5 overexpression in primary keratinocytes, it was also noticed that KLK5 expression in the induced KC-Tet-GFP cells was reduced. Interestingly, the expression of downstream molecule DSG1 was also declined together with KLK5 down-regulation in keratinocytes. According to previous publications, GFP protein was reported to cause cell apoptosis, leading to increased permeability in contracted cells and later disappeared under fluorescent microscope (Ansari, Ahmed et al. 2016). The increased staining of CPP32 in GFP-transfected cells as an apoptosis marker indicated similar resutls (Hsiao-Sheng Liu 1999). The transduced and induced KC-Tet-GFP cells displayed significant GFP expression, which might result in abnormal expressions of some proteins, such as KLK5 and DSG1 in this study.

Based on the results above, this inducible model in keratinocytes showed a useful tool for dynamically investigating KLK5 overexpression and skin barrier function.

Chapter 6: Discussion

Skin barrier dysfunction and immuno-dysregulation are two major characteristics in AD and they can be caused by many factors. The abnormality of KLK5 regulation has been considered as one of factors (Zhu, Underwood et al. 2017). Studies have shown that KLK5 is not only related to skin barrier integrity by regulating DSG1 (Descargues, Deraison et al. 2006), but also regulates immune response via PAR2-NFκb pathway (Steinhoff, Buddenkotte et al. 2005, Briot, Deraison et al. 2009). Thus, KLK5 may be an important molecule which link to both skin barrier and immune response in the skin. This project intended to investigate the pathological role of increased KLK5 in the immune response in the skin by studying the transcriptome of keratinocytes with KLK5 overexpression and the possibility of Th2 differentiation among naive $CD4^+$ T cells using the conditional media collected from keratinocytes overexpressing KLK5.

6.1 Transcriptomic changes in keratinocytes overexpressing KLK5

The transcriptome study in keratinocytes revealed down-regulated *TGFBR1* and *FLG2* expressions due to KLK5 overexpression. The differentiated genes found in RNA-seq did not show obvious pathways related to immune response in my study, but revealed down-regulated TGF-β signaling, which was indirectly related to immune response. Previous studies have reported that the TGF-β signaling was a crucial regulator for inflammatory response, cell apoptosis and differentiation (Tzavlaki and Moustakas 2020). Since TGF-β signaling tends to be tumor suppressive (ROBERT J.COFFEY 1988, Liarte, Bernabe-Garcia et al. 2020), this downregulation might promote keratinocyte proliferation in AD, where a thickened epidermal layer was found. Other studies also reported TGF-β1 was associated to keratinocyte differentiation (Hang-Rae Cho 2004). Its expression was increased during calcium-induced HaCaT keratinocyte differentiation (Hang-

Rae Cho 2004). Moreover, TGF-β1 signaling is also known to inhibit IL-2 production and to prevent the activation and differentiation of naïve T cells (Lopamudra Das 2008, Liarte, Bernabe-Garcia et al. 2020). The decreased TGF-β1 signaling might boost IL-2 expression, which was detected in the culture media from keratinocytes overexpressing KLK5 in my study. This might facilitate Th2 differentiation among naïve CD4+ T cells. TGF-β might also inhibit IgE level as the study in B cells addressed TGF-β secretion could be promoted by Toll-like Receptor 9-induced Smad7 suppression, which lead to decreased IgE expression (Ham, Lee et al. 2021). Since IgE is increased in AD patients, it is worthy of investigation of the relation between KLK5-induced TGF-β suppression and elevated IgE level. Apart from Smad7, the decreased expression in *TGFBR1* might potentially lead to reduced phosphorylation of downstream factors, such as SMAD2/3 and initiation of TGF-β signaling (Vander Ark, Cao et al. 2018). In a Smad 3-deficient murine AD model, the mRNA expressions of pro-inflammatory cytokines IL-6 and IL-1β drastically reduced in the skin (Anthoni, Wang et al. 2007). However, this was controversial to the increased IL-6 production found in my study from keratinocyte culture media with KLK5 overexpression. Besides, there was no difference of Smad2, Smad3 and Smad7 expressions in KC-KLK5 cells compared to KC-GFP from RNA-seq data. But the phosphorylated Smad protein could be further investigated as the interactions might be protein level rather than transcriptomic level. These different findings suggested more research towards the role of KLK5 overexpression-induced TGF-β signaling suppression in AD.

Apart from TGF-β signaling found in the RNA-seq study, *FLG2* might be another target. Although it was not showed from the analysis in RNA-seq pooled dataset,

the reduced *FLG2* expression was found in the 1st donor in RNA-seq and confirmed in RT-qPCR study with more donors. Previous studies reported that the *FLG2* variation is most likely to be associated with persistent AD among African Americans but not Brazilians (Margolis, Gupta et al. 2014, Hertz, Azulay-Abulafia et al. 2020). Due to the similarities shared between *FLG* and *FLG2*, the possible patho-mechanism between *KLK5* and *FLG2* requires further investigations.

As for other differential signaling pathways highlighted from RNA-seq pooled dataset, the RIP1-mediated necrosis was the third differentially expressed signaling pathway in KC-KLK5 cells compared to KC-GFP cells. The downregulations in *BIRC2*, *UBE2D1, SDCBP* and *CHMP2B* gene expressions in KC-KLK5 cells, which participate in RIP1-mediated IKK complex recruitment (Meylan, Burns et al. 2004, Vanden Berghe, Linkermann et al. 2014), might suggest the regulations of necrosis in KC-KLK5 cells. Protein encoded by *BIRC2* is identified as apoptosis inhibitor (Mike Rothe 1995, Peter Liston and Korneluk 1996), and positively regulates canonical NF-κB signaling and suppresses non-canoninal pathway (Bertrand, Milutinovic et al. 2008, Dubrez-Daloz, Dupoux et al. 2008, Vallabhapurapu, Matsuzawa et al. 2008, Gyrd-Hansen and Meier 2010). The deletion of p65 and c-Rel in canonical NF-κB signaling has been reported to cause spontaneous dermatitis (Grinberg-Bleyer, Dainichi et al. 2015). This suggested the decreased *BIRC2* in the study has potential to anti-apoptosis and promote dermatitis via NF-κB pathway. The *SDCBP* gene encoded protein could increase TGF-β1 signaling by emphasizing the expression of TGF-β type I receptor at cell surface (Hwangbo, Tae et al. 2016). Thus, the decreased *SDCBP* gene expression might indicate declined TGF-β signaling, which was consistent

with the down-regulation of TGF-β signaling revealed from RNA-seq. Besides, the data analysis for the 1st donor revealed the genes related to keratinization in the epidermis and genes related to p53 signaling. Partial reason might be higher KLK5 overexpression could lead to more differential pathways highlighted in epidermis, ie. keratinization in the 1st donor. More donors with high KLK5 overexpression level (>3-fold) could be included in further study to confirm the transcriptomic changes in keratinocytes due to KLK5 overexpression.

Previous research reported that PAR2 was activated by KLK5 overexpression in keratinocytes (Briot, Deraison et al. 2009). However, this is more of the effect of transient KLK5 overexpression rather than the constant overexpression as PAR2 was found desensitized in the keratinocytes overexpressing KLK5 persistently (Zhu, Underwood et al. 2017). This was supported by our RNA-seq data as PAR2 did not display differentially transcriptomic change in keratinocytes with persistent KLK5 overexpression. It suggested the differences between transient and constant KLK5 overexpression, representing acute and chronic AD conditions. Alternatively, the influences of KLK5 overexpression on PAR2 might be the changes at protein level not transcriptome level.

As the direct pathway related to immune response was not found in differentially expressed genes in keratinocytes overexpressing KLK5 and the fold change of indirect TGF-β signaling was marginal, there might be other possibilities regarding this. The large donor variation observed in the study could arise from different aspects. First, as the ethnics was not strictly controlled during donor recruitment, different genetic backgrounds could boost diversities in the transcriptomes. Second, various levels of increased KLK5 expression might

influence the outcome of RNA-seq as the transcriptome was influenced by KLK5 overexpression at different levels. Third, even if similar KLK5 expression levels were used in the study, each donor might react to it at certain levels, leading to the various responses observed in a small sample size study. This suggested to recruitment more samples in the study. Alternatively, as the transcriptomic study focused on the transcriptomes in keratinocytes, the changes due to KLK5 overexpression might exist at protein level not transcriptomic level. As the function and activity of proteins were not checked in keratinocytes overexpressing KLK5, it is hard to conclude if the KLK5 overexpression only influences the transcriptome or the proteins in keratinocytes. Thus, the proteomics is proposed to check the changes at protein level in keratinocytes due to KLK5 overexpression.

6.2 The relation between keratinocytes overexpressing KLK5 and Th2 skewed immune response

Different pro-inflammatory/inflammatory cytokine expressions were detected in keratinocytes due to KLK5 overexpression, including the up-regulated IL-2, IL-6 and IL-8 as well as down-regulated TSLP. These cytokines have many functions in the immune response. As reported previously, IL-2 is essential for T cell proliferation and differentiation (Ross and Cantrell 2018), which was first discovered as T cell growth factor in 1976 (Doris A. Morgan, Francis W. Ruscetti et al. 1976). It can bind to IL-2 receptor on $CD4^+$ T cells to initiate IL-2 dependent STAT5-mediated IL-4Rα axis and maintain IL-4α production (Javier Cote-Sierra 2004, Liao, Schones et al. 2008). This provided evidence to support the enhanced secretions from keratinocytes overexpressing KLK5 containing IL-2 might facilitate Th2 differentiation among $CD4^+$ T cells.

IL-6 is produced by both professional antigen presenting cells (APCs) like monocytes and macrophages as well as nonprofessional APCs like epithelial and endothelial cells (Philippe Paquet 1996). Keratinocytes have been proved to produce and secret IL-6 previously (Kirnbauer, Kock et al. 1989, Philippe Paquet 1996), as detected in this project. It was also published that the addition of IL-1β and TNF-α could significantly enhance the IL-6 expression in keratinocyte cultured (Kirnbauer, Kock et al. 1989, Philippe Paquet 1996, Hirano 2021). This also matched with the increased IL-1β expression in my detection, pointing out the possible cause of elevated IL-6 in keratinocytes with KLK5 overexpression that the KLK5 overexpression might secret more IL-1β to drive IL-6 expression. IL-6 has been shown to induce nuclear factor of activated T cells c2 (NFATc2)-mediated transcription in $CD4^+$ T cells to facilitate Th2 differentiation in $CD4^+$ T cells and boost IL-4 secretion (Diehl, Chow et al. 2002). It can also upregulate the suppressor of cytokine signaling 1 (SOCS1) expression and inhibit Interferon gamma (IFNγ)-induced STAT1 phosphorylation to reduce Th1 activity (Sean Diehl and Rinco 2000). In addition, it was also discovered that IL-4 production was boosted after IL-6 stimulation followed by STAT3 binding and activating c-Maf promoter (Yang, Ochando et al. 2005). These are the evidence to support the direct function of IL-6 on Th2 differentiation, which could partial explain the mild Th2 differentiation among $CD4^+$ T cells detected in this study. Besides, IL-6 is also found to interact with other immune cells, such as B cells. IL-6 could activate and stimulate B cells to produce antibodies when meeting the specific antigens (Toshio Hirano 1986, TOSHIO HIRANO 1987, Hirano 2021). This brought a possibility of its function in the humoral immunity that the up-regulated IL-6 could boost B cells to recognize the similar antigens caused AD and produce abundant

antibodies towards it. Interestingly, it was discovered that IL-6 also has growth stimulatory effect on keratinocytes (Philippe Paquet 1996, Hirano 2021). But IL-6 only caused thickened Stratum corneum with little keratinocyte hyperproliferation and without leukocyte infiltration in transgenic mice (Swope, Abdel-Malek et al. 1991). This might partially contribute to the skin barrier dysfunction in AD as the keratinocytes try to compensate for the disrupted skin barrier.

Based on these, the hypothesis of this study was established that the cultured media from keratinocytes containing these increased cytokines due to KLK5 overexpression could facilitate Th2 differentiation in human $CD4^+$ T cells. My results showed slight Th2 differentiation among $CD4^+$ T cells but without statistical significance. As discussed previously, the donor variation could partially contribute to this non-significance. Another possibility is that these pro-inflammatory molecules facilitate Th2 differentiation among $CD4^+$ T cells mildly. Alternatively, these increased pro-inflammatory molecules might regulate immune response via different pathways, for example, through the interactions with B cells, dendritic cells and neutrophils. As stated above, these molecules could regulate antigen presenting cells, of which the functions are processing and presenting external allergens to T cells. Through this way, these pro-inflammatory molecules could regulate Th2 differentiation indirectly. Thus, further studies should focus on the interactions between keratinocytes overexpressing KLK5 and other immune cells like B cells, dendritic cell and pan T cells.

Apart from the cytokines discussed above, an interesting finding in this study was the downregulation of TSLP in the cultured media from keratinocytes overexpressing KLK5. Previous publications reported the enhanced TSLP

expression in AD-skin lesions (Soumelis, Reche et al. 2002). Compared to the normal and non-lesional skin from AD patients, TSLP significantly elevated in the AD-lesional skin by immunostaining (Soumelis, Reche et al. 2002). The TSLP transgenic mice developed eczematous-like skin with Th2 immune response (Yoo, Omori et al. 2005). However, due to the complicated conditions of skin samples, it was hard to conclude if the increased TSLP was caused by KLK5 overexpression or other factors in these studies. Previous work in our group showed increased TSLP in KC-KLK5 cells (Zhu, Underwood et al. 2017). However, this was performed in one donor only. To confirm this, I recruited more donors in this study and tested the pro-inflammatory cytokines and chemokines secretions in keratinocytes overexpressing KLK5 cell model. The increased TSLP was not detected in both mRNA and protein level. A similar result was reported in the British Society Investigative Dermatology annual meeting in 2023 by the research group led by Professor Sara Brown. They developed a 3D cell culture model for AD and found no increased TSLP at mRNA and protein level. Both our studies suggest that keratinocytes may not be a responsive cell type in terms of TSLP production in AD.

6.3 The influences of inducible KLK5 overexpression on keratinocytes

I further established a primary keratinocyte model with inducible KLK5 overexpression to explore the reversible effect of KLK5 overexpression in my PhD study. This is the first primary cell model with inducible KLK5 overexpression. The idea of creating this cells model is to study the pathological role of KLK5 overexpression in keratinocytes dynamically. By controlling KLK5 expression in keratinocytes using doxycycline, the clinical features could be mimicked to characterise different KLK5 expression levels in AD skin as well as its reversible

effects. The normal KLK5 expression could be presentable by no induction of KLK5 overexpression in keratinocytes, which is similar to non-lesional skin in AD, while the increased KLK5 expression was mimicked by the induction using doxycycline in keratinocytes as lesional skin in AD. The established model was validated by checking GFP and KLK5 expressions. No 'leakage' of signals for both transgenes were observed. The transgene signals could be induced by doxycycline within 24 hours and reached to the peak at 48 hours, which could keep as long as requested without cytotoxicity. In addition, the overexpressions of transgenes including KLK5 and GFP could be stopped once withdrawing doxycycline induction, illustrating the expressions of transgenes could be tightly controlled. Although the KLK5 expression in the induced KC-Tet-GFP cells used as control was decreased, the similar expression of internal control GAPDH showed the protein was detectable. The downstream molecule of KLK5, DSG1, was also found decreased when GFP expression was induced. This might be due to the abundant GFP protein being induced and detected by Western blotting that it might lower other proteins to some extent, such as KLK5 overexpression and its downstream molecule. As GFP protein has been reported to promote cell apoptosis (Hsiao-Sheng Liu 1999, Ansari, Ahmed et al. 2016), abnormal expressions might be detected in some proteins while robust proteins like GAPDH may be affected to a less extent.

Furthermore, I also confirmed that the induced KLK5 overexpression was also functional by the over-degradation of the downstream molecule DSG1. In contrast, when the induction was removed, KLK5 level elevated to endogenous level and DSG1 was restored. All of these indicated that this newly developed

inducible KLK5 expression model can be a useful tool for further investigations of the interactions between KLK5 overexpression and other molecules.

6.4 Further work

Based on what has been discussed above, future investigations could focus on three perspectives. First, for the influence of KLK5 overexpression on keratinocytes, the down-regulation in TGF-β signaling should be confirmed at protein level as well as its downstream molecules. The functions of declined *FLG2* expression should be further investigated, especially in epidermal development. Another question regarding RNA-seq remains as if increasing sample size could find more potential gene candidates. It also drew my attention if the KLK5 overexpression might influence keratinocytes more at protein level rather than at transcriptomes, ie through protein-protein interactions. Thus, proteomics could be used to verify this.

Second, in terms of the interactions between keratinocytes overexpressing KLK5 and immune cells, as the p value for the comparison of Th2 differentiation among $CD4^+$ T cells in RM-KLK5 group and RM-GFP group was close to the significant level 0.05, it remains unclear if recruiting more donors might cover the statistically non-significance caused by large donor variations. Besides, it is also worthy to investigate if the increased pro-inflammatory cytokines and chemokines regulate immune response in pan T cells not just naïve $CD4^+$ T cells. This could be adaptive immune response regarding the recurring antigens not just priming Th2 differentiation. Besides, the study could also focus on if these elevated pro-inflammatory cytokines and chemokines interact with antigen presenting cells like dendritic cells, macrophages and B cells etc. Alternatively, more pro-

inflammatory/inflammatory molecules should be tested to find potential targets influenced by KLK5 overexpression in keratinocytes.

Third, for the primary keratinocyte model with inducible KLK5 overexpression, more donors should be included in the study to confirm the inducible transgene expressions in keratinocytes and the reversible effect with doxycycline withdrawal. This model could be used in future investigations on the pathological role of KLK5 overexpression in AD, such as testing the pro-inflammatory molecules' secretions in keratinocytes before and after doxycycline removal, skin manifestations before and after doxycycline treatment, transcriptomic and protein changes with and without doxycycline induction. If possible, they can also be used for the study on interactions between keratinocytes and immune cells.

To sum up, if there were another 6 months for the lab work, the first work to be conducted would be validating the decreased TGF-β1 signaling and FLG2 expression at protein level by Western blotting. This might lead to find potential target of KLK5 overexpression. The second piece of work would be repeating the inducible KLK5 overexpression in another two donors to confirm the model consistency. Once the model is consistent, it could be used for further investigations, including testing changes of secreted cytokines with/without the removal of doxycycline induction etc. The third part would be testing interactions between keratinocytes overexpressing KLK5 and pan T cells or dendritic cells using same technique but different selection kit for immune cells. If this is successful, a complicated model might be established to study interactions between keratinocytes with KLK5 overexpression, dendritic cells and T cells.

6.5 Conclusion

This study revealed that the overexpression of KLK5 in keratinocytes did not directly mediate immune response at transcriptomic level. However, the TGF-β signaling and *FLG2* expression was found down-regulated in keratinocytes due to KLK5 overexpression. The enhanced expressions of IL-2 and IL-6 were also found in keratinocytes overexpressing KLK5. These elevated cytokines and chemokines could mildly regulate Th2 differentiation in naïve $CD4^+$ T cells. These study outcomes suggested KLK5 overexpression could influence keratinocyte transcriptome and enhance $CD4^+$ T cells differentiation to Th2 cells. In addition, an inducible KLK5 overexpression primary keratinocyte model was developed and characterised. It was confirmed in this model that KLK5 overexpression could be induced by doxycycline and decreased to endogenous level when the treatment of doxycycline withdrew. This provides a useful tool for further investigations of KLK5 function in skin barrier.

Reference

Alberola, G., J. M. Schroder, C. Froment and M. Simon (2019). "The Amino-Terminal Part of Human FLG2 Is a Component of Cornified Envelopes." J Invest Dermatol **139**(6): 1395-1397.

Ali, N., B. Zirak, R. S. Rodriguez, M. L. Pauli, H. A. Truong, K. Lai, R. Ahn, K. Corbin, M. M. Lowe, T. C. Scharschmidt, K. Taravati, M. R. Tan, R. R. Ricardo-Gonzalez, A. Nosbaum, M. Bertolini, W. Liao, F. O. Nestle, R. Paus, G. Cotsarelis, A. K. Abbas and M. D. Rosenblum (2017). "Regulatory T Cells in Skin Facilitate Epithelial Stem Cell Differentiation." Cell **169**(6): 1119-1129 e1111.

Ansari, A. M., A. K. Ahmed, A. E. Matsangos, F. Lay, L. J. Born, G. Marti, J. W. Harmon and Z. Sun (2016). "Cellular GFP Toxicity and Immunogenicity: Potential Confounders in in Vivo Cell Tracking Experiments." Stem Cell Rev Rep **12**(5): 553-559.

Anthoni, M., G. Wang, C. Deng, H. J. Wolff, A. I. Lauerma and H. T. Alenius (2007). "Smad3 signal transducer regulates skin inflammation and specific IgE response in murine model of atopic dermatitis." J Invest Dermatol **127**(8): 1923-1929.

Barresi, C., C. Stremnitzer, V. Mlitz, S. Kezic, A. Kammeyer, M. Ghannadan, K. Posa-Markaryan, C. Selden, E. Tschachler and L. Eckhart (2011). "Increased sensitivity of histidinemic mice to UVB radiation suggests a crucial role of endogenous urocanic acid in photoprotection." J Invest Dermatol **131**(1): 188-194.

Bertrand, M. J., S. Milutinovic, K. M. Dickson, W. C. Ho, A. Boudreault, J. Durkin, J. W. Gillard, J. B. Jaquith, S. J. Morris and P. A. Barker (2008). "cIAP1 and cIAP2 facilitate cancer cell survival by functioning as E3 ligases that promote RIP1 ubiquitination." Mol Cell **30**(6): 689-700.

Bieber, T. (2008). "Atopic Dermatitis." The new england journal of medicine **358**(14): 12.

Biniek, K., K. Levi and R. H. Dauskardt (2012). "Solar UV radiation reduces the barrier function of human skin." Proc Natl Acad Sci U S A **109**(42): 17111-17116.

Bissett, D. L., J. F. McBride and L. F. Patrick (1987). "Role of protein and calcium in stratum corneum cell cohesion." Arch Dermatol Res **279**(3): 184-189.

Bonnart, C., C. Deraison, M. Lacroix, Y. Uchida, C. Besson, A. Robin, A. Briot, M. Gonthier, L. Lamant, P. Dubus, B. Monsarrat and A. Hovnanian (2010). "Elastase 2 is expressed in human and mouse epidermis and impairs skin barrier function in Netherton syndrome through filaggrin and lipid misprocessing." J Clin Invest **120**(3): 871-882.

Borgono, C. A. and E. P. Diamandis (2004). "The emerging roles of human tissue kallikreins in cancer." Nat Rev Cancer **4**(11): 876-890.

Bradley, J. R. (2008). "TNF-mediated inflammatory disease." J Pathol **214**(2): 149-160.

Brattsand, M. and T. Egelrud (1999). "Purification, molecular cloning, and expression of a human stratum corneum trypsin-like serine protease with possible function in desquamation." J Biol Chem **274**(42): 30033-30040.

Brattsand, M., K. Stefansson, C. Lundh, Y. Haasum and T. Egelrud (2005). "A proteolytic cascade of kallikreins in the stratum corneum." J Invest Dermatol **124**(1): 198-203.

Briot, A., C. Deraison, M. Lacroix, C. Bonnart, A. Robin, C. Besson, P. Dubus and A. Hovnanian (2009). "Kallikrein 5 induces atopic dermatitis-like lesions through PAR2-mediated thymic stromal lymphopoietin expression in Netherton syndrome." J Exp Med **206**(5): 1135-1147.

Cammareri, P., A. M. Rose, D. F. Vincent, J. Wang, A. Nagano, S. Libertini, R. A. Ridgway, D. Athineos, P. J. Coates, A. McHugh, C. Pourreyron, J. H. Dayal, J. Larsson, S. Weidlich, L. C. Spender, G. P. Sapkota, K. J. Purdie, C. M. Proby, C. A. Harwood, I. M. Leigh, H. Clevers, N. Barker, S. Karlsson, C. Pritchard, R. Marais, C. Chelala, A. P. South, O. J. Sansom and G. J. Inman (2016). "Inactivation of TGFbeta receptors in stem cells drives cutaneous squamous cell carcinoma." Nat Commun **7**: 12493.

Candi, E., R. Schmidt and G. Melino (2005). "The cornified envelope: a model of cell death in the skin." Nat Rev Mol Cell Biol **6**(4): 328-340.

Caubet, C., N. Jonca, M. Brattsand, M. Guerrin, D. Bernard, R. Schmidt, T. Egelrud, M. Simon and G. Serre (2004). "Degradation of corneodesmosome proteins by two serine proteases of the kallikrein family, SCTE/KLK5/hK5 and SCCE/KLK7/hK7." J Invest Dermatol **122**(5): 1235-1244.

Celine Deraison, C. B., Frederic Lopez, Celine Besson, Ross Robinson, Arumugam Jayakumar, Fredrik Wagberg, Maria Brattsand, Jean Pierre Hachem, Goran Leonardsson, and Alain Hovnanian (2007). "LEKTI Fragments Specifically Inhibit KLK5, KLK7, and KLK14 and Control Desquamation through a pH-dependent Interaction." Molecular Biology of the Cell **18**: 13.

Chin, A. C., W. Y. Lee, A. Nusrat, N. Vergnolle and C. A. Parkos (2008). "Neutrophil-mediated activation of epithelial protease-activated receptors-1 and -2 regulates barrier function and transepithelial migration." J Immunol **181**(8): 5702-5710.

Christian Jobin, L. H., Cynthia A. Bradham, Konrad Streetz, David A. Brenner and R. Balfour Sartor (1999). "TNF Receptor-Associated Factor-2 Is Involved in Both IL-1 β and TNF-α Signaling Cascades Leading to NF- κB Activation and IL-8 Expression in Human Intestinal Epithelial Cells." Journal of Immunology **162**: 9.

Clark, R. A. (2010). "Skin-resident T cells: the ups and downs of on site immunity." J Invest Dermatol **130**(2): 362-370.

Clayton, K., A. F. Vallejo, J. Davies, S. Sirvent and M. E. Polak (2017). "Langerhans Cells-Programmed by the Epidermis." Front Immunol **8**: 1676.

Collin, M. and P. Milne (2016). "Langerhans cell origin and regulation." Curr Opin Hematol **23**(1): 28-35.

Cork, M. J., S. G. Danby, Y. Vasilopoulos, J. Hadgraft, M. E. Lane, M. Moustafa, R. H. Guy, A. L. Macgowan, R. Tazi-Ahnini and S. J. Ward (2009). "Epidermal barrier dysfunction in atopic dermatitis." J Invest Dermatol **129**(8): 1892-1908.

Cork, M. J., D. A. Robinson, Y. Vasilopoulos, A. Ferguson, M. Moustafa, A. MacGowan, G. W. Duff, S. J. Ward and R. Tazi-Ahnini (2006). "New perspectives on epidermal barrier dysfunction in atopic dermatitis: gene-environment interactions." J Allergy Clin Immunol **118**(1): 3-21; quiz 22-23.

Das, L. and A. D. Levine (2008). "TGF-beta inhibits IL-2 production and promotes cell cycle arrest in TCR-activated effector/memory T cells in the presence of sustained TCR signal transduction." J Immunol **180**(3): 1490-1498.

Das, P., P. Mounika, M. L. Yellurkar, V. S. Prasanna, S. Sarkar, R. Velayutham and S. Arumugam (2022). "Keratinocytes: An Enigmatic Factor in Atopic Dermatitis." Cells **11**(10).

Deckers, I. A., S. McLean, S. Linssen, M. Mommers, C. P. van Schayck and A. Sheikh (2012). "Investigating international time trends in the incidence and prevalence of atopic eczema 1990-2010: a systematic review of epidemiological studies." PLoS One **7**(7): e39803.

Descargues, P., C. Deraison, C. Bonnart, M. Kreft, M. Kishibe, A. Ishida-Yamamoto, P. Elias, Y. Barrandon, G. Zambruno, A. Sonnenberg and A. Hovnanian (2005). "Spink5-deficient mice mimic Netherton syndrome through degradation of desmoglein 1 by epidermal protease hyperactivity." Nat Genet **37**(1): 56-65.

Descargues, P., C. Deraison, C. Prost, S. Fraitag, J. Mazereeuw-Hautier, M. D'Alessio, A. Ishida-Yamamoto, C. Bodemer, G. Zambruno and A. Hovnanian (2006). "Corneodesmosomal cadherins are preferential targets of stratum corneum trypsin- and chymotrypsin-like hyperactivity in Netherton syndrome." J Invest Dermatol **126**(7): 1622-1632.

Di, W. L., J. E. Mellerio, C. Bernadis, J. Harper, A. Abdul-Wahab, S. Ghani, L. Chan, M. Martinez-Queipo, H. Hara, A. M. McNicol, F. Farzaneh, J. McGrath, A. Thrasher and W. Qasim (2013). "Phase I study protocol for ex vivo lentiviral gene therapy for the inherited skin disease, Netherton syndrome." Hum Gene Ther Clin Dev **24**(4): 182-190.

Diehl, S., C. W. Chow, L. Weiss, A. Palmetshofer, T. Twardzik, L. Rounds, E. Serfling, R. J. Davis, J. Anguita and M. Rincon (2002). "Induction of NFATc2 expression by interleukin 6 promotes T helper type 2 differentiation." J Exp Med **196**(1): 39-49.

Dienz, O. and M. Rincon (2009). "The effects of IL-6 on CD4 T cell responses." Clin Immunol **130**(1): 27-33.

Doris A. Morgan, Francis W. Ruscetti and R. Gallo (1976). "Selective in Vitro Growth of T Lymphocytes from Normal Human Bone Marrows." Science **193**(4257): 2.

Dubrez-Daloz, L., A. Dupoux and J. Cartier (2008). "IAPs: more than just inhibitors of apoptosis proteins." Cell Cycle **7**(8): 1036-1046.

ECKERT, R. L. (1989). "Structure function and differentiation of the keratinocyte." PHYSIOLOGICAL REVIEWS **69**(4): 31.

Egelrud, T., P. A. Hofer and A. Lundstrom (1988). "Proteolytic degradation of desmosomes in plantar stratum corneum leads to cell dissociation in vitro." Acta Derm Venereol **68**(2): 93-97.

Egelrud, T. and A. Lundstrom (1991). "A chymotrypsin-like proteinase that may be involved in desquamation in plantar stratum corneum." Arch Dermatol Res **283**(2): 108-112.

Ekholm, I. E., M. Brattsand and T. Egelrud (2000). "Stratum corneum tryptic enzyme in normal epidermis: a missing link in the desquamation process?" J Invest Dermatol **114**(1): 56-63.

Elias, P. M. (1983). "Epidermal lipids, barrier function, and desquamation." J Invest Dermatol **80**(1 Suppl): 44s-49s.

Emami, N. and E. P. Diamandis (2007). "Human tissue kallikreins: a road under construction." Clin Chim Acta **381**(1): 78-84.

Ettehadi, P., M. W. Greaves, D. Wallach, D. Aderka and R. D. Camp (1994). "Elevated tumour necrosis factor-alpha (TNF-alpha) biological activity in psoriatic skin lesions." Clin Exp Immunol **96**(1): 146-151.

Fadadu, R. P., K. Abuabara, J. R. Balmes, J. M. Hanifin and M. L. Wei (2023). "Air Pollution and Atopic Dermatitis, from Molecular Mechanisms to Population-Level Evidence: A Review." Int J Environ Res Public Health **20**(3).

Fortugno, P., L. Furio, M. Teson, M. Berretti, M. El Hachem, G. Zambruno, A. Hovnanian and M. D'Alessio (2012). "The 420K LEKTI variant alters LEKTI proteolytic activation and results in protease deregulation: implications for atopic dermatitis." Hum Mol Genet **21**(19): 4187-4200.

Furue, M., T. Chiba, G. Tsuji, D. Ulzii, M. Kido-Nakahara, T. Nakahara and T. Kadono (2017). "Atopic dermatitis: immune deviation, barrier dysfunction, IgE autoreactivity and new therapies." Allergol Int **66**(3): 398-403.

Gao, P. S., N. M. Rafaels, D. Mu, T. Hand, T. Murray, M. Boguniewicz, T. Hata, L. Schneider, J. M. Hanifin, R. L. Gallo, L. Gao, T. H. Beaty, L. A. Beck, D. Y. Leung and K. C. Barnes (2010). "Genetic variants in thymic stromal lymphopoietin are associated with atopic dermatitis and eczema herpeticum." J Allergy Clin Immunol **125**(6): 1403-1407 e1404.

Getsios, S., C. L. Simpson, S. Kojima, R. Harmon, L. J. Sheu, R. L. Dusek, M. Cornwell and K. J. Green (2009). "Desmoglein 1-dependent suppression of EGFR signaling promotes epidermal differentiation and morphogenesis." J Cell Biol **185**(7): 1243-1258.

Goettig, P. and V. Magdolen (2013). Kallikrein-Related Peptidase 5. Handbook of Proteolytic Enzymes**:** 2772-2778.

Goodman, R. E., F. Nestle, Y. M. Naidu, J. M. Green, C. B. Thompson, B. J. Nickoloff and L. A. Turka (1994). "Keratinocyte-derived T cell costimulation induces preferential production of IL-2 and IL-4 but not IFN-gamma." J Immunol **152**(11): 5189-5198.

Grinberg-Bleyer, Y., T. Dainichi, H. Oh, N. Heise, U. Klein, R. M. Schmid, M. S. Hayden and S. Ghosh (2015). "Cutting edge: NF-kappaB p65 and c-Rel control epidermal development and immune homeostasis in the skin." J Immunol **194**(6): 2472-2476.

Grone, A. (2002). "Keratinocytes and cytokines." Veterinary Immunology and Immunopathology **88**: 12.

Gyrd-Hansen, M. and P. Meier (2010). "IAPs: from caspase inhibitors to modulators of NF-kappaB, inflammation and cancer." Nat Rev Cancer **10**(8): 561-574.

Ham, W. K., E. J. Lee, M. S. Jeon, H. Y. Kim, G. Agrahari, E. J. An, C. H. Bang, D. S. Kim and T. Y. Kim (2021). "Treatment with phosphodiester CpG-ODN ameliorates atopic dermatitis by enhancing TGF-beta signaling." BMB Rep **54**(2): 142-147.

Hang-Rae Cho, S.-B. H., Young Il Kim, Jin-Woo Lee, Nack-In Kim (2004). "Differential Expression of TGF-beta Isoforms During Differentiation of HaCaT Human Keratinocyte Cells: Implication for the Separate Role in Epidermal Differentiation." J Korean Med Sci **19**: 6.

He, R., M. K. Oyoshi, L. Garibyan, L. Kumar, S. F. Ziegler and R. S. Geha (2008). "TSLP acts on infiltrating effector T cells to drive allergic skin inflammation." Proc Natl Acad Sci U S A **105**(33): 11875-11880.

Hershko, A. Y. (2017). "Insights into the mast cell-microbiome connection in the skin." J Allergy Clin Immunol **139**(4): 1137-1139.

Hertz, A., L. Azulay-Abulafia, A. P. D. Nascimento, C. Y. Ohara, F. C. Kuschnir and L. C. Porto (2020). "Analysis of filaggrin 2 gene polymorphisms in patients with atopic dermatitis." An Bras Dermatol **95**(2): 173-179.

Hirano, T. (2021). "IL-6 in inflammation, autoimmunity and cancer." Int Immunol **33**(3): 127-148.

Hovnanian, A. (2013). "Netherton syndrome: skin inflammation and allergy by loss of protease inhibition." Cell Tissue Res **351**(2): 289-300.

Hsiao-Sheng Liu, M.-S. J., Chao-Kai Chou, Ping-Hong Chen, and Nir-Jihn Ke (1999). "Is Green Fluorescent Protein Toxic to the Living Cells." Biochemical and Biophysical Research Communications **260**: 6.

Hsu, Y. C. and E. Fuchs (2022). "Building and Maintaining the Skin." Cold Spring Harb Perspect Biol **14**(7).

Hwangbo, C., N. Tae, S. Lee, O. Kim, O. K. Park, J. Kim, S. H. Kwon and J. H. Lee (2016). "Syntenin regulates TGF-beta1-induced Smad activation and the epithelial-to-mesenchymal transition by inhibiting caveolin-mediated TGF-beta type I receptor internalization." Oncogene **35**(3): 389-401.

IAN R. SCOTT, C. R. H. a. J. G. B. (1982). "HISTIDINE-RICH PROTEIN OF THE KERATOHYALIN GRANULES SOURCE OF THE FREE AMINO ACIDS, UROCANIC ACID AND PYRROLIDONE CARBOXYLIC ACID IN THE STRATUM CORNEUM." Biochimica et Biophysica Acta **719**: 10.

Javier Cote-Sierra, G. F., Liying Guo, Lynda Chiodetti, Howard A. Young, Jane Hu-Li, Jinfang Zhu, and William E. Paul (2004). "Interleukin 2 plays a central role in Th2 differentiation." Chromatin Immunopresipitation Analysis **101**(11): 6.

Jonathan N.W.N. Barker, M. L. J., Raj S. Mitra, Elahe Crockett-Torabe, Joseph C Fantone, Steven L.Kunkel, Jeffery S. Warren, Vishva M. Dixit and Brian J. Nickoloff (1991). "Modulation of Keratinocyte-derived Interleukin-8 Which Is Chemotactic for Neutrophils and T Lymphocytes." American Journal of Pathology **139**(4): 8.

Joo, K. M., J. Y. Han, E. D. Son, G. W. Nam, H. Y. Chung, H. J. Jeong, J. C. Cho and K. M. Lim (2012). "Rapid, simultaneous and nanomolar determination of pyroglutamic acid and cis-/trans-urocanic acid in human stratum corneum by hydrophilic interaction liquid chromatography (HILIC)-electrospray ionization tandem mass spectrometry." J Chromatogr B Analyt Technol Biomed Life Sci **897**: 55-63.

Kalinska, M., U. Meyer-Hoffert, T. Kantyka and J. Potempa (2016). "Kallikreins - The melting pot of activity and function." Biochimie **122**: 270-282.

Kanehisa, M. (2019). "Toward understanding the origin and evolution of cellular organisms." Protein Sci **28**(11): 1947-1951.

Kanehisa, M., M. Furumichi, Y. Sato, M. Kawashima and M. Ishiguro-Watanabe (2023). "KEGG for taxonomy-based analysis of pathways and genomes." Nucleic Acids Res **51**(D1): D587-D592.

Kany, S., J. T. Vollrath and B. Relja (2019). "Cytokines in Inflammatory Disease." Int J Mol Sci **20**(23).

Kawabata, A. (2002). "PAR-2: structure, function and relevance to human diseases of the gastric mucosa." Expert Rev Mol Med **4**(16): 1-17.

Kim, J. E. and H. S. Kim (2019). "Microbiome of the Skin and Gut in Atopic Dermatitis (AD): Understanding the Pathophysiology and Finding Novel Management Strategies." J Clin Med **8**(4).

Kim, Y. and K. M. Lim (2021). "Skin barrier dysfunction and filaggrin." Arch Pharm Res **44**(1): 36-48.

Kirnbauer, R., A. Kock, T. Schwarz, A. Urbanski, J. Krutmann, W. Borth, D. Damm, G. Shipley, J. C. Ansel and T. A. Luger (1989). "IFN-beta 2, B cell differentiation factor 2, or hybridoma growth factor (IL-6) is expressed and released by human epidermal cells and epidermoid carcinoma cell lines." J Immunol **142**(6): 1922-1928.

Kishibe, M. (2019). "Physiological and pathological roles of kallikrein-related peptidases in the epidermis." J Dermatol Sci **95**(2): 50-55.

Komatsu, N., K. Saijoh, C. Kuk, A. C. Liu, S. Khan, F. Shirasaki, K. Takehara and E. P. Diamandis (2007). "Human tissue kallikrein expression in the stratum corneum and serum of atopic dermatitis patients." Exp Dermatol **16**(6): 513-519.

Komatsu, N., K. Saijoh, M. Sidiropoulos, B. Tsai, M. A. Levesque, M. B. Elliott, K. Takehara and E. P. Diamandis (2005). "Quantification of human tissue kallikreins in the stratum corneum: dependence on age and gender." J Invest Dermatol **125**(6): 1182-1189.

Kortekaas Krohn, I., J. L. Aerts, K. Breckpot, C. Goyvaerts, E. Knol, F. Van Wijk and J. Gutermuth (2022). "T-cell subsets in the skin and their role in inflammatory skin disorders." Allergy **77**(3): 827-842.

Kristensen, M., C. Q. Chu, D. J. Eedy, M. Feldmann, F. M. Brennan and S. M. Breathnach (1993). "Localization of tumour necrosis factor-alpha (TNF-alpha) and its receptors in normal and psoriatic skin: epidermal cells express the 55-kD but not the 75-kD TNF receptor." Clin Exp Immunol **94**(2): 354-362.

Langan, S. M., A. D. Irvine and S. Weidinger (2020). "Atopic dermatitis." Lancet **396**(10247): 345-360.

Laughter, M. R., M. B. C. Maymone, S. Mashayekhi, B. W. M. Arents, C. Karimkhani, S. M. Langan, R. P. Dellavalle and C. Flohr (2021). "The global burden of atopic dermatitis: lessons from the Global Burden of Disease Study 1990-2017." Br J Dermatol **184**(2): 304-309.

Leung, D. Y. (2000). "Atopic dermatitis: new insights and opportunities for therapeutic intervention." J Allergy Clin Immunol **105**(5): 860-876.

Liao, W., D. E. Schones, J. Oh, Y. Cui, K. Cui, T. Y. Roh, K. Zhao and W. J. Leonard (2008). "Priming for T helper type 2 differentiation by interleukin 2-mediated induction of interleukin 4 receptor alpha-chain expression." Nat Immunol **9**(11): 1288-1296.

Liarte, S., A. Bernabe-Garcia and F. J. Nicolas (2020). "Role of TGF-beta in Skin Chronic Wounds: A Keratinocyte Perspective." Cells **9**(2).

Liu, X., R. Zhu, Y. Luo, S. Wang, Y. Zhao, Z. Qiu, Y. Zhang, X. Liu, X. Yao, X. Li and W. Li (2021). "Distinct human Langerhans cell subsets orchestrate reciprocal functions and require different developmental regulation." Immunity **54**(10): 2305-2320 e2311.

Lodyga, M. and B. Hinz (2020). "TGF-beta1 - A truly transforming growth factor in fibrosis and immunity." Semin Cell Dev Biol **101**: 123-139.

Lopamudra Das, A. D. L. (2008). "TGF-beta Inhibits IL-2 Production and Promotes Cell Cycle Arrest in TCR-Activated Effector/Memory T Cells in the Presence of Sustained TCR Signal Transduction." The Journal of Immunology: 9.

Loset, M., S. J. Brown, M. Saunes and K. Hveem (2019). "Genetics of Atopic Dermatitis: From DNA Sequence to Clinical Relevance." Dermatology **235**(5): 355-364.

Losquadro, W. D. (2017). "Anatomy of the Skin and the Pathogenesis of Nonmelanoma Skin Cancer." Facial Plast Surg Clin North Am **25**(3): 283-289.

Lundstrom, A. and T. Egelrud (1990). "Evidence that cell shedding from plantar stratum corneum in vitro involves endogenous proteolysis of the desmosomal protein desmoglein I." J Invest Dermatol **94**(2): 216-220.

Lundwall, A. and M. Brattsand (2008). "Kallikrein-related peptidases." Cell Mol Life Sci **65**(13): 2019-2038.

Manabe, M., M. Sanchez, T. T. Sun and B. A. Dale (1991). "Interaction of filaggrin with keratin filaments during advanced stages of normal human epidermal differentiation and in ichthyosis vulgaris." Differentiation **48**(1): 43-50.

Margolis, D. J., J. Gupta, A. J. Apter, T. Ganguly, O. Hoffstad, M. Papadopoulos, T. R. Rebbeck and N. Mitra (2014). "Filaggrin-2 variation is associated with more persistent atopic dermatitis in African American subjects." J Allergy Clin Immunol **133**(3): 784-789.

Martin, M. J., M. Estravis, A. Garcia-Sanchez, I. Davila, M. Isidoro-Garcia and C. Sanz (2020). "Genetics and Epigenetics of Atopic Dermatitis: An Updated Systematic Review." Genes (Basel) **11**(4).

Masurier, N., D. P. Arama, C. El Amri and V. Lisowski (2018). "Inhibitors of kallikrein-related peptidases: An overview." Med Res Rev **38**(2): 655-683.

Matsui, T. and M. Amagai (2015). "Dissecting the formation, structure and barrier function of the stratum corneum." Int Immunol **27**(6): 269-280.

Mette Deleuran, A. R. E., Kirsten Paludan, Carsten Schou and Kristian Thestrup-pedersen (1998). "Purifed Der p1 and p2 Patch Tests in Patients with Atopic Dermatitis: Evidence for Both Allergenicity and Proteolytic Irritancy." Acta Derm Venereol **78**: 241-243.

Meylan, E., K. Burns, K. Hofmann, V. Blancheteau, F. Martinon, M. Kelliher and J. Tschopp (2004). "RIP1 is an essential mediator of Toll-like receptor 3-induced NF-kappa B activation." Nat Immunol **5**(5): 503-507.

Mike Rothe, M.-G. P., William J. Henzel, T. Merrill Ayres, and David V. Goeddel (1995). "The TNFR2-TRAF Signaling Complex Contains Two Novel Proteins Related to Baculoviral Inhibitor of Apoptosis Proteins." Cell **83**: 10.

Minoru Kanehisa, S. G. (2000). "KEGG kyoto encyclopedia of genes and genomes." Nucleic Acids Research **28**(1): 4.

Morizane, S. (2019). "The Role of Kallikrein-Related Peptidases in Atopic Dermatitis." Acta Med.Okayama **73**: 1-6.

Morizane, S., K. Sunagawa, H. Nomura and M. Ouchida (2022). "Aberrant serine protease activities in atopic dermatitis." J Dermatol Sci **107**(1): 2-7.

Murphy, J. E., C. Robert and T. S. Kupper (2000). "Interleukin-1 and cutaneous inflammation: a crucial link between innate and acquired immunity." J Invest Dermatol **114**(3): 602-608.

Najor, N. A., G. N. Fitz, J. L. Koetsier, L. M. Godsel, L. V. Albrecht, R. Harmon and K. J. Green (2017). "Epidermal Growth Factor Receptor neddylation is regulated by a desmosomal-COP9 (Constitutive Photomorphogenesis 9) signalosome complex." Elife **6**.

Nauroy, P. and A. Nystrom (2020). "Kallikreins: Essential epidermal messengers for regulation of the skin microenvironment during homeostasis, repair and disease." Matrix Biol Plus **6-7**: 100019.

Nedoszytko, B., E. Reszka, D. Gutowska-Owsiak, M. Trzeciak, M. Lange, J. Jarczak, M. Niedoszytko, E. Jablonska, J. Romantowski, D. Strapagiel, J. Skokowski, A. Siekierzycka, R. J. Nowicki, I. T. Dobrucki, A. Zaryczanska and L. Kalinowski (2020). "Genetic and Epigenetic Aspects of Atopic Dermatitis." Int J Mol Sci **21**(18).

Nguyen, A. V. and A. M. Soulika (2019). "The Dynamics of the Skin's Immune System." Int J Mol Sci **20**(8).

Nomura, H., M. Suganuma, T. Takeichi, M. Kono, Y. Isokane, K. Sunagawa, M. Kobashi, S. Sugihara, A. Kajita, T. Miyake, Y. Hirai, O. Yamasaki, M. Akiyama and S. Morizane (2020). "Multifaceted Analyses of Epidermal Serine Protease Activity in Patients with Atopic Dermatitis." Int J Mol Sci **21**(3).

Oikonomopoulou, K., K. K. Hansen, M. Saifeddine, I. Tea, M. Blaber, S. I. Blaber, I. Scarisbrick, P. Andrade-Gordon, G. S. Cottrell, N. W. Bunnett, E. P. Diamandis and M. D. Hollenberg (2006). "Proteinase-activated receptors, targets for kallikrein signaling." J Biol Chem **281**(43): 32095-32112.

Oikonomopoulou, K., K. K. Hansen, M. Saifeddine, N. Vergnolle, I. Tea, M. Blaber, S. I. Blaber, I. Scarisbrick, E. P. Diamandis and M. D. Hollenberg (2006). "Kallikrein-mediated cell signalling: targeting proteinase-activated receptors (PARs)." Biol Chem **387**(6): 817-824.

Palmer, C. N., A. D. Irvine, A. Terron-Kwiatkowski, Y. Zhao, H. Liao, S. P. Lee, D. R. Goudie, A. Sandilands, L. E. Campbell, F. J. Smith, G. M. O'Regan, R. M. Watson, J. E. Cecil, S. J. Bale, J. G. Compton, J. J. DiGiovanna, P. Fleckman, S. Lewis-Jones, G. Arseculeratne, A. Sergeant, C. S. Munro, B. El Houate, K. McElreavey, L. B. Halkjaer, H. Bisgaard, S. Mukhopadhyay and W. H. McLean (2006). "Common loss-of-function variants of the epidermal barrier protein filaggrin are a major predisposing factor for atopic dermatitis." Nat Genet **38**(4): 441-446.

Parrado, A. C., A. Canellada, T. Gentile and E. B. Rey-Roldan (2012). "Dopamine agonists upregulate IL-6 and IL-8 production in human keratinocytes." Neuroimmunomodulation **19**(6): 359-366.

Pasupuleti, M., A. Schmidtchen and M. Malmsten (2012). "Antimicrobial peptides: key components of the innate immune system." Crit Rev Biotechnol **32**(2): 143-171.

Pellerin, L., J. Henry, C. Y. Hsu, S. Balica, C. Jean-Decoster, M. C. Mechin, B. Hansmann, E. Rodriguez, S. Weindinger, A. M. Schmitt, G. Serre, C. Paul and M. Simon (2013). "Defects of filaggrin-like proteins in both lesional and nonlesional atopic skin." J Allergy Clin Immunol **131**(4): 1094-1102.

Peter Liston, N. R., Katsuyuki Tamai, Charles Lefebvre, Stephen Baird, Gabriele Cherton-Horvat, Reza Farahani, Michael McLean, Joh-E IkedaII, and A. M. R. G. Korneluk (1996). "Suppression of apoptosis in mammalian cells by NAIP and a related family of IAP genes." Nature **379**: 5.

Philippe Paquet, G. P. (1996). "lnterleukin-6 and the Skin." Ini Arch Allergy Immunol **109**: 10.

Piipponen, M., D. Li and N. X. Landen (2020). "The Immune Functions of Keratinocytes in Skin Wound Healing." Int J Mol Sci **21**(22).

Polak, M. E., L. Newell, V. Y. Taraban, C. Pickard, E. Healy, P. S. Friedmann, A. Al-Shamkhani and M. R. Ardern-Jones (2012). "CD70-CD27 interaction augments CD8+ T-cell activation by human epidermal Langerhans cells." J Invest Dermatol **132**(6): 1636-1644.

Polak, M. E., C. Y. Ung, J. Masapust, T. C. Freeman and M. R. Ardern-Jones (2017). "Petri Net computational modelling of Langerhans cell Interferon Regulatory Factor Network predicts their role in T cell activation." Sci Rep **7**(1): 668.

Proksch, E. (2018). "pH in nature, humans and skin." J Dermatol **45**(9): 1044-1052.

Rawlings, A. V. and C. R. Harding (2004). "Moisturization and skin barrier function." Dermatol Ther **17 Suppl 1**: 43-48.

Rene de Waal Malefyt, J. A., Bruce Bennett, Carl G. Figdor and Jan E de Vries (1991). "Interleukin 10 Inhibits Cytokine Synthesis by Human Monocytes-An Autoregulatory Role of IL-10 Produced by Monocytes." Journal of experimental medicine **174**: 12.

Ridolo, E., I. Martignago, G. G. Riario-Sforza and C. Incorvaia (2018). "Allergen immunotherapy in atopic dermatitis." Expert Rev Clin Immunol **14**(1): 61-68.

ROBERT J.COFFEY, J., CHARLES C.BASCOM,NANCY J.SIPES, RAMONA GRAVES-DEAL, BERNARD E. WEISSMAN, AND HAROLD L. MOSES (1988). "Selective Inhibition of Growth-Related Gene Expression in Murine Keratinocytes by Transforming Growth Factor." MOLECULAR AND CELLULAR BIOLOGY **8**(8): 6.

Ross, S. H. and D. A. Cantrell (2018). "Signaling and Function of Interleukin-2 in T Lymphocytes." Annu Rev Immunol **36**: 411-433.

Sakabe, J., M. Yamamoto, S. Hirakawa, A. Motoyama, I. Ohta, K. Tatsuno, T. Ito, K. Kabashima, T. Hibino and Y. Tokura (2013). "Kallikrein-related peptidase 5 functions in proteolytic processing of profilaggrin in cultured human keratinocytes." J Biol Chem **288**(24): 17179-17189.

Schenkel, J. M., K. A. Fraser, L. K. Beura, K. E. Pauken, V. Vezys and D. Masopust (2014). "T cell memory. Resident memory CD8 T cells trigger protective innate and adaptive immune responses." Science **346**(6205): 98-101.

Sean Diehl, J. A., Angelika Hoffmeyer, Tyler Zapton, James N. Ihle, Erol Fikrig, and a. M. Rinco (2000). "Inhibition of Th1 Differentiation by IL-6 Is Mediated by SOCS1." Immunity **13**: 11.

Soumelis, V., P. A. Reche, H. Kanzler, W. Yuan, G. Edward, B. Homey, M. Gilliet, S. Ho, S. Antonenko, A. Lauerma, K. Smith, D. Gorman, S. Zurawski, J. Abrams, S. Menon, T. McClanahan, R. de Waal-Malefyt Rd, F. Bazan, R. A. Kastelein and Y. J. Liu (2002).

"Human epithelial cells trigger dendritic cell mediated allergic inflammation by producing TSLP." Nat Immunol **3**(7): 673-680.

Stander, S. (2021). "Atopic Dermatitis." N Engl J Med **384**(12): 1136-1143.

Stefansson, K., M. Brattsand, D. Roosterman, C. Kempkes, G. Bocheva, M. Steinhoff and T. Egelrud (2008). "Activation of proteinase-activated receptor-2 by human kallikrein-related peptidases." J Invest Dermatol **128**(1): 18-25.

Steinhoff, M., J. Buddenkotte, V. Shpacovitch, A. Rattenholl, C. Moormann, N. Vergnolle, T. A. Luger and M. D. Hollenberg (2005). "Proteinase-activated receptors: transducers of proteinase-mediated signaling in inflammation and immune response." Endocr Rev **26**(1): 1-43.

Sun, Z., J. H. Kim, S. H. Kim, H. R. Kim, K. Zhang, Y. Pan, M. K. Ko, B. M. Kim, H. Chu, H. R. Lee, H. L. Kim, J. H. Kim, X. Fu, Y. M. Hyun, K. N. Yun, J. Y. Kim, D. W. Lee, S. Y. Song, C. P. Lin, R. A. Clark, K. H. Lee, T. S. Kupper and C. O. Park (2021). "Skin-resident natural killer T cells participate in cutaneous allergic inflammation in atopic dermatitis." J Allergy Clin Immunol **147**(5): 1764-1777.

Swope, V. B., Z. Abdel-Malek, L. M. Kassem and J. J. Nordlund (1991). "Interleukins 1 alpha and 6 and tumor necrosis factor-alpha are paracrine inhibitors of human melanocyte proliferation and melanogenesis." J Invest Dermatol **96**(2): 180-185.

Szklarczyk, D., R. Kirsch, M. Koutrouli, K. Nastou, F. Mehryary, R. Hachilif, A. L. Gable, T. Fang, N. T. Doncheva, S. Pyysalo, P. Bork, L. J. Jensen and C. von Mering (2023). "The STRING database in 2023: protein-protein association networks and functional enrichment analyses for any sequenced genome of interest." Nucleic Acids Res **51**(D1): D638-D646.

Tamagawa-Mineoka, R. and N. Katoh (2020). "Atopic Dermatitis: Identification and Management of Complicating Factors." Int J Mol Sci **21**(8).

Tatsuno, K., T. Fujiyama, H. Yamaguchi, M. Waki and Y. Tokura (2015). "TSLP Directly Interacts with Skin-Homing Th2 Cells Highly Expressing its Receptor to Enhance IL-4 Production in Atopic Dermatitis." J Invest Dermatol **135**(12): 3017-3024.

Toshio Hirano, K. Y., Hisashi Harada, Tetsuya Taga, Yasuo Watanabe, Tadashi Matsuda, Shin-ichiro Kashiwamura, Koichi Nakajima, Koichi Koyama, Akihiro Iwamatsut, Susumu Tsunasawat, Fumio Sakiyamat, Hiroshi Matsui, Yoshiyuki Takahara, Tadatsugu Taniguchi, Tadamitsu Kishimoto (1986). "Complementary DNA for a novel human interleukin (BSF-2) that induces B lymphocytes to produce immunoglobulin." Nature **324**: 4.

TOSHIO HIRANO, T. T., KIYOSHI YASUKAWA, KOICHI NAKAJIMA, NAOKO NAKANO, FUMIHIKO TAKATSUKI, MASATOSHI SHIMIZU, ATSUKO MURASHIMA, SUSUMU TSUNASAWA, FUMIO SAKIYAMA, AND TADAMITSU KISHIMOTO (1987). "Human B-cell differentiation factor defined by an anti-peptide antibody and its possible role in autoantibody production." Proc. Natl. Acad. Sci **84**: 4.

Tsuji, G., A. Hashimoto-Hachiya, M. Kiyomatsu-Oda, M. Takemura, F. Ohno, T. Ito, S. Morino-Koga, C. Mitoma, T. Nakahara, H. Uchi and M. Furue (2017). "Aryl hydrocarbon receptor activation restores filaggrin expression via OVOL1 in atopic dermatitis." Cell Death Dis **8**(7): e2931.

Tzavlaki, K. and A. Moustakas (2020). "TGF-beta Signaling." Biomolecules **10**(3).

Vallabhapurapu, S., A. Matsuzawa, W. Zhang, P. H. Tseng, J. J. Keats, H. Wang, D. A. Vignali, P. L. Bergsagel and M. Karin (2008). "Nonredundant and complementary functions of TRAF2 and TRAF3 in a ubiquitination cascade that activates NIK-dependent alternative NF-kappaB signaling." Nat Immunol **9**(12): 1364-1370.

Vanden Berghe, T., A. Linkermann, S. Jouan-Lanhouet, H. Walczak and P. Vandenabeele (2014). "Regulated necrosis: the expanding network of non-apoptotic cell death pathways." Nat Rev Mol Cell Biol **15**(2): 135-147.

Vander Ark, A., J. Cao and X. Li (2018). "TGF-beta receptors: In and beyond TGF-beta signaling." Cell Signal **52**: 112-120.

Voegeli, R., A. V. Rawlings, M. Breternitz, S. Doppler, T. Schreier and J. W. Fluhr (2009). "Increased stratum corneum serine protease activity in acute eczematous atopic skin." Br J Dermatol **161**(1): 70-77.

Wallach, D. and A. Taieb (2014). "Atopic dermatitis/atopic eczema." Chem Immunol Allergy **100**: 81-96.

Walley, A. J., S. Chavanas, M. F. Moffatt, R. M. Esnouf, B. Ubhi, R. Lawrence, K. Wong, G. R. Abecasis, E. Y. Jones, J. I. Harper, A. Hovnanian and W. O. Cookson (2001). "Gene polymorphism in Netherton and common atopic disease." Nat Genet **29**(2): 175-178.

Wallmeyer, L., K. Dietert, M. Sochorova, A. D. Gruber, B. Kleuser, K. Vavrova and S. Hedtrich (2017). "TSLP is a direct trigger for T cell migration in filaggrin-deficient skin equivalents." Sci Rep **7**(1): 774.

Walt, F. M. (1989). "Terminal differentiation of epidermal keratinocytes." Current Opinion in Cell Biology: 9.

Wu, Z., B. Hansmann, U. Meyer-Hoffert, R. Glaser and J. M. Schroder (2009). "Molecular identification and expression analysis of filaggrin-2, a member of the S100 fused-type protein family." PLoS One **4**(4): e5227.

Y.NIWA, H. S., K.KAWAHIRA, T.TERASHIMA, T.NAKAMURA AND H.AKAMATSU (2003). "Protein oxidative damage in the stratum corneum: evidence for a link between environmental oxidants and the changing prevalence and nature of atopic dermatitis in Japan." British Journal of Dermatology **149**: 7.

Yamasaki, K., K. Kanada, D. T. Macleod, A. W. Borkowski, S. Morizane, T. Nakatsuji, A. L. Cogen and R. L. Gallo (2011). "TLR2 expression is increased in rosacea and stimulates enhanced serine protease production by keratinocytes." J Invest Dermatol **131**(3): 688-697.

Yamasaki, K., J. Schauber, A. Coda, H. Lin, R. A. Dorschner, N. M. Schechter, C. Bonnart, P. Descargues, A. Hovnanian and R. L. Gallo (2006). "Kallikrein-mediated

proteolysis regulates the antimicrobial effects of cathelicidins in skin." FASEB J **20**(12): 2068-2080.

Yanez, D. C., C. I. Lau, M. M. Chawda, S. Ross, A. L. Furmanski and T. Crompton (2019). "Hedgehog signaling promotes T(H)2 differentiation in naive human CD4 T cells." J Allergy Clin Immunol **144**(5): 1419-1423 e1411.

Yang, G., J. K. Seok, H. C. Kang, Y. Y. Cho, H. S. Lee and J. Y. Lee (2020). "Skin Barrier Abnormalities and Immune Dysfunction in Atopic Dermatitis." Int J Mol Sci **21**(8).

Yang, Y., J. Ochando, A. Yopp, J. S. Bromberg and Y. Ding (2005). "IL-6 plays a unique role in initiating c-Maf expression during early stage of CD4 T cell activation." J Immunol **174**(5): 2720-2729.

Yoo, J., M. Omori, D. Gyarmati, B. Zhou, T. Aye, A. Brewer, M. R. Comeau, D. J. Campbell and S. F. Ziegler (2005). "Spontaneous atopic dermatitis in mice expressing an inducible thymic stromal lymphopoietin transgene specifically in the skin." J Exp Med **202**(4): 541-549.

Yousef, G. M. and E. P. Diamandis (1999). "The new kallikrein-like gene, KLK-L2. Molecular characterization, mapping, tissue expression, and hormonal regulation." J Biol Chem **274**(53): 37511-37516.

Yousef, H., M. Alhajj and S. Sharma (2023). Anatomy, Skin (Integument), Epidermis. StatPearls. Treasure Island (FL) ineligible companies. Disclosure: Mandy Alhajj declares no relevant financial relationships with ineligible companies. Disclosure: Sandeep Sharma declares no relevant financial relationships with ineligible companies.

Zanetti, M. (2005). "The role of cathelicidins in the innate host defenses of mammals." Curr Issues Mol Biol **7**(2): 179-196.

Zeboudj, L., M. Maitre, L. Guyonnet, L. Laurans, J. Joffre, J. Lemarie, S. Bourcier, W. Nour-Eldine, C. Guerin, J. Friard, A. Wakkach, E. Fabre, A. Tedgui, Z. Mallat, P. L. Tharaux and H. Ait-Oufella (2018). "Selective EGF-Receptor Inhibition in CD4(+) T Cells Induces Anergy and Limits Atherosclerosis." J Am Coll Cardiol **71**(2): 160-172.

Zhu, Y., J. Underwood, D. Macmillan, L. Shariff, R. O'Shaughnessy, J. I. Harper, C. Pickard, P. S. Friedmann, E. Healy and W. L. Di (2017). "Persistent kallikrein 5 activation induces atopic dermatitis-like skin architecture independent of PAR2 activity." J Allergy Clin Immunol **140**(5): 1310-1322 e1315.

Appendix 1-Primers

Primer	Sequence
Check mRNA	
KLK5	
Forward	CAAGACCCCCCTGGATGTGG
Reverse	CCGAGACGGACTCTGAAAACT
GAPDH	
Forward	CCCATCACCATCTTCCAGGA
Reverse	CCAGTGAGCTTCCCGTTCAGC
TGFBR1	
Forward	GTTGGTACCCAAGGAAAGCC
Reverse	TCGAGAACTTCAGGGGCCAT
LCE3D	
Forward	GGCTGAGCTAGGGGTTTTC
Reverse	GATGAGGTCAGGCACAAGCA
FLG2	
Forward	ACCAAGCAAGATGGGGAGTG
Reverse	GTCTGGATCATCTGGGTTCTTCA
ASPRV1	
Forward	AGGACCAGGGAGACTATGGG
Reverse	GGCACTTTGCCAATCTTCCC
CRCT1	
Forward	ACCAGTTGCTGCTGCTT
Reverse	CCTGAGCTCCGGTTGTTG
SPRR2E	
Forward	GGAGAACCTGATTCTGAGACTC
Reverse	CAGGGCTGTGGACACTTT
Amplification	
Infusion-TetOne-GFP	
Forward	CCCTCGTAAAGAATTCATGGTGAGCAAGGGC GAGG
Reverse	GAGGTGGTCTGGATCCTTACTTGTACAGCTCG TCCATGCC
GA-TetOne-KLK5	

Continued

Forward	CTTATACCAACTTTCCGTACCACTTCCTACCCT
	CGTAAAGCCACCATGGCTACAGCAAGACCCC
Reverse	TCATTGGCTGTCCAGCTTAGCTCGCAGGGGA
	GGTGGTCTGGATCCTTACTTGTACAGCTCGTC
	CATGCC
Sequence check	
Tet-GFP vector	
GFPmid Reverse	GGGCACAAGCTGGAGTAC
End insert Forward	GGAAGCTGCGCCTGTCTT
Tet-KLK5 vector	
GFPmid Reverse	GGGCACAAGCTGGAGTAC
KLK5end Reverse	CGATACCGTCGACCTCG
KLK5mid Reverse	CCACTCTAACGACCTCATGC
KLK5midcheck Forward	GGGTAATCTCCCCAGGACAC
End insert Forward	GGAAGCTGCGCCTGTCTT

Appendix 2-Antibodies

Antibody	Host	Product code	Dilution
KLK5	Goat	AF1108	1:10000
DSG1	Mouse	651111	1:1000
GFP	Rabbit	A11122	1:1000
GAPDH	Rabbit	3683S	1:3000
Actin	Rabbit	5125S	1:2000
Vinculin	Mouse	SAB4200080	1:250000
Anti-Goat	Rabbit	81-1620	1:5000
Anti-Mouse	Goat	926-80010	1:5000
Anti-Rabbit	Mouse	RG96	1:7000
CD4-PE	Mouse	12-0048-41	0.0006ug/ul
CD45RA-FITC	Mouse	304105	0.01ug/ul
CD45RO-APC	Mouse	17-0457-41	0.0003ug/ul
CD25-APC	Mouse	302609	0.005ug/ul
CD69-FITC	Mouse	310903	0.005ug/ul
GATA3-PE	Rat	12-9966-41	0.0006ug/ul
PE Mouse IgG2b, κ Isotype	Mouse	12-4732-81	0.0006ug/ul
FITC Mouse IgG2b, κ Isotype	Mouse	400309	0.01ug/ul
APC Mouse IgG2a, κ Isotype	Mouse	17-4724-81	0.0003ug/ul
APC Mouse IgG1, κ Isotype	Mouse	400119	0.005ug/ul
FITC Mouse IgG1, κ Isotype	Mouse	400107	0.005ug/ul
PE Rat IgG2b, κ Isotype	Rat	12-4031-81	0.0006ug/ul

Appendix 3-Differentiated genes from pooled RNA-seq dataset

ID	P_{adj}	Fold Change	log_2Fold Change
KLK5	0.034	2.254	1.173
PABPC3	0.017	1.742	0.801
RPL23P8	0.030	1.672	0.742
PPRC1	0.022	1.484	0.570
GBP1	0.033	1.478	0.563
PHF12	0.037	1.478	0.563
MMP2	0.043	1.431	0.517
BGN	0.049	1.421	0.507
TOB2	0.033	1.419	0.505
PTMS	0.033	1.418	0.503
DRAP1	0.041	1.408	0.494
PRDX3	0.048	0.727	-0.460
DCBLD2	0.034	0.727	-0.459
CD24	0.049	0.715	-0.485
KLF3	0.048	0.711	-0.492
RABGGTB	0.045	0.705	-0.505
SERPINB3	0.033	0.705	-0.504
ITM2B	0.033	0.704	-0.507
LAMP2	0.044	0.703	-0.507
SDCBP	0.049	0.696	-0.522
CREG1	0.048	0.695	-0.525
BZW1	0.040	0.692	-0.531
SERPINB13	0.033	0.691	-0.534
ARL6IP1	0.047	0.690	-0.536
SIKE1	0.035	0.686	-0.544
PTP4A1	0.034	0.684	-0.547
POMP	0.039	0.682	-0.552
TMEM33	0.039	0.682	-0.552
GGH	0.049	0.682	-0.552
EIF3E	0.042	0.680	-0.556
YIPF6	0.044	0.680	-0.555

Continued

ID	P_{adj}	Fold Change	log_2Fold Change
IMPAD1	0.034	0.678	-0.560
IER3IP1	0.030	0.675	-0.568
SERPINB4	0.017	0.674	-0.570
CAND1	0.049	0.674	-0.568
HIGD1A	0.022	0.673	-0.572
GLO1	0.041	0.671	-0.576
CD46	0.048	0.670	-0.578
ABCD3	0.040	0.667	-0.584
MMADHC	0.033	0.666	-0.585
SLC6A14	0.036	0.664	-0.591
KPNA3	0.042	0.662	-0.596
LYPLA1	0.049	0.660	-0.600
CMPK1	0.030	0.659	-0.601
HINT3	0.033	0.659	-0.601
RAP1B	0.030	0.657	-0.606
LYST	0.044	0.657	-0.606
MFSD1	0.017	0.656	-0.609
BRWD1	0.049	0.656	-0.607
TMEM45A	0.017	0.655	-0.611
SLC6A15	0.048	0.654	-0.613
BTF3L4	0.027	0.653	-0.614
SDHD	0.050	0.652	-0.617
CDK6	0.044	0.650	-0.621
CCNC	0.034	0.649	-0.624
SH3BGRL	0.034	0.648	-0.627
MAL2	0.033	0.644	-0.636
TMBIM4	0.048	0.642	-0.639
SPTSSB	0.034	0.640	-0.644
SCYL2	0.048	0.640	-0.643
SLC39A8	0.034	0.639	-0.646
LINC01578	0.044	0.639	-0.645
STT3B	0.023	0.638	-0.648
SCAMP1	0.042	0.637	-0.650

Continued

ID	P_{adj}	Fold Change	log_2Fold Change
C6orf62	0.043	0.635	-0.656
FMO2	0.027	0.635	-0.655
CHMP2B	0.034	0.635	-0.654
NAA50	0.040	0.634	-0.659
CLDN12	0.044	0.634	-0.658
DESI2	0.033	0.633	-0.659
TRAPPC6B	0.042	0.631	-0.665
NCKAP1	0.039	0.630	-0.667
DSTN	0.018	0.628	-0.672
PTGES3	0.025	0.628	-0.672
SYPL1	0.022	0.627	-0.673
TGFBR1	0.048	0.624	-0.680
INSIG2	0.044	0.623	-0.683
UBE2D1	0.049	0.623	-0.682
ZDHHC20	0.028	0.622	-0.686
VPS50	0.033	0.622	-0.685
UGCG	0.042	0.622	-0.684
NEBL	0.030	0.620	-0.690
VPS13A	0.040	0.620	-0.690
ARAP2	0.035	0.619	-0.691
SC5D	0.024	0.618	-0.695
SNX14	0.048	0.618	-0.695
PNLIPRP3	0.021	0.618	-0.694
ARL8B	0.022	0.617	-0.697
CRIPT	0.048	0.614	-0.705
TM9SF3	0.033	0.614	-0.703
PPP1CB	0.045	0.613	-0.706
STARD4	0.048	0.613	-0.706
RAB27B	0.046	0.612	-0.707
YIPF4	0.047	0.611	-0.711
TMEM106B	0.045	0.609	-0.714
AASDHPPT	0.032	0.605	-0.725
MMGT1	0.033	0.605	-0.724

Continued

ID	P_{adj}	Fold Change	log_2Fold Change
TBC1D23	0.022	0.604	-0.728
MUC15	0.028	0.604	-0.727
COPS2	0.032	0.603	-0.729
NDFIP2	0.017	0.602	-0.733
RHOQ	0.048	0.602	-0.732
RNF139	0.049	0.601	-0.734
LANCL1	0.018	0.597	-0.744
ZBED5	0.033	0.596	-0.747
CD164	0.030	0.596	-0.746
NEK7	0.036	0.593	-0.754
XPO1	0.034	0.592	-0.757
CMTM6	0.017	0.592	-0.755
CCBL2	0.025	0.592	-0.755
LTN1	0.038	0.590	-0.760
TMEM167A	0.021	0.588	-0.767
ELOVL7	0.026	0.588	-0.767
FAM135A	0.033	0.586	-0.772
OSTM1	0.039	0.585	-0.772
DCUN1D1	0.033	0.582	-0.781
NAA30	0.037	0.578	-0.791
EXOC5	0.027	0.576	-0.797
MARCH7	0.018	0.574	-0.800
MSMO1	0.017	0.571	-0.808
GSKIP	0.033	0.570	-0.812
TRAM1	0.017	0.567	-0.818
KITLG	0.033	0.564	-0.826
TMEM30A	0.017	0.561	-0.833
BIRC2	0.032	0.559	-0.840
CCNG1	0.018	0.552	-0.858

Appendix 4-Differentiated genes from individual RNA-seq dataset

ID	Fold Change (GFP vs KLK5)	Log_2Fold Change (GFP vs KLK5)	Fold Change (UT vs GFP)
Differentiated genes from the RNA-seq of 1st donor			
AASDHPPT	0.493	-1.021	0.935
ALOX12B	3.247	1.699	0.890
AMMECR1	0.499	-1.003	0.848
ANXA9	2.093	1.066	1.483
ARAP2	0.491	-1.025	0.919
ARL15	0.496	-1.013	0.800
ARL5A	0.451	-1.149	1.088
ARL8B	0.462	-1.114	0.955
ARRDC3	0.412	-1.278	1.108
ASPRV1	4.326	2.113	1.440
ATL2	0.498	-1.006	0.884
AZGP1	3.408	1.769	1.500
BIRC2	0.372	-1.428	0.979
C1GALT1	0.410	-1.285	1.040
C5orf51	0.418	-1.258	0.962
C6orf62	0.488	-1.036	0.995
CALML5	2.110	1.077	0.852
CCBL2	0.493	-1.021	1.025
CCNG1	0.449	-1.155	1.063
CCNG2	0.499	-1.002	0.849
CD164	0.399	-1.324	1.005
CDK6	0.495	-1.013	0.967
CMTM6	0.457	-1.129	0.984
CMTR2	0.372	-1.426	0.934
CNFN	6.243	2.642	1.045
CNOT6L	0.493	-1.021	1.001
COPS2	0.501	-0.998	1.135
CRCT1	3.130	1.646	1.253
CRIPT	0.455	-1.138	1.158

Continued

ID	Fold Change (GFP vs KLK5)	Log_2Fold Change (GFP vs KLK5)	Fold Change (UT vs GFP)
CRNN	2.623	1.391	1.560
CUL5	0.485	-1.045	1.050
CXADR	0.471	-1.086	0.917
CYSRT1	2.220	1.150	1.070
DCUN1D1	0.409	-1.291	1.075
DYNLT3	0.469	-1.092	1.039
EDEM3	0.473	-1.079	1.004
ELOVL7	0.490	-1.029	0.938
EPT1	0.417	-1.262	1.018
EXOC5	0.432	-1.211	0.989
FAM126B	0.455	-1.138	1.021
FAM135A	0.440	-1.184	0.935
FAM199X	0.464	-1.107	1.027
FAM69A	0.494	-1.016	0.938
FAM8A1	0.464	-1.107	1.010
FLG2	4.616	2.207	1.795
GLS	0.463	-1.110	0.953
GMFB	0.284	-1.817	1.207
GSKIP	0.374	-1.419	1.141
HACD2	0.478	-1.064	0.987
HECA	0.479	-1.063	0.950
HINT3	0.501	-0.997	1.022
HMOX1	2.197	1.136	1.271
ICE2	0.500	-1.000	0.985
IFITM1	2.052	1.037	0.884
IL36RN	2.348	1.232	1.244
KIAA1033	0.406	-1.300	1.006
KITLG	0.420	-1.250	1.048
KLK5	3.441	1.783	1.183
KLK6	2.350	1.233	1.339
KRT1	2.703	1.435	1.308
LANCL1	0.438	-1.192	1.000

Continued

ID	Fold Change (GFP vs KLK5)	Log_2Fold Change (GFP vs KLK5)	Fold Change (UT vs GFP)
LINC00657	0.489	-1.033	0.900
LRRC58	0.473	-1.081	0.874
LTN1	0.471	-1.086	0.880
LYPD5	2.102	1.072	1.107
MAL2	0.490	-1.028	0.992
MAN2A1	0.450	-1.151	1.004
MARCH7	0.495	-1.013	1.058
MIB1	0.466	-1.101	1.004
MMGT1	0.446	-1.165	1.028
MSMO1	0.501	-0.997	1.021
MX2	2.492	1.317	0.648
NAA30	0.400	-1.323	0.984
NAA50	0.460	-1.122	0.951
NAE1	0.499	-1.003	1.049
NCKAP1	0.497	-1.010	0.984
NEBL	0.431	-1.215	1.075
NEK7	0.478	-1.065	1.042
NR1D2	0.482	-1.054	1.024
NT5C3A	0.423	-1.240	1.053
OASL	2.385	1.254	1.024
ORC4	0.493	-1.020	1.014
OSBPL8	0.484	-1.048	1.012
OSTM1	0.497	-1.010	0.903
PMEL	0.334	-1.582	0.766
PPP1CB	0.430	-1.219	1.003
PRKD3	0.454	-1.140	0.938
PRSS27	2.077	1.054	1.258
PTGES3	0.472	-1.084	0.958
RAB27B	0.451	-1.149	1.126
RAP2A	0.487	-1.039	0.993
RB1	0.495	-1.013	0.983
RHOQ	0.425	-1.233	0.978

Continued

ID	Fold Change (GFP vs KLK5)	Log_2Fold Change (GFP vs KLK5)	Fold Change (UT vs GFP)
RNASE7	3.680	1.880	0.962
RNF139	0.459	-1.123	1.065
RPS6KA3	0.433	-1.206	0.998
RRM2B	0.444	-1.172	1.056
SCAMP1	0.471	-1.085	0.988
SCOC	0.293	-1.770	1.060
SCYL2	0.499	-1.002	0.988
SESN3	0.434	-1.203	0.784
SLC25A36	0.415	-1.270	0.936
SLC35F5	0.496	-1.011	1.077
SLC38A2	0.381	-1.393	0.777
SLC5A3	0.492	-1.023	1.057
SLC7A11	0.420	-1.251	0.988
SMCHD1	0.441	-1.182	0.941
SNX14	0.489	-1.032	1.054
SPNS2	2.917	1.544	1.486
SPOPL	0.477	-1.068	0.998
SPRR1A	2.151	1.105	1.093
SPRR2A	2.332	1.221	1.484
SPRR2E	2.985	1.578	1.346
TAOK1	0.498	-1.004	0.908
TBC1D23	0.485	-1.045	1.045
TCEA1	0.476	-1.072	0.924
TCHHL1	2.059	1.042	1.673
TGFBR1	0.471	-1.085	1.023
TM9SF3	0.479	-1.063	1.065
TMEM106B	0.465	-1.104	1.033
TMEM167A	0.488	-1.034	0.968
TMEM168	0.429	-1.222	1.068
TMEM30A	0.462	-1.115	1.090
TMEM87B	0.467	-1.098	0.893
TMX3	0.377	-1.407	1.006

Continued

ID	Fold Change (GFP vs KLK5)	Log_2Fold Change (GFP vs KLK5)	Fold Change (UT vs GFP)
TPM2	2.055	1.039	1.202
TRAM1	0.437	-1.195	1.090
TVP23B	0.382	-1.387	1.049
TWF1	0.493	-1.019	1.037
TYRP1	0.304	-1.720	0.698
UBA6	0.419	-1.255	0.997
UBE2W	0.450	-1.154	0.978
UHMK1	0.354	-1.499	0.983
VBP1	0.458	-1.127	1.012
WFDC12	6.098	2.608	1.291
WFDC21P	2.019	1.013	1.019
XPO1	0.409	-1.288	0.979
ZBED5	0.497	-1.008	0.902
ZBTB33	0.455	-1.136	0.871
ZDHHC21	0.450	-1.151	0.959
ZMAT3	0.460	-1.119	1.004
ZMPSTE24	0.438	-1.191	1.114
ZNF770	0.385	-1.376	0.895
Differentiated genes from the RNA-seq of 2nd donor			
ENO3	2.000	1.000	0.721
ACER3	0.490	-1.030	1.324
ADGRG6	0.452	-1.145	1.058
AP4E1	0.418	-1.258	1.134
ARHGAP29	0.418	-1.258	0.804
ARL5A	0.311	-1.684	0.845
BCAP29	0.485	-1.044	1.011
BIRC2	0.478	-1.064	0.996
CCNG1	0.394	-1.343	0.941
CDK19	0.494	-1.017	0.982
CMTR2	0.493	-1.020	1.113
COPS2	0.501	-0.997	0.860
CUL4B	0.443	-1.175	0.933

Continued

ID	Fold Change (GFP vs KLK5)	Log_2Fold Change (GFP vs KLK5)	Fold Change (UT vs GFP)
CUL5	0.485	-1.044	1.048
CXADR	0.451	-1.148	1.060
DDX60L	0.489	-1.032	0.926
DKK1	0.471	-1.085	0.871
DMXL1	0.495	-1.016	1.162
DSTN	0.477	-1.066	0.926
ELOVL4	0.443	-1.175	0.898
ELOVL7	0.435	-1.201	0.964
EMB	0.420	-1.251	0.856
FAM135A	0.447	-1.160	1.030
FAM214A	0.432	-1.212	0.985
FAM89A	0.466	-1.103	0.919
FBXL3	0.429	-1.221	1.023
GGCT	0.500	-0.999	0.755
GLS	0.458	-1.127	0.781
GMFB	0.363	-1.463	1.158
H3F3AP4	0.470	-1.088	0.843
HOPX	0.417	-1.261	0.750
HS2ST1	0.456	-1.131	1.144
IDE	0.501	-0.998	0.861
IL18	0.399	-1.327	0.708
INSIG2	0.484	-1.048	0.885
KATNBL1	0.484	-1.046	1.030
KIAA1033	0.492	-1.024	0.971
KITLG	0.446	-1.164	1.366
LINC01578	0.462	-1.114	1.070
LMBRD1	0.472	-1.084	1.006
LTN1	0.453	-1.144	0.829
MALAT1	0.367	-1.447	1.929
MAN2A1	0.483	-1.050	1.129
MARCH7	0.419	-1.255	0.835
METTL5	0.490	-1.030	0.972

Continued

ID	Fold Change (GFP vs KLK5)	Log_2Fold Change (GFP vs KLK5)	Fold Change (UT vs GFP)
MME	0.478	-1.064	0.799
MOSPD1	0.483	-1.051	0.838
MSMO1	0.394	-1.345	0.936
NAA30	0.470	-1.089	1.025
NAE1	0.471	-1.086	1.045
NCKAP1	0.490	-1.029	1.049
NEAT1	0.409	-1.288	1.720
NEK7	0.424	-1.236	0.995
NT5C3A	0.440	-1.184	0.843
ORC4	0.448	-1.158	0.977
OSTM1	0.435	-1.199	1.002
PIK3CB	0.497	-1.010	0.940
PMEL	0.472	-1.082	0.786
PNPLA8	0.499	-1.002	1.003
PPP1CB	0.497	-1.010	0.874
RAB27B	0.493	-1.022	0.962
RHOQ	0.493	-1.020	0.972
RICTOR	0.480	-1.059	1.063
RNF139	0.421	-1.248	1.131
RORA	0.502	-0.995	0.771
SC5D	0.498	-1.005	1.023
SCOC	0.393	-1.348	0.994
SLC25A46	0.493	-1.021	1.004
SLC38A2	0.400	-1.323	1.015
SLC39A8	0.474	-1.078	1.110
SLC5A3	0.400	-1.321	0.667
SLC6A14	0.489	-1.033	1.041
SLC6A15	0.488	-1.034	1.260
SLMO2	0.497	-1.007	0.928
SNX14	0.452	-1.146	1.182
SREK1IP1	0.493	-1.020	0.947
TM9SF3	0.462	-1.113	1.073

Continued

ID	Fold Change (GFP vs KLK5)	Log_2Fold Change (GFP vs KLK5)	Fold Change (UT vs GFP)
TMEM106B	0.470	-1.089	1.080
TMEM126B	0.462	-1.114	0.857
TMEM167A	0.461	-1.119	0.976
TMEM30A	0.396	-1.335	1.158
TMEM70	0.442	-1.178	1.012
TRAM1	0.436	-1.197	1.012
TRAPPC6B	0.487	-1.039	0.978
TRAPPC8	0.465	-1.105	0.941
TYRP1	0.367	-1.445	0.833
UBA6	0.436	-1.197	1.059
UBE2W	0.441	-1.180	0.936
UBLCP1	0.449	-1.154	1.261
UGCG	0.406	-1.300	0.940
USP38	0.462	-1.115	0.775
VBP1	0.448	-1.157	1.025
VPS13A	0.449	-1.155	1.088
XIST	0.470	-1.090	3.032
XPO1	0.464	-1.108	0.962
YIPF4	0.417	-1.262	0.979
YOD1	0.392	-1.350	0.649
ZBTB33	0.480	-1.059	1.128
ZDHHC21	0.498	-1.005	0.899
ZNF277	0.488	-1.036	0.892
ZNF770	0.433	-1.207	1.015
ZNF841	0.480	-1.060	1.069

Appendix 5-Maps for inducible lentiviral vectors

Tet-GFP inducible lentiviral vector

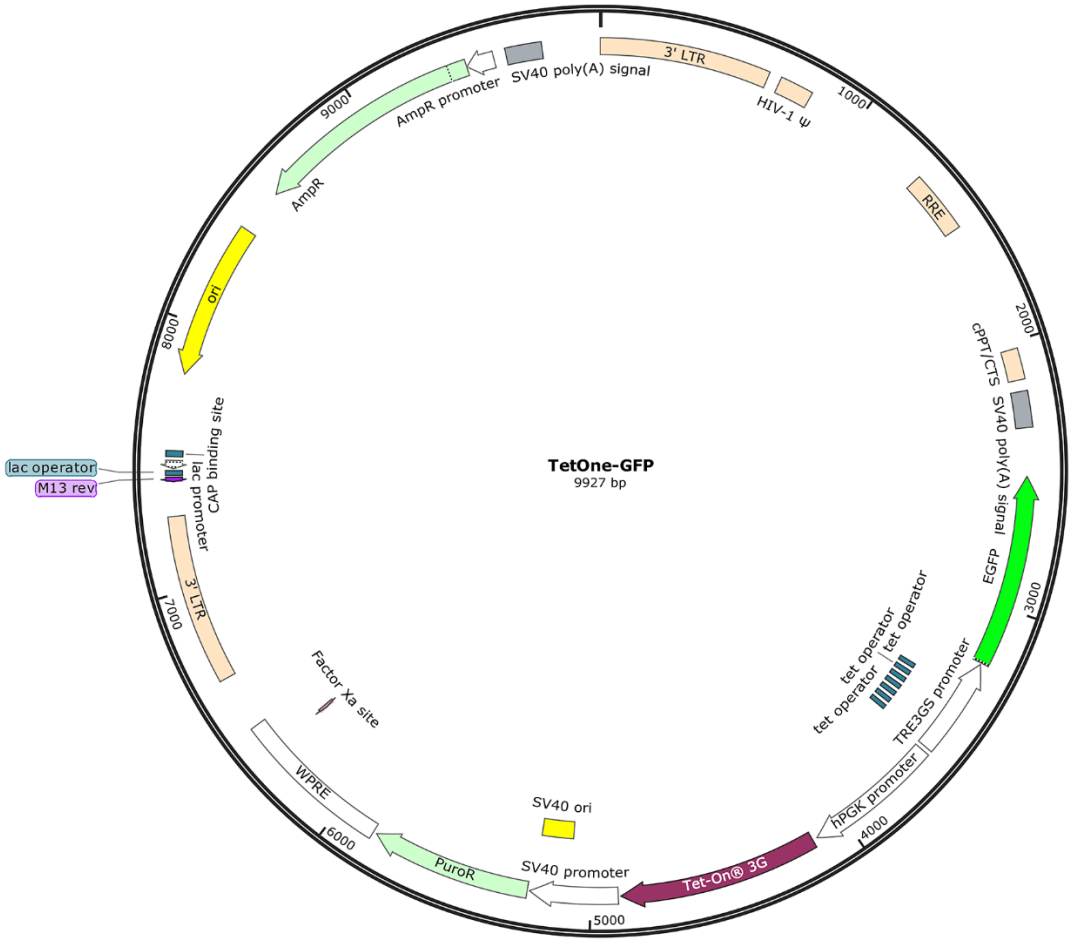

Tet-KLK5 inducible lentiviral vector